University of Alberta

Molecular and Developmental Characterization of *Drosophila melanogaster atm*

by

Michael Eric Pedersen 

A thesis submitted to the Faculty of Graduate Studies and Research in partial fulfillment of the requirements for the degree of Master of Science

in

Molecular Biology and Genetics

Department of Biological Sciences

Edmonton, Alberta

Fall 2005

Your file Votre référence
ISBN: 0-494-09262-9
Our file Notre référence
ISBN: 0-494-09262-9

University of Alberta

Library Release Form

Name of Author: *Michael Eric Pedersen*

Title of Thesis: *Molecular and Developmental Characterization of Drosophila melanogaster atm*

Degree: *Master of Science*

Year this Degree Granted: *2005*

_____

Signature

Aug. 31st/05

Abstract:

ATM is a protein kinase involved in the cellular response to DNA double strand breaks (DSBs). This project is concerned with the characterization of the *Drosophila melanogaster* homolog of ATM. Research was focused on three fronts. First, mutant alleles of *atm* were sequenced, and two poorly characterized regions of the protein were identified as being important for ATM function. Second, the cellular responsibilities of ATM were examined and I demonstrate that ATM is important for somatic DSB repair. Finally, oogenesis and eye development were examined to determine if there is a link between the *atm* phenotypes observed in these tissues and the established functions of ATM. I demonstrate that there is *p53* dependent apoptosis in proliferating cells of *atm* eye discs, likely a consequence of compromised genomic stability. Furthermore, I have demonstrated that ATM is required during oogenesis for the proper repair of DSBs during meiotic recombination.

Table Of Contents

List of Tables

List of Figures

List of Abbreviations

ATM – Ataxia Telangiectasia Mutated

AT – Ataxia Telangiectasia

PI(3)K – Phosphoinositol (3) Kinase

DNA-PKcs – DNA Protein Kinase Catalytic Subunit

ATR – ATM Related

DSB – Double Strand Break

MRN – Mre11, Rad50, and Nbs1

HR – Homologous Recombination

NHEJ – Non-Homologous End Joining

FAT – FRAP, ATM, TRRAP

FATC – FRAP, ATM, TRRAP C-terminal

Df – Deficiency

PH3 – Phospho Histone-3

BrdU – Bromodeoxyuridine

FMW – First Mitotic Wave

SMW – Second Mitotic Wave

A/P – Anterior/Posterior

D/V – Dorsal/Ventral

IR – Ionizing Radiation

Chapter 1: Introduction

Section 1.1 - The cellular role of ATM

ATM is a large, multifunctional protein kinase involved in the cellular response to double strand breaks (DSBs), a type of DNA damage where both strands of the double helix are severed. ATM has been a topic of interest since it was found to be associated with a human disease, ataxia telangiectasia (AT) (Gatti et. al., 1988; Wei et. al., 1990; Savitsky et. al., 1995; Uziel et. al., 1996). AT is characterized by a variety of symptoms that begin to manifest themselves at around 2 years of age. The hallmark of the AT disease is progressive neurodegeneration that leads to ataxia, a loss of motor coordination. The purkinje neurons of the CNS seems to be particularly susceptible to neurodegeneration in AT individuals. These large neurons are located in the cerebellum and are involved in the control and refinement of motor activities. Other AT symptoms include vaso-dilation around the eyes (termed telangiectases), immunodeficiency, sterility, and susceptibility to certain forms of cancer, including leukemia and lymphoma (Taylor et. al., 1996). Furthermore, AT individuals are extremely sensitive to ionizing radiation (IR), which makes treatment of these cancers by radiotherapy difficult. Because AT patients tend to die in their 20's, AT is primarily a childhood disorder.

The ATM protein is a member of a large family of protein kinases, which possess a kinase domain similar to phosphoinositol-3 kinase (PI(3)K). This domain has been found in many kinases that phosphorylate either lipids (phosphoinositol) or proteins. In the case of ATM, all known targets for phosphorylation are proteins. The ATM protein specifically recognizes certain SQ or TQ sequence motifs and phosphorylates the serine or threonine residue (O'Neill et. al., 2000; Kim et. al., 1999). The sequence of regions surrounding the SQ/TQ motif also influences ATM phosphorylation; with negatively charged or hydrophobic amino acids near the serine or threonine residue being suggested to promote phosphorylation by ATM (Kim et. al., 1999). Several other kinases involved in the response to DSBs also possess a PI(3)K-like domain and are evolutionarily related to ATM. These include the DNA protein kinase catalytic subunit (DNA-PKcs) and the ATM-paralog, ATR (ATM–Related), proteins which serve partially redundant functions with ATM (Abraham, 2004).

Because ATM is associated with a human disease, it has been extensively studied in mammalian cell cultures. Much is known about ATM activation and function based on these studies. Under normal cellular conditions, ATM is thought to be held inactive as a dimer (Bakkenist and Kastan, 2003). Once DSBs occur, ATM has been proposed to release itself from this dimer through autophosphorylation (Fig. 1-1) Bakkenist and Kastan, 2003). Activation of ATM also requires the inhibition of the protein phosphatase PP2A, which is capable of removing the autophosphorylation event when active and bound to ATM (Goodarzi et. al., 2004). The autophosphorylation of ATM has also been shown to require Mre11, Nbs1, and Rad50 (Carson et. al., 2003; Uziel et. al., 2003), components of the MRN complex that interact with ATM in multiple ways to carry out the DSB response. The activation process may also involve DNA binding by ATM near the actual DSB site in addition to autophosphorylation (as shown in Fig. 1-1), an idea which has been proposed based on the presence of a DNA binding domain in 3D models of the ATM protein (Llorca et. al., 2003) and supported by the observation that autophosphorylation and dimer disassociation, by itself, is not sufficient to activate the kinase domain (Goodarzi et. al., 2004). Once ATM is activated, it phosphorylates a variety of targets involved in the DSB response (Fig. 1-1). These targets include proteins involved in DSB repair, checkpoint components that prevent progression through the cell cycle until repair is complete, and promoters of apoptosis (Abraham, 2001; Kastan and Lim, 2000). These latter interactions are thought to be important for removing cells if many DSBs are present that can not be repaired.

In eukaryotes, DSBs are repaired by two very different mechanisms: homologous recombination (HR) (reviewed in Shinohara and Ogawa, 1995) and non-homologous end joining (NHEJ) (reviewed in Tsukamoto and Ikeda, 1998). HR is a process similar to meiotic recombination, where a recombination intermediate forms at the damaged site between the damaged chromosome and its homolog. During the repair process, the 5' ends of the DNA molecules at the breaksite are resected, giving rise to single stranded DNA (ssDNA) (Fig. 1-2). This ssDNA is recognized by a complex of repair proteins, including Rad51, Rad52, and Rad54. Once bound to the ssDNA, this complex allows the detection of homologous regions on the other chromosome and promotes strand invasion (Fig. 1-2). During the strand invasion process, the ssDNA portion of the damaged

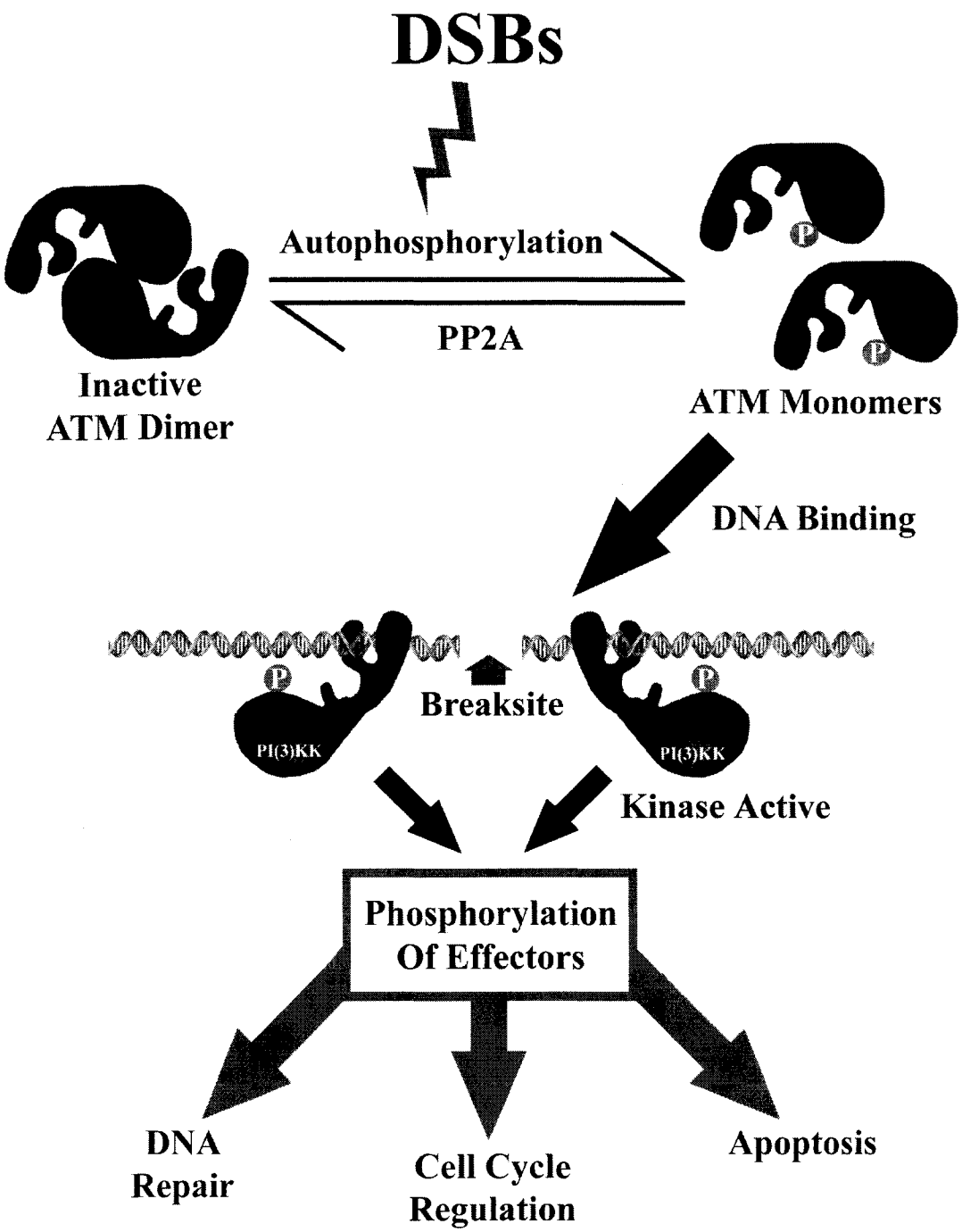

Fig. 1-1 – Current model of ATM activation in response to DNA DSBs. Under normal cellular conditions, ATM is thought to be held inactive in the cell as a dimer. When DNA DSBs are present, a autophosphorylation event occurs, causing dissociation of ATM. This phosphorylation event is antagonized by the PP2A phosphatase. Once in monomeric form, ATM may bind to DNA surrounding the DSB site. Upon DNA binding, ATM undergoes a conformational change, which activates the PI(3)KK kinase domain. Kinase active ATM proceeds to phosphorylate a variety of effectors involved in the cellular response to DSBs, including DNA repair, cell cycle regulation, and apoptosis.

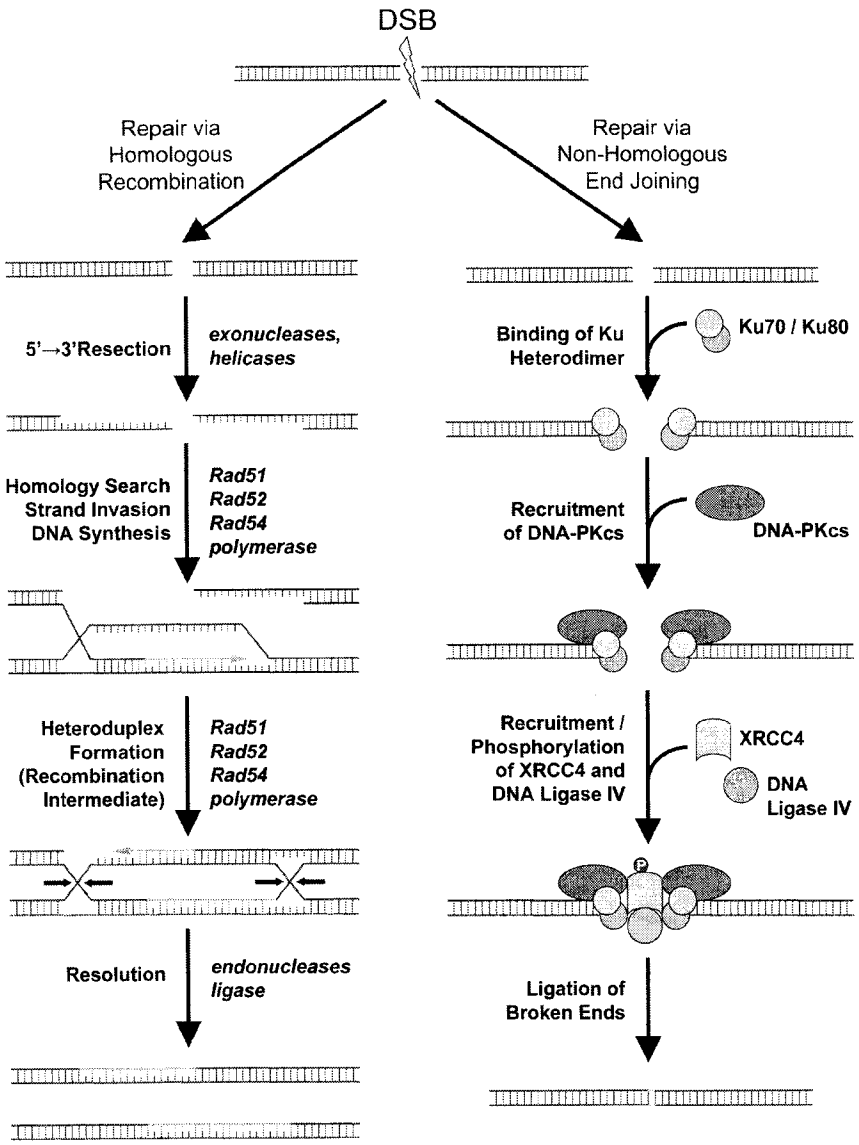

Fig. 1-2 – Current models for DSB repair via homologous recombination and non-homologous end joining. In homologous recombination (left), the 5' ends of the DNA molecules at the breaksite are resected. The resulting single stranded DNA is recognized by a complex of repair proteins (including Rad51, Rad52, and Rad54), which then carry out the homology search and strand invasion processes that result in the formation of a heteroduplex between the damaged chromosome (blue), and its homolog (red). DNA synthesis then occurs across the break site, using the homologous chromosome as a template (pink strand with arrow), and the two chromosomes become further associated to form what is called a double Holliday junction intermediate. The Holliday junctions are then resolved, which involves endonuclease cleavages (arrows) and ligation of the resulting nicks. In non-homologous end joining, the DNA ends are recognized by Ku70 and Ku80. These proteins recruit DNA-PKcs, which in turn recruits and activates XRCC4 and DNA Ligase IV via phosphorylation. These proteins are responsible for joining the DNA ends with a ligation reaction that is independent of sequence homology.

chromosome displaces the same-sense strand from the homologous chromosome, thereby allowing the formation of a heteroduplex molecule involving strands from both chromosomes (Fig. 1-2). DNA synthesis occurs across the break site, using the homologous chromosome as a template (Fig. 1-2, pink strand and arrow), and the two chromosomes become further associated to form what is called a double Holliday junction intermediate (Fig. 1-2). The final step in the repair process is the resolution of the Holliday junctions, which involves endonuclease cleavages (Fig. 1-2, black arrows) and ligation of the resulting nicks, resulting in two intact chromosomes (Fig. 1-2). The advantage of this type of DNA repair is that it ensures that the correct DNA ends are joined together, based on homologous sequence information derived from the homologous chromosome. In contrast, NHEJ is an inherently error-prone DNA repair process, involving the fusion of non-homologous DNA molecules thought to primarily involve DNA-PKcs in most metazoans (Meek et. al., 2004; Dore et. al., 2004). The structure of DNA-PKcs is similar to ATM in that they both contain similar conserved domains, including the PI(3)K-like kinase domain. In NHEJ, the DNA ends at the break site are recognized by the Ku proteins, Ku70 and Ku80 (Fig. 1-2). These proteins are thought to be involved in localization of DNA-PKcs to the break site and promote DNA-PKcs kinase activity (Fig. 1-2) (Yaneva et. al., 1997, Smith and Jackson, 1999). DNA-PKcs kinase activity is important for activating and recruiting DNA Ligase IV and XRCC4, two factors that cooperate to ligate the DNA ends (Fig. 1-2) (Meek et. al., 2004). This method of repairing DSBs is error-prone since there is no sequence based method of ensuring that the correct DNA ends are joined.

The idea that ATM functions in the DNA repair process is primarily based on the observation that when ATM-deficient human tissue culture cells are exposed to DSB inducing agents, there is a significant increase in the frequency of chromosomal breaks relative to controls (Morgan et. al., 1997; Cornforth and Bedford, 1985). The exact molecular mechanisms that connect ATM to HR and/or NHEJ remain uncertain however, and are likely to be quite complex. One of several links between ATM and both the HR and NHEJ repair pathways has come out of work done on the MRN complex. The MRN complex is composed of three proteins: Mre11, Rad50, and Nbs1. Although the MRN complex appears to be required for the activation of ATM in response to DSBs (Carson

et. al., 2003; Uziel et. al., 2003), it has also been demonstrated that ATM activates Nbs1 via phosphorylation, suggesting that ATM reciprocally modulates the activity of the MRN complex (Fig. 1-3A) (Lim et. al., 2000; Gatei et. al., 2000, Zhao et. al., 2000, Wu et. al., 2000). The MRN complex has been linked to DSB repair by both HR and NHEJ based on studies in the budding yeast, *Saccharomyces cerevisiae* (Fig. 1-3A) (Ivanov et. al., 1994, Bressan et. al., 1999; Schiestl et. al., 1994, Moore and Haber, 1996; Boulton and Jackson, 1998). However, there are still some open questions as to the exact nature of the MRN complex's role and conflicting opinions on whether it is a required component of the repair process in all organisms (Kastan and Lim, 2000; D'Amours and Jackson, 2002). While DNA repair through NHEJ and HR has been shown to be defective in Mre11, Rad50, or Xrs2 (Nbs1) mutants in *S. cerevisiae*, such a role has not been firmly established in mammals (D'Amours and Jackson, 2002; Bressan et. al, 1999). Although this debate has not been fully resolved, if the MRN complex does have dual functions in DSB repair by HR and NHEJ, it is likely that ATM is involved as well (Fig. 1-3A).

A stronger case linking ATM directly to DNA repair through HR has also been made that does not necessarily rely on the MRN complex connection. It has been demonstrated that Rad51, a component of the HR repair complex involved in setting up the recombination intermediate, fails to properly localize to the breaksite in ATM mutants (Yuan et. al., 2003; Chen et. al., 1999; Morrison et. al., 2000). However, the question remains, what aspect of ATM function is involved with promoting HR complex formation? ATM dependent phosphorylation events no doubt play some role. For example, ATM can phosphorylate c-Abl, a protein which is thought to interact with Rad51 to promote recombination complex formation (Fig. 1-3A) (Yuan et. al., 2003; Baskaran et. al., 1997; Kastan and Lim, 2000). ATM is also required for phosphorylation of Brca1 (Lee et. al., 2000; Li et. al., 2000), a protein that interacts physically with Rad51 and is important for the HR process (Fig. 1-3A) (Scully et. al., 1997; Gowen et. al., 1998; Moynahan et. al., 1999). Taken together, these results suggest that ATM phosphorylates substrates which are critical components of the HR complex or in the recruitment of the complex to the site of DSBs. However, since ATM has been suggested to have a role in mediating the formation of large protein complexes (Kastan and Lim, 2000; Perry and

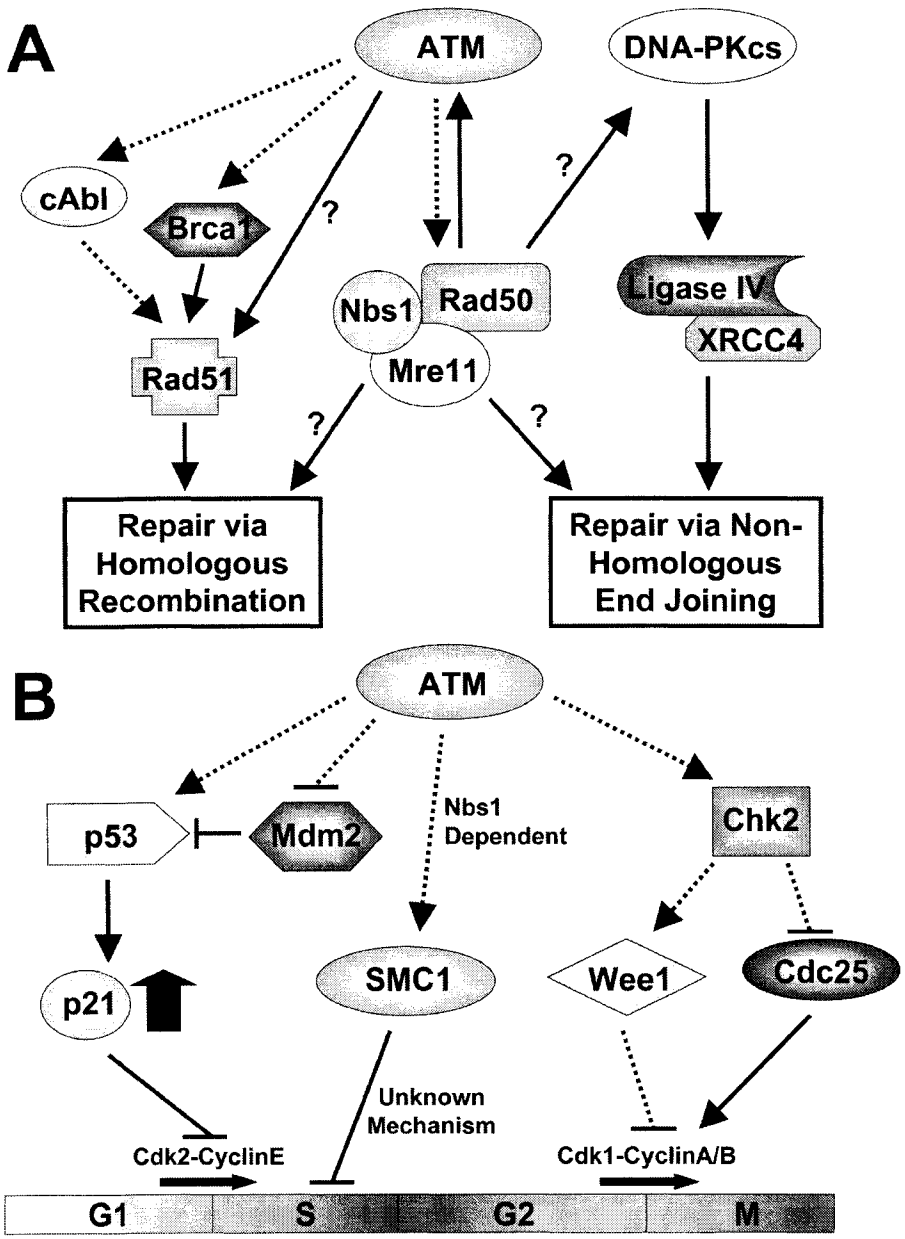

Fig. 1-3 – Known targets of ATM involved in the DSB repair process and cell cycle checkpoints. (A) Traditionally, ATM is thought to activate DNA repair proteins involved in the homologous recombination process, including cAbl and Brca1. Although DNA-PKcs is traditionally thought of as being more important for non-homologous end joining, ATM may also play a role in this process via its interactions with the MRN complex. (B) ATM can also activate numerous targets involved in cell cycle checkpoint responses to DSBs. The G1/S checkpoint is activated by ATM's interactions with p53 and Mdm2. The Intra-S phase checkpoint is not well understood, but seems to involve interactions between ATM and both SMC1 and Nbs1. The G2/M checkpoint is carried out by Chk2 phosphorylation. Dotted arrows indicate known phosphorylation events while solid arrows indicate interaction via other mechanisms. Question marks indicate hypothetical or uncertain connections.

Kleckner, 2003), it is also possible that ATM has a more direct scaffolding role in mediating recombination complex assembly.

In addition to interacting with proteins involved in DNA repair, ATM functions in controlling cell cycle progression when DSBs are present (Abraham, 2001; Kastan and Lim, 2000). Cell cycle regulation in response to DNA damage involves activation of cell cycle checkpoints, including the G1 checkpoint, the intra-S phase checkpoint, and the G2/M checkpoint. These checkpoint pathways have been extensively studied by inducing DSBs by exposure to sources of ionizing radiation (IR). IR treatments causes the creation of highly reactive oxidative radicals that can cause DSBs in chromosomes (Fridovich, 1995). These DSBs then induce these checkpoint responses at different stages of the cell cycle. In the G1 checkpoint response, cells are prevented from exiting G1 phase and beginning DNA replication. Active ATM is thought to trigger the G1 checkpoint by phosphorylating p53 on serine residue 15 (Fig. 1-3B) (Shieh et. al., 1997; Siliciano et. al., 1997; Kastan et. al., 1992; Canman et. al., 1998; Banin et. al., 1998). p53 is a transcription factor normally associated with apoptosis. Although the apoptotic role of p53 may come into play if damage in the cell accumulates, p53 is also implicated in G1 checkpoint responses by transcriptional upregulation of p21, a cell cycle regulator that inhibits the Cdk2-cyclin E complex that is required for entry into S-phase (Fig. 1-3B) (Morgan and Kastan, 1997; Kastan et. al., 1991; Giaccia and Kastan, 1998). ATM has also been shown to phosphorylate other proteins that help regulate p53 function, including a regulator of p53 degradation called Mdm2 (Haupt et. al., 1997; Khosravi et. al., 1999; Maya et. al., 2001), and Chk2, which helps up-regulate p53 activity by phosphorylation of serine residue 20 (Hirao et. al., 2000; Chehab et. al., 2000; Shieh et. al., 2000; Matsuoka et. al., 1998). The G1 checkpoint response to DSBs is further complicated by the observation that the ATM paralog, ATR, can also regulate p53 in response to DSBs, suggesting that there is redundancy within the G1 checkpoint pathway (Tibbetts et. al., 1999).

In the intra-S phase checkpoint response to DSBs, cells are halted during S-phase until damage is repaired. This helps ensure that the DNA damage is not replicated and passed on to the daughter cell. In normal cells, this checkpoint can be induced by exposing cells to IR and inducing DSBs. In ATM deficient cell lines however, cells

continue to replicate their genomes despite IR treatment, a phenotype referred to as radioresistant DNA synthesis (RDS) (Houldsworth and Lavin, 1980). This observation implies that ATM has a critical function in the intra S-phase checkpoint. One current model suggests that ATM regulates the S-phase checkpoint through cooperation with Nbs1, a component of the MRN complex (Falck et. al., 2002; Lim et. al., 2000; Gatei et. al., 2000; Zhao et. al., 2000; Wu et. al., 2000). A current model postulates that Nbs1 is required for the recruitment of ATM to DSB foci where it can phosphorylate many targets (Kitagawa et. al., 2004). One such target is SMC1, a cohesin protein involved in sister chromatid cohesion (Fig. 1-3B) (Kitagawa et. al., 2004; Yazdi et. al., 2002). SMC1 has been shown to play a key role in activation of the intra-S phase checkpoint, although the specifics of this role remain unclear (Fig. 1-3B) (Yazdi et. al., 2002; Kitagawa et. al., 2004). In support of this model is the observation that cell lines deficient for Nbs1 or SMC1 display a radioresistant DNA synthesis phenotype, similar to that seen in ATM deficient cell lines (Shiloh, 1997, Kitagawa et. al., 2004).

The third and final cell cycle checkpoint that is thought to involve ATM is the G2/M or "pre-mitotic" checkpoint, which prevents cells with damaged DNA from entering mitosis. The G2/M checkpoint is thought to involve cooperative regulation between parallel pathways (Fig. 1-4) (Xu et. al., 2002; Beamish and Lavin, 1994; Rudolph and Latt, 1989, Scott et. al., 1994). In one pathway ATM activates the Chk2 kinase, which in turn is thought to regulate cell cycle proteins, including Cdc25 and Wee-like kinases, to regulate the cell cycle (Fig.1-3B, 1-4) (Matsuoka et. al., 2000; Ahn et. al., 2000; Peng et. al., 1997). In the other pathway, ATR is thought to activate Chk1, a paralog of Chk2 that is thought to have a similar role in regulating the same cell cycle proteins (Fig. 1-4) (Liu et. al., 2000; Zhao and Piwnica-Worms, 2001). The dependency on these two parallel pathways seems to vary depending on the cell cycle stage during which DNA damage is induced (Xu et. al., 2002). Cells exposed to IR during G2 phase seem to require ATM in order to induce the checkpoint (Xu et. al., 2002). On the other hand, ATM deficient cells irradiated during S-phase or G1 phase arrest properly, suggesting a role for ATR in inducing the checkpoint in these cells (Xu et. al., 2002; Brown and Baltimore, 2003). Therefore, there appear to be temporal differences in the requirement for ATM in the G2/M checkpoint. The relationship between the ATR and

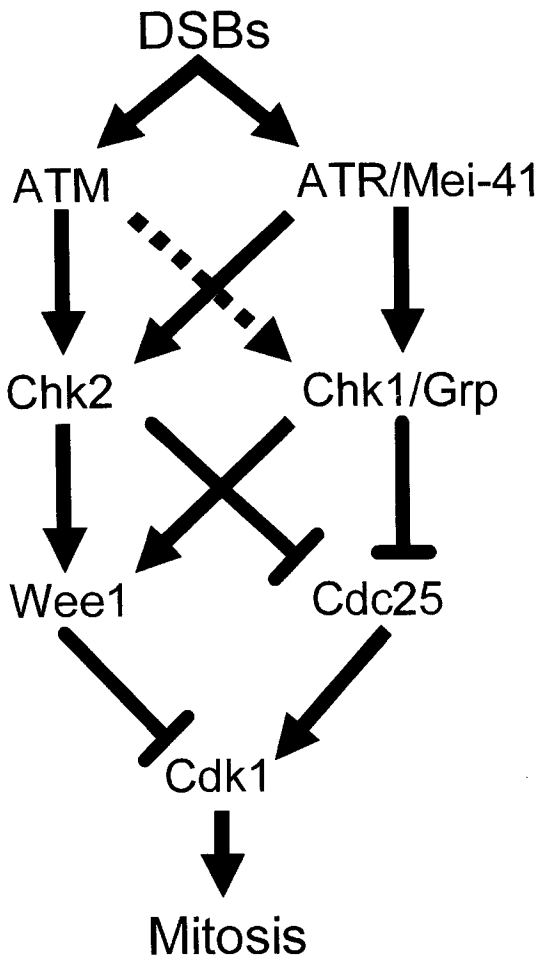

Fig. 1-4 – G2/M checkpoint pathways. In response to DSBs, ATM and ATR kinases are activated and proceed to activate Chk1 and Chk2 kinases by phosphorylation. Although Chk2 is often thought of as a target of ATM and Chk1 is thought of as a target of ATR, there are certain contexts where interactions between ATR and Chk2 have been established. The same may be true of ATM and Chk1 (dotted arrow). When Chk1 and Chk2 are activated, they both act on the same cell cycle regulatory machinery to carry out the G2/M checkpoint. This involves inhibitory phosphorylation of Cdc25, an activator of Cdk1, and a activating phosphorylation of Wee1, an inhibitor of Cdk1. These two events cooperate to downregulate Cdk1 function, which is responsible for driving the cell cycle into mitosis. Thus, checkpoint activation prevents entry into mitosis. Note that in *Drosophila*, ATR and Chk1 are called Mei-41 and Grp, respectively.

ATM pathways is further complicated by the observation that in *Drosophila*, the ATR homolog *mei-41* can regulate Chk2, a "traditional" ATM substrate, in at least two specific developmental contexts (Fig. 1-4) (Abdu et. al., 2002; Xu et. al., 2001; Brodsky et. al., 2000). This suggests that there is likely redundancy between the ATM and ATR pathways and that they are not simply two separate pathways acting in parallel in all contexts.

Section 1.2 - A Drosophila melanogaster *model for* atm

In view of the complexities involved in understanding the role of ATM in different aspects of the response to DNA damage, our laboratory has developed a *Drosophila* model for addressing these issues. A previous graduate student, Elizabeth Silva, performed a forward genetic screen using ethyl methanesulfonate as a mutagen, to isolate mutant alleles of the *Drosophila melanogaster* homolog of *atm*. The goal was to develop a model for ataxia telangiectasia in which *in vivo* and genetic experiments can be easily conducted in a multicellular organism that could help to elucidate some of the uncertainties discussed earlier concerning ATM function. The screen was successful in obtaining eight independent alleles of *atm* (Silva et. al., 2004). Seven of these alleles display non-conditional lethality during the pharate adult stage. The eighth (atm^{8}) is a temperature sensitive conditional lethal. When raised at 25°C, atm^{8} hemizygotes display pupal lethality similar to that seen when each of the other seven alleles are hemizygous. When raised at 22°C, however, the flies are fully viable and display no obvious mutant phenotypes. At 24°C, the viability of the flies is affected, however adult flies can be recovered that exhibit a variety of distinct developmental phenotypes. These include rough eyes caused by disorganization of the ommatidial (Fig. 1-5A and B), notched wings (Fig. 1-5C and D), missing or abnormal bristles, female sterility, and a locomotor defect (Silva et. al., 2004). Pharate adults that are mutant for the other seven alleles, atm^{1}-atm^{7} also exhibit these phenotypes. The locomotor defect was quantified using climbing assays and we determined that although the flies present a severe defect when they initially eclose, the defect does not get progressively worse as flies age (Silva et. al., 2004). This is different from human ATM where progressive neurodegeneration is a hallmark of ataxia telangiectasia. This may simply reflect the fact that when adult flies

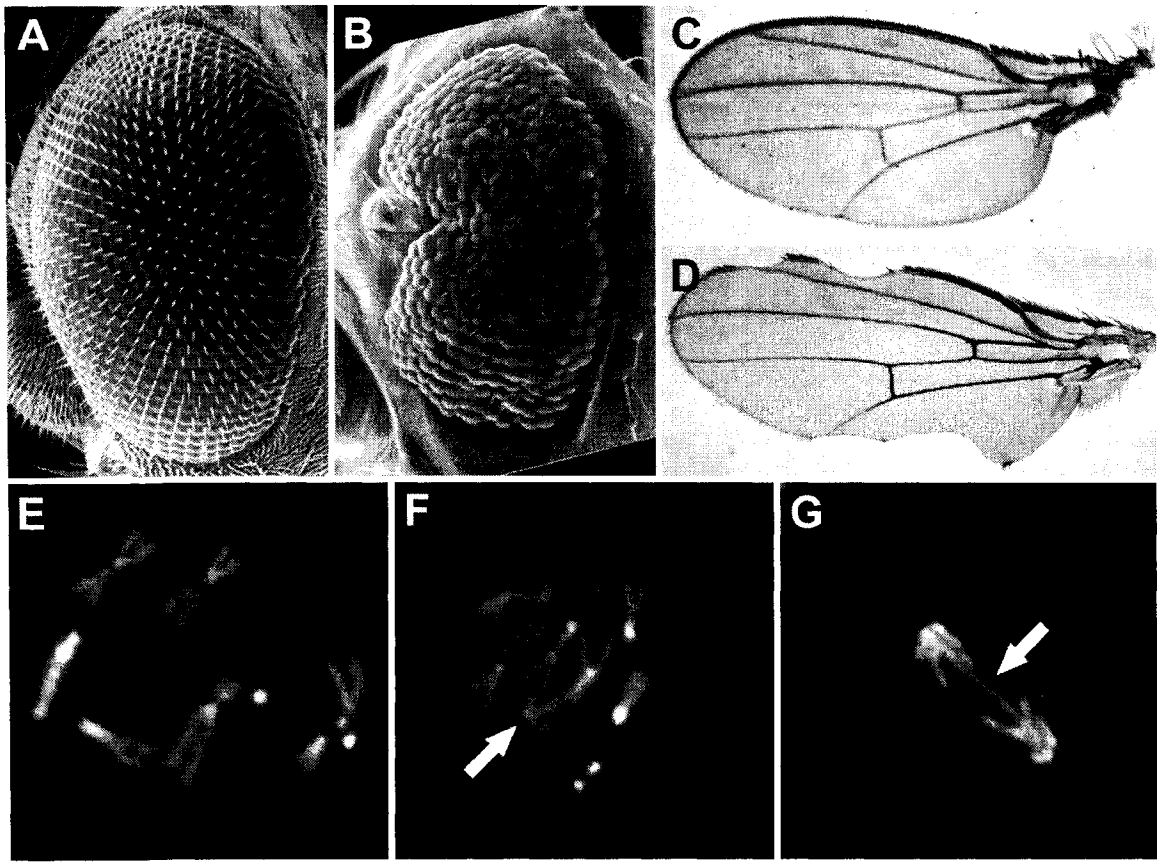

Fig. 1-5 – Previously characterized phenotypes associated with *atm* mutants. (A) In wild type flies, the ommatidia are well organized and arranged in a characteristic pattern. (B) In *atm* mutants, the ommatidia are disorganized and the eye is rough. (C) Wild type wing blades are smooth and intact. (D) *atm* mutant wing blades exhibit notching and gaps. (E) Larval neuroblasts can be squashed and the DNA can be stained with hoechst, allowing individual chromosomes to be seen. Normally, the telomeres of different chromosomes do not associated with one another. (F) In *atm* mutant neuroblasts however, telomere fusion events (white arrow) have been observed at high frequencies. (G) If chromosomes enter mitosis with fused telomere, it can result in the formation of anaphase bridges (white arrow), where chromosomes that are trying to segregate from one another remain connected. This can result in ectopic chromosome breakage.

eclose, all patterning and growth in the brain has been completed, unlike mammals where considerable post-natal brain development occurs. Further examination of our *atm* mutants by collaborators at the University of California, Santa Cruz revealed that *atm* larval neuroblasts exhibit telomere fusions and other major chromosomal aberrations at an extremely high frequency (Fig. 1-5E-G) (Silva et. al., 2004). Such fusions can result in DNA DSBs, when the resulting dicentric chromosomes are captured by opposite spindle poles during mitosis (Fig. 1-5G) (Ahmad and Golic, 1999, McClintock, 1939). These results suggest that *Drosophila* ATM serves an essential function required for the proper maintenance of telomeres. Other groups have gone on to demonstrate that *Drosophila* ATM is required for the localization of two telomeric proteins, HP1 and HOAP, which are thought to be required for capping the telomeres and preventing illegitimate fusions (Bi et. al., 2004; Oikemus et. al., 2004). Despite substantial differences between the structure of *Drosophila* telomeres and those of other eukaryotes, a role for ATM in normal telomere maintenance has also been shown in human tissue culture cells and *Saccharomyces cerevisiae* mutants for Tel1, a homolog of *atm*. Abnormal telomere shortening has been observed in ATM deficient human cell lines (Pandita et. al., 1995; Metcalfe et. al., 1996; Xia et. al., 1996). In *S. cerevisiase*, *Tel1* mutants show a similar phenotype characterized by chromosome loss and telomere shortening (Lustig and Petes, 1986; Greenwell et. al., 1995). A role for ATM in the maintenance of telomeres makes sense since a telomere is a chromosome end, that in that sense resembles a DSB. It is interesting that ATM seems to have contradictory roles in promoting the joining of chromosome ends during DSB repair but preventing the fusion of the natural ends of chromosomes, the telomeres. Mutants also recently became available that affect the *Drosophila* homologs of Rad50 and Mre11, two of the core components of the MRN complex. It is interesting that these mutants have a remarkably similar phenotype to our *atm* mutants, including rough eyes and telomere fusion defects (Ciapponi et. al., 2004; Bi et. al., 2004). In other organisms, MRN and ATM cooperate to activate repair proteins and cell cycle checkpoints in response to DSBs. The similarity between the *rad50*, *mre11*, and *atm* phenotypes suggests that these pathways might also be conserved in *Drosophila*. Furthermore, these results are consistent with a model where Mre11 and Rad50 act together with ATM to ensure the proper maintenance of telomeres.

The purpose of this project was to further characterize the structure and function of *Drosophila* ATM. The first goal was to sequence the eight alleles of *atm* that were isolated from Elizabeth Silva's screen. It was expected that the location and nature of the mutations might provide some clues as to regions of the protein that are important for ATM function. In this regard we have identified several regions of the protein, both within and outside conserved domains, that are critical for ATM function. The second goal of the project was to determine if the cellular phenotypes that are seen in human ATM deficient cell lines also occur in *Drosophila*. This includes sensitivity to IR and the failure to implement cell cycle checkpoints in response to IR. We have demonstrated that, like AT cell lines, ATM mutants are hypersensitive to IR. However, our results suggest that ATM is dispensable for the G2/M checkpoint response 1 hour following the induction of DSBs. Other groups (Song et. al., 2004; Oikemus et. al., 2004) have since demonstrated that there is a requirement for ATM in the G2/M checkpoint response to DSBs, but that this role is confined to the "early" response, 25 min. following DSB induction, a time point that we did not examine.

We have also examined eye development in *atm* mutants to determine if there is a link between known cellular roles for the ATM kinase and the rough eye phenotype and lethality of the whole organism. This project has demonstrated that both the lethality and rough eye phenotype are caused by *p53* dependent apoptosis, implying that p53 activation is not dependent on ATM activity in *Drosophila*. Based on these data, we propose that the apoptosis seen in our *atm* mutants is a response to chromosome breakage induced by telomere fusion events during periods of cell proliferation and argue that DNA DSB repair and telomere maintenance are the core conserved functions of ATM kinases.

The final goal of my project was to examine oogenesis in an attempt to determine why viable *atm* mutant females are sterile. This analysis has revealed that ATM has an essential function in the somatic cells of the ovaries. Furthermore, these studies have demonstrated that ATM is required in germline cells for the timely repair of DSBs during meiotic recombination. Failure to properly repair these developmentally timed DSBs results in the activation of a checkpoint that halts the development of eggs with compromised genomic stability.

Chapter 2: Sequencing of the *atm* alleles

Section 2.1- Introduction

The first aspect of my project was to sequence our eight alleles of *atm*. These alleles were isolated from a screen performed by Elizabeth Silva, a previous grad student in our laboratory. Before this screen, the gene was annotated in the *Drosophila* genome sequence as CG6535. Prior to the availability of the *Drosophila* genome sequence it was incorrectly reported that the *Drosophila* homolog of ATM was *mei-41*, a gene now known to be the ATM-related (ATR) homolog. Our own analysis as well as a more recent publication reported that CG6535 is actually the closest *Drosophila* homolog of ATM, while *mei-41* is the homolog of human ATR (Table 2-1) (Doré et. al., 2004). The degree of homology is most apparent when the conserved regions of the protein are aligned alone. This includes the FAT domain, FATC domain, and the PI(3)K-like kinase domain. The PI(3)K-like kinase domain in particular has a high degree of amino acid identity (57%) between fly and human ATM (Table 2-1). However, the protein is very large (3056 a.a. in humans, 2768 a.a. in *Drosophila*) and the majority of the protein is relatively poorly conserved, with no easily identifiable domains. This raises the question as to what the rest of the protein is doing. Since ATM is reported to interact with many different protein partners, these regions may be involved in specific protein-protein interactions. Consistent with this idea, a series of repeating HEAT domains, which are thought to act as scaffolds for the macromolecular assembly of large protein complexes, have been identified in ATM and other members of the PI(3)K-like superfamily (Fig. 2-1) (Perry and Kleckner, 2003). Each HEAT repeat involves two interlacing anti-parallel alpha-helices separated by a short linker region. The repeats have a flexible consensus sequence that can tolerate a high degree of sequence variability as long as the three-dimensional structure of the repeat remains intact (Perry and Kleckner, 2003). *Drosophila* ATM has been predicted to contain 28 such repeats scattered throughout the non-conserved regions of the protein (Fig. 2-1) (Perry and Kleckner, 2003). Another recent study has also reported that the weakly conserved region of the protein might have specific protein binding responsibilities. It has been demonstrated that amino acids 81-106 of human ATM are important for *in vivo* interactions with Brca1 and p53 as well as being required for ATM localization to DSB foci (Fernandes et. al., 2005). A similar

	Percent Identity Between Proteins			
	Mei-41 / hATR	Mei-41 / hATM	dATM / hATR	dATM / hATM
Amino Terminal Region	**14%**	10%	9%	**14%**
FAT Domain	**24%**	15%	12%	**19%**
PI3K-like Kinase Domain	**53%**	35%	35%	**57%**
FATC Domain	**48%**	42%	41%	**48%**
Whole Protein	**21%**	14%	12%	**21%**

Table 2-1 – *Drosophila* ATM (dATM) and mei-41 are the fly homologs of human ATM (hATM) and ATR (hATR) respectively. Domain locations were identified in the ATR and ATM homologs from *Drosophila* and humans using the NCBI Conserved Domain Search tool (Marchler-Bauer and Bryant, 2004). For each region of the protein, alignments were performed between each of the fly proteins and each of the human proteins using the Clustal W alignment tool (Thompson et. al., 1994; Higgens et. al., 1996). Percent amino acid identity between the two aligned proteins was determined by Clustal W and is displayed here. There is higher degree of amino acid identity between Mei-41 and hATR (bold) than between Mei-41 and hATM. This is true in each of the subregions as well as the entire protein. In the case of dATM there is a higher degree of amino acid identity with hATM (bold) than with hATR.

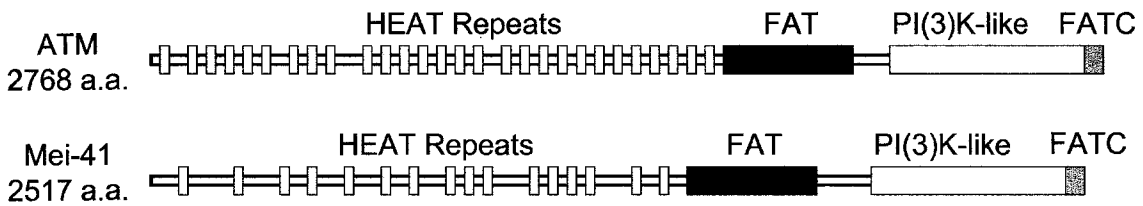

Fig. 2-1 – Protein structures of *Drosophila melanogaster* ATM and Mei-41. ATM and Mei-41 have similar protein structures in that they both contain a FAT domain (black), a PI(3)K-like kinase domain (white), a FATC domain (dark gray), and a series of HEAT repeats (light gray) in the amino terminal half of the protein. *Drosophila* ATM is predicted to have 28 of these HEAT repeats, whereas Mei-41 is predicted to have only 16.

region in *Drosophila* ATM can not be identified based on sequence similarity; however, it is possible that sequences encoding similar structural motifs are maintained that fulfill similar roles, despite these sequence differences. Together, these two studies suggest that the poorly conserved regions of the protein are important for interactions with other proteins.

Although the specific roles of the large non-conserved region of ATM are still unclear, more is known about the functions of the conserved domains of ATM, based on studies of human cell cultures. The FAT and FATC domains are found near the carboxy terminus of the protein, flanking either side of the PI(3)K-like kinase domain (Fig. 2-1). FAT stands for FRAP, ATM, TRRAP, reflecting the super-family of proteins in which this domain is found. FATC stands for FAT Carboxy-terminal, reflecting the presence of the domain at the carboxy terminus of the protein. A critical phosphorylation site is present within the FAT domain at serine residue 1981 (Bakkenist and Kastan, 2003). When inactive, this site is un-phosphorylated and ATM is thought to be present as a dimer. Autophosphorylation of this site promotes dimer disassociation and allows ATM to function. The S1981 residue is not conserved in *Drosophila* ATM, although there are other potential autophosphorylation sites within the FAT domain that could serve an equivalent function (SQ starting at position 1821, TQ starting at 1596 and 1842). The function of the FATC domain is even more poorly understood, however clues have emerged from 3D protein modeling of the related protein DNA-PKcs (DNA protein kinase catalytic subunit), which also contains homologous FAT, PI(3)K-like, and FATC domains (Rivera-Calzada et. al, 2005). When DNA-PKcs binds DNA near the double strand break, the FATC region appears to be involved in stabilizing a conformational change that activates the PI(3)K-kinase domain. 3D modeling of ATM has shown that the FAT, PI(3)K-like, and FATC domains might possess a similar 3D structure to that seen in DNA-PKcs (Llorca et. al., 2003), suggesting that FATC might play a similar regulatory role in modulating ATM kinase activity.

In comparison to the FAT and FATC regions, the role of the kinase domain is better understood. Much of ATM's known activities involve the phosphorylation of a plethora of proteins involved in the DNA damage response. ATM's kinase activity targets the amino acid motifs SQ or TQ and phosphorylates the serine or threonine residue (Kim

et. al., 1999; O'Neill et. al., 2000). The kinase region of the protein seems to be one of the most important regions of the protein. Not only is this domain absolutely required for phosphorylation by ATM, but transfection of AT mutant fibroblasts with the kinase domain alone can partially suppress some of the ATM cellular phenotypes (Morgan et. al., 1997). This includes restoration of IR induced S-phase arrest, lowered radiosensitivity, and reduction of chromosomal instability normally associated with AT cell lines (Morgan et. al., 1997).

The first goal of my project was to sequence the eight alleles of *atm* that Liz Silva isolated in her screen. This presented an opportunity to see if any of the mutations were due to effects on specific domains of the protein. It was hoped that some of the mutations might cause single amino acid changes that affect the function of the protein. This would help us identify essential regions of the protein either within or outside of the conserved domains. Furthermore, sequencing of the *atm* alleles might help explain some unusual features of the alleles. The first of these unusual features was the temperature sensitivity of atm^{8} (first discovered by Stanley Tiong in our laboratory). At 22°C the physical appearance and viability of atm^{8} hemizygotes is approximately wild type. The eyes, wings, and climbing ability all appear normal and the fly is partly fertile. At 24°C the viability of the flies decreases dramatically and the flies that do manage to eclose exhibit the full range of *atm* phenotypes. At 25°C atm^{8} behaves essentially as a null allele in that the hemizygotes are lethal during the pharate adult stage with almost full penetrance. The phenotypes associated with atm^{8} were always examined in hemizygotes since extraneous second site mutations prevents the atm^{8} chromosome from being homozygous viable under any conditions.

Another odd feature of the *atm* alleles that we expected sequencing would shed light on was the observation that atm^{1} through atm^{7} all seem to exhibit variable degrees of antimorphic effects (Silva, 2002). The clearest example of this effect is that when atm^{8} is made transheterozygous with any one of these other, antimorphic alleles, the phenotype at 24°C is worse than seen in atm^{8} hemizygotes with the *Df(3R)PG4* deficiency. This implies that carrying one copy of alleles atm^{1} through atm^{7} is somehow worse than completely lacking a copy of the gene. When these *atm* alleles are heterozygous with a

wild type allele however, there is no obvious dominant negative effect on the expression or function of the wild type copy of *atm*.

The sequencing of the *atm* alleles had two major goals. The first was to determine if the unusual genetic features described above might have a molecular explanation. A single missense mutation was found in atm^{8} that is likely responsible for the temperature sensitive effects on ATM function. The molecular lesions that are associated with the other alleles are all predicted to affect the structure of the encoded protein, although they do not provide any obvious explanation for their antimorphic effects. The second goal of the sequencing project was to analyze the mutations to see if they provide clues as to which regions of the protein are important for function. Many of the mutations are premature stop codons that truncate the protein upstream of the conserved domains at the carboxy terminus. This confirms that these regions are critical for *Drosophila* ATM function, as they are in human ATM. One allele that eliminates ATM function (atm^{4}) was found to have a single amino acid change in a poorly conserved region of the protein. A large portion of this poorly conserved region has been suggested to contain repeating HEAT domains in ATM and other PI(3)K-like family members (Perry and Kleckner, 2003). According to bioinformatic analysis performed by this group (Perry and Kleckner, 2003), the location of the atm^{4} mutation may be part of one of these HEAT repeats. Although this hypothesis has not been tested, the strong *atm* phenotype caused by this allele does suggest that this poorly-conserved region of the protein is very important for some aspect of ATM's function. Another portion of the protein that has been shown here to be important is the FATC domain. The atm^{8} mutation is located within the FATC domain and results in not only a dysfunctional protein but also in the temperature sensitive effect. Together, these atm^{8} and atm^{4} sequencing results have demonstrated that the FATC domain and amino-terminal region, two relatively poorly understood regions of the protein, are critical for the *in vivo* function of *Drosophila* ATM.

Section 2.2- Materials and Methods

Isolation of DNA from *atm* mutants

For each of the eight *atm* alleles, $p^{p}\ atm^{X}\ e$ / *TM6b* flies were crossed to *Ki* p^{p}*Df(3R)PG4* / *TM6b* virgin females. The *PG4* deficiency is a large deficiency which uncovers *atm* and

some nearby genes (none of which have any obvious dominant effects). From these crosses p^p *atm*^{X} *e* / *Ki* p^p*Df(3R)PG4* flies were recovered that were hemizygous for each of the *atm* alleles. These flies were used for DNA isolation and sequencing. Hemizygotes were used instead of homozygotes because the presence of extraneous recessive lethal mutations on the *atm* chromosomes that were likely produced during the genetic screen used to obtain the *atm* mutant alleles. A wild type *atm* allele was also sequenced from p^p*e* flies to control for any variation associated with the genetic background. The p^p*e* stock was initially used in the screen for *atm* and is the most suitable control for DNA polymorphisms that are unrelated to the mutant phenotype.

Because *atm* mutants are lethal during the pharate adult stage, pharate adults had to be dissected from their pupal cases and used for DNA extractions. *atm* hemizygous pupae can be identified based on the absence of the Tb marker present on the *TM6b* balancer chromosome and by the presence of the *atm* rough eye phenotype which can be observed in these pharate adults. One of two protocols were used for DNA extraction. In one, a small scale DNA preparation was performed from 5 pharate adults. Flies were ground up in a 1.5mL centrifuge tube in 200 µl TESS buffer (10mM Tris-Cl, pH 7.5; 60mM EDTA, 0.15mM spermine; 0.15mM spermidine) and then incubated in 400µg/ml proteinase K for 15 minutes at 37°C. Next, 200 µl TES buffer was added (0.2M Tris-Cl, pH 9.0; 30mM EDTA; 2% SDS) and the solution was incubated at 60°C for another 15 minutes. The solution was next extracted with 150µl of 1:1 phenol/chloroform, heated to 65°C, shaken for 2 minutes, and then centrifuged for 4 minutes. The aqueous layer was removed and a similar extraction was performed with chloroform alone. Finally, an Amersham GFX PCR DNA and gel band purification kit was used to remove salts from the DNA. Although this kit is intended to clean up PCR products it worked well for this purpose as well. The preparation produced 90µl of genomic DNA and approximately 1µl was used for each 10µl of PCR reaction. In the second protocol for DNA extraction a Qiagen DNA purification kit was used that is intended for animal tissues (DNeasy Tissue Kit). The manufacturer's protocol was followed when using this kit. From 65 pharate adults 200µl of DNA was recovered and 0.25µl was used per 20µl PCR reaction. The second protocol for DNA isolation provided a much higher concentration of DNA and performed better during subsequent PCR reactions.

PCR Reactions

Because *atm* is a large gene, sequencing required that the genomic region be divided up into fourteen overlapping 900 bp regions. The sequenced region also included ~500 bp upstream and ~2000 bp downstream of the start and stop codons, respectively. In total, the sequenced region spanned 12.3 kb. Each ~900 bp region was amplified with a set of primers that were optimized for annealing temperature using an Eppendorf Gradient Mastercycler PCR machine. These primers were designed by Elizabeth Silva, a previous graduate student in the laboratory. The annealing temperatures used for the different primer pairs are summarized in Appendix A along with the primer names and sequences. In order to get a concentrated solution of amplification product for use in sequencing, two rounds of PCR were performed. In the first round, genomic DNA was used for a template (amount was dependent on the protocol of DNA isolation used, see above). The PCR reaction was run on a 1% agarose gel and the correct band was cut out and purified using the Amersham GFX PCR DNA and gel band purification kit. The recovered PCR product was used as a template for a second PCR reaction with identical conditions, using 2μl of template per 20μl PCR reaction. Following the second reaction, the PCR mix was purified directly, without the use of a gel, using the Amersham GFX PCR DNA and gel band purification kit. The recovered template was assayed for concentration and purity by running 0.5-1μl on a 1% agarose gel. Estimation of concentration was performed by comparison the band's intensity to a standard from the Invitrogen 1 Kb+ DNA ladder. The concentrations of $MgCl_2$, dNTPs, and primers used during PCR reactions was 1.5 mM, 0.2 mM and 0.2 μM respectively and all reactions were carried out using Invitrogen Taq polymerase (0.025 units/ml) and provided buffer. The standard reaction was initial denaturation at 95°C for 3 minutes followed by 25 cycles of denaturation for 1 minute, annealing for 30 seconds (see Appendix A for temperatures), and elongation at 72°C for 1 minute. Following the final cycle there was a final elongation step at 72°C for 5 minutes.

Sequencing Reactions and Alignment

Sequencing reactions were performed using each of the fourteen 900 bp PCR products for all eight alleles of *atm* plus the wild type control. For each region, four separate primers were used for sequencing in order to ensure that the product would be sequenced entirely on both strands. Two of the sequencing primers were the original two used to amplify the region, these primers are located on the ends of the region and were called A and B preceded by the region number (ie "1A" and "1B" for region 1). The other two are embedded within the region, about halfway in, facing outward (one on each strand). These embedded primers were called C and D and were designed by myself using Primer A, an online sequencing program for primer design (Rozen and Skaletsky, 2000). Sequencing mix was as follows: 0.1-0.2 pmol template DNA (approximately 0.1 ng per base pair of template), 0.26 μM primer, 4μl Big Dye sequencing pre-mix (Applied Biosystems), 4μl pre-mix buffer, and autoclaved distilled water up to 20μl. The Big Dye system incorporates fluorescently labeled terminators into the sequencing reaction product. The use of a different label for each type of base allows the reaction product to be run in a single lane of the sequencing gel. The sequencing reaction involved heating to 95°C for 20 seconds, 50°C for 15 seconds, and 60°C for 1 minute, repeated for 25 cycles. Following the reaction, the DNA was precipitated and the salts were removed. 2μl of sodium acetate/EDTA buffer (1.5 M sodium acetate pH > 8.0 and 250 mM EDTA) was added to each reaction to facilitate precipitation followed by 80 μl of 95% ethanol. The solution was vortexed well and then centrifuged for 15 minutes at 12 000 rpm. Supernatant was removed by aspiration and the tube was filled with 70% ethanol. The tubes were then centrifuged briefly before removing the supernatant again. The pellet was dried by placing the tubes, lid open, at 37°C for 2-5 minutes. The dried pellet was sent to the department's Molecular Biology Services Unit (MBSU) where the DNA was resuspended, ran on a gel, and sequenced using a ABI Prism (Model 373) sequencer. Readouts of the sequence were provided in electronic format which were compatible with the software program GeneTool 2.0, as well as chromatogram printouts that showed the peaks of fluorescence used to determine the sequence. GeneTool 2.0 was used to align the sequences from the different alleles of *atm* along with the wild type allele that was sequenced. The chromatogram itself was analyzed to ensure that the sequencing reaction

was clean and that sequence at the beginning and the end of the reactions, where quality had deteriorated, was disregarded. After alignment with GeneTool 2.0, the region was then scanned for any sequence variations within the *atm* alleles compared to the $p^p e$ control sequence. When mutations were found, they were verified by repeating the PCR and sequencing of the region from the start, using a new genomic DNA preparation. This ensured that the mutation was real and not present by chance or because of the poor fidelity of Taq polymerase. Finally, the location of the different mutations were analyzed to determine the location and predicted effects of each identified mutation on the ATM protein.

RT-PCR

In atm^5, a mutation was identified that is predicted to interfere with a splice junction. To determine if this mutation actually affected splicing of the mRNA, RT-PCR was performed. RNA isolation was performed with a Qiagen RNeasy RNA isolation kit according to the manufacturer's protocol. RNA concentration and purity was determined by analyzing a portion of the recovered RNA on a spectrophotometer. Primers were positioned on either side of the affected intron and RT-PCR was performed. These primers were designed using Primer A and are listed in Appendix A. Ideal annealing temperature for the primers was determined and then RT-PCR was performed using a Qiagen One-Step RT-PCR Kit. The reaction mixture was setup as described in the manufacturer's protocol. The RT-PCR reaction involved an initial incubation for 30 minutes at 50°C, allowing for the reverse transcriptase activity. Following this, the reverse transcriptase was deactivated with a 15 minute incubation at 95°C. Next, there was a standard PCR reaction that uses the reverse transcriptase product as the template. This reaction involved denaturation at 94°C for 1 minute, annealing at 62°C for 1 minute, and elongation at 72°C for 1 minute. 30 cycles of this were performed followed by a 10 minute elongation step at 72°C to ensure that all PCR products were fully elongated. The RT-PCR product was run on an agarose gel and analyzed for the presence or absence of the spliced mRNA species.

Section 2.3- Results

The *atm* alleles were sequenced and mutations were found in all eight alleles. The nature of these mutations are summarized in Fig. 2-2A and Table 2-2. The majority of the changes result in premature stop codons, truncating the protein early (Fig. 2-2A, Table 2-2). The atm^5 allele was unique in that it contained two separate mutations. The first was a change in a 5' splice site of intron 21. The mutation would be expected to prevent normal splicing of intron 21, resulting in its inclusion into the mature mRNA sequence. Because intron 21 contains an in-frame stop codon, this change would result in premature truncation of the protein. The second mutation was a single amino acid change in the kinase domain. Although this might normally be expected to affect the protein, it might not have an effect since the splice site mutation, and subsequent protein truncation, is upstream of this mutation. Therefore, the region of the protein containing this change is not expected to be translated. To verify that the first mutation does actually result in altered splicing, RT-PCR was performed on total RNA from atm^5 mutants. Primers were chosen within exons flanking the affected intron (Fig. 2-2B). In wild type flies, both processed and unprocessed RNAs are present. This results in two bands on the gel after RT-PCR, the spliced species (85 b.p.) and the unspliced species (150 b.p.) (Fig. 2-2B and C). In atm^5 mutants however the spliced species (85 b.p.) is absent, supporting our prediction that the splicing out of intron 21 is affected by the 5' splice site mutation (Fig. 2-2B and C).

In addition to mutations leading to premature stop codons, there were two other mutations leading to a single amino acid change in the protein. One was in atm^4, that changed a leucine residue to a histidine. This change was present near the amino terminus, in a relatively poorly conserved region of the protein. To verify that this was the only mutation present, atm^4 was resequenced in its entirety. No other mutations were found, suggesting that this mutation does affect the function of the protein. The other single amino acid change was found in atm^8, the temperature sensitive allele of *atm*. The mutation is present within the FATC domain, in the final amino acid of the protein. The change is expected to change a leucine residue to phenylalanine, a non-conservative amino acid substitution.

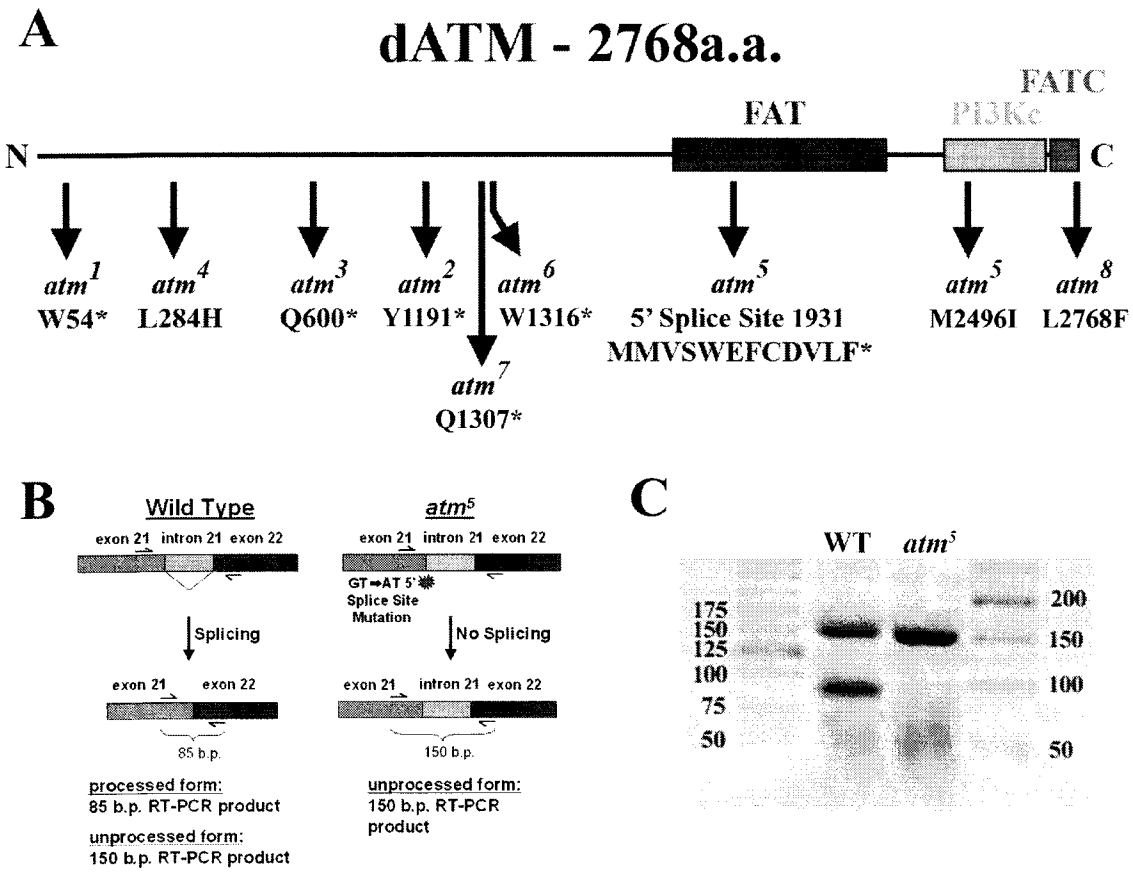

Fig 2-2 – Location of *atm* alleles and RT-PCR strategy. (A) The location and consequences of the mutations in the different *atm* alleles are shown along the 2768 amino acid dATM protein. All eight alleles have mutations predicted to effect protein structure. atm^1, atm^2, atm^3, atm^6, and atm^7 have mutations predicted to result in premature stop codons (indicated with *). atm^4 and atm^8 have missense mutations while atm^5 has two separate mutations, one of which is predicted to result in a splicing defect in intron 17. (B) RT-PCR strategy to test effect of atm^5 mutation of the splicing of intron 17. Position of RT-PCR primers are indicated with arrows. (C) In wild type flies two products are obtained from RT-PCR using total RNA as the template. These products of 85 b.p. and 150 b.p correspond to the spliced and unspliced species respectively. The atm^5 mutant has only a single RT-PCR product of 150 b.p., suggesting that the atm^5 mutation does effect the splicing of intron 17. DNA ladders are shown in the left and right side lanes for a size comparison.

Allele	Codon Change	Type	Genomic Position (b.p.)	Consequence
atm[1]	TGG -> TGA	Transition	162	W -> Opal Stop
atm[2]	TAT -> TAA	Transversion	4297	Y -> Ochre Stop
atm[3]	CAA -> TAA	Transition	2007	Q -> Ochre Stop
atm[4]	CTC -> CAC	Transversion	1074	L -> H
atm[5]	GT -> AT	Transition	6909	Intron 21 Retained, Stop
atm[5]	ATG -> ATA	Transition	8858	M -> I
atm[6]	TGG -> TAG	Transition	4724	W -> Amber Stop
atm[7]	CAG -> TAG	Transition	4696	Q -> Amber Stop
atm[8]	CTT -> TTT	Transition	9850	L -> F

Table 2-2 – Description of mutations in alleles of *atm*. The exact codon change in every mutation is shown, as well as whether the change is a transition (purine > purine or pyrimidine > pyrimidine) or a transversion (purine > pyrimidine or pyrimidine > purine). The genomic position refers to the position of the change in the genomic *atm* region, with the initial A of the start codon being position 1. The consequence refers to the effect of the mutation on the protein structure of ATM.

Section 2.4- Discussion

Section 2.4.1 – Mutations were identified in all eight atm *alleles*

After isolation of our eight alleles of *Drosophila atm*, it was necessary to confirm that the mutant phenotypes we observed were due specifically to a lack of functional ATM, and not an effect on another gene product. To confirm this, an *atm* transgene was used to rescue the mutant phenotype of all eight alleles (Silva et. al., 2004). Next, all eight of our *Drosophila atm* alleles were sequenced to confirm the presence of molecular lesions. Each allele was found to contain at least one sequence variation when compared to the $p^p e$ control sequence, all of which are predicted to affect ATM protein structure through either missense mutations or premature stop codons. Furthermore, most of the mutations are either G->A or C->T transitions, changes which are commonly induced by EMS, the mutagen used during the screen (Table 2-2). Apart from this confirmation that the phenotypes are due to specific mutations in *atm*, the sequencing project had two major goals. The first was to develop a molecular explanation for the abnormal characteristics of the *atm* alleles: namely the apparent antimorphic nature of alleles atm^1 – atm^7 and the temperature sensitivity of atm^8. The second goal was to determine if any of the mutations provide clues as to critical regions of the ATM protein, either within or outside of the conserved regions. Although there are still unresolved issues, the results from the sequencing data do help to address these points (see subsequent sections).

Section 2.4.2 – Five atm *alleles have premature stop codons resulting in truncation prior to the conserved domains of the protein*

Mutations resulting directly in premature stop codons were found in five of the alleles: atm^1, atm^2, atm^3, atm^6, and atm^7. These mutations are all located in the amino-terminal half of the protein. This means that they all truncate ATM prior to the conserved domains that reside in the C-terminal half of the protein. This result confirms the importance of these conserved regions for ATM function, a result which is not surprising since these regions have previously been shown to be critical for human ATM function. Because these five mutations all result in apparent null alleles, this result suggests that the amino terminal part of the *Drosophila* ATM protein has no function by itself and that the FAT, PI(3)K-like, and FATC regions are absolutely required for ATM function.

Section 2.4.3 – atm^4's *single missense mutation suggests an important roll for the non-conserved region of the protein*

In *atm^4* the only mutation is a missense at residue 284 of the protein. This change is predicted to change a leucine to a histidine. This is a non-conservative change since leucine is a relatively small and hydrophobic residue whereas histidine is a large and basic residue. Although this allele has only a single amino acid change in a relatively poorly conserved portion of the protein, the mutant phenotype of *atm^4* hemizygotes is as severe as that seen with any of the premature stop codon mutations. This suggests that the non-conserved region of the protein where the *atm^4* mutation is located serves an essential function. Possible functions that have been proposed for the non-conserved region include forming protein scaffolds and binding to DNA (Perry and Kleckner, 2003; Fernandes et. al., 2005; Llorca et. al., 2003). The role of ATM in the formation of protein scaffolds is thought to involve a series of repeating HEAT domains in the non-conserved N-terminal regions of the protein (Perry and Kleckner, 2003). Such HEAT domains have been found in many different species within several members of the PI(3)K-like family, including ATMs, ATR, and TOR. According to bioinformatics analysis performed by another group (Perry and Kleckner, 2003), the amino acid affected in the *atm^4* mutant is predicted to be within one of these HEAT repeats. Specifically, the last amino acid of the fifth repeat. Although this is circumstantial evidence, it is consistent with the *atm^4* mutation affecting a HEAT repeat. This model would predict that the *atm^4* protein product is non-functional since it is unable to help assemble large protein complexes that are involved in the response to DSBs. Another possible function for this region of the protein is DNA binding. 3D modeling of the ATM protein in humans has suggested that part of the non-conserved region of the protein might form a claw-like structure that can wrap around DNA (Llorca et. al., 2003). If the *atm^4* mutation affects an appropriate part of the protein, this DNA binding function may be compromised. A third possibility is that this mutation affects ATM protein folding. A change from a hydrophobic residue such as leucine to a large and basic histidine might disrupt the proper folding of ATM if this residue is in a appropriate location. Improper folding might result in protein mislocalization, malfunction, and/or degradation. Regardless of the exact mechanism of

effect, this result is interesting because it suggests that the non-conserved region of the protein does indeed have a necessary function. This function is absolutely required for functional ATM since the phenotype of *atm*^{4} hemizygotes is as severe as the null alleles which have large carboxy-terminal truncations.

Section 2.4.4 – atm^{5} *has a 5' splice junction mutation that affects splicing of the mRNA and truncates the protein*

Although *atm*^{5} contained two mutations, only the mutation affecting the splicing of intron 21 is predicted to have an effect. Since the failure to remove this intron results in a premature stop codon, the second missense mutation in the downstream kinase domain would not be expected to result in a change in the portion of the protein that is actually translated. It was confirmed that the first mutation does in fact affect the splicing of intron 21 using RT-PCR (Fig 2-2B and C). It is important to note however that this experiment does not address the possibility of there being different ATM splice isoforms. If *Drosophila atm* has splice variants that do not include the exon 21 - exon 22 region they may be affected by the second downstream mutation. This second mutation is interesting because it is present in the conserved PI(3)K-like kinase domain (Fig. 2-2A). This is known to be a conserved and important region of human ATM. The change specifically changes a methionine residue to an isoleucine. Because this residue is conserved between human, mouse, and *Drosophila* ATM, it may be an important amino acid for the function of the kinase domain. However, in order for this mutation to have an effect on ATM there would have to be splice variants that skip the exon 21 - exon 22 region. The existence of such a splice variant is unlikely since the exon 21 - exon 22 region encodes a portion of the FAT domain, an important region for ATM function and regulation. Although there have been two other splice isoforms identified for human ATM, one is very small and likely non-functional while the other does not skip the FAT domain (ascension numbers NP612150 and NP612149). Therefore, there is no precedent for a splicing pattern that might allow the second mutation in *atm*^{5} to be expressed. The only conclusion that can be made concerning *atm*^{5} at this time is that it likely produces a truncated protein product and behaves as a null. It this regard, it is similar to the other *atm* alleles that produce truncated proteins, *atm*^{1}, *atm*^{2}, *atm*^{3}, *atm*^{6}, and *atm*^{7}.

Section 2.4.5 –antimorphic effects of $atm^1 - atm^7$

One major goal of the sequencing project was to explain why seven of the *atm* alleles demonstrate antimorphic behavior. When each of these antimorphic alleles (*atm*^{1}-*atm*^{7}) are made transheterozygous with *atm*^{8} under temperature conditions permissive for viability, the resulting phenotype is worse then when *atm*^{8} is hemizygous with the *Df(3R)PG4* deficiency. This suggests some sort of dominant interference by the antimorphic alleles that makes the phenotype worse than in mutants lacking a copy of the gene altogether. However, this affect is not severe enough to show a phenotype in flies which are heterozygous for the antimorphic alleles and a wild type allele. Out of the seven antimorphic alleles, six of them encode truncated versions of the protein which eliminate the conserved regions, whereas the seventh (*atm*^{4}) is a missense mutation in the non-conserved amino-terminus. Why would these truncated versions of the protein have a dominant negative effect? One possibility emerges from work suggesting that in human tissue culture cells, inactive ATM forms dimers (Bakkenist and Kastan, 2003). Autophosphorylation events between ATM molecules causes these dimers to disassociate, a requirement for ATM activation. If a truncated version of the protein was still capable of interacting with full length copies of ATM, it might interfere with these autophosphorylation events and subsequent protein activation. With one wild type copy of the protein, the cell might be able to cope with the resulting decrease in ATM activity. However, when in combination with the temperature sensitive allele (*atm*^{8}) this dominant interference would be expected to enhance the mutant phenotypes. This is because ATM function is already partly compromised by the *atm*^{8} mutation and therefore sensitive to further decreases in function. There are problems with this hypothesis. First, some of the *atm* alleles are predicted to produce very short truncated proteins. *atm*^{1} produces a protein only 53 a.a. long, but its antimorphic effect is as potent as that seen for longer truncated proteins such as *atm*^{7} (967 a.a.) and *atm*^{6} (976 a.a.). Unless the first 53 a.a. are sufficient for dimer assembly, this is a strong argument against this explanation. The second problem with this explanation is that it does not provide a simple explanation for why *atm*^{4} behaves as a antimorphic allele, since *atm*^{4} contains a missense mutation instead of a premature stop codon. Perhaps a simpler way to explain the antimorphic effect is that there are second site mutation(s) on the *atm*^{1} - *atm*^{7} chromosomes which enhance the *atm*

phenotype. It is unlikely however, that seven separate alleles would each have obtained a second site enhancer. Alternatively, there might be second site mutation(s) on the *Df(3R)PG4* chromosome which actually partly suppress the atm^8 phenotype and make this an artificial result. No further work has been done to determine whether one of these possibilities, or some other explanation, is correct. However, characterization of the mutations in these alleles is a important piece of information for anyone interested in pursuing this problem further.

Section 2.4.6 –Analysis of the atm^8 *temperature sensitive mutation suggests an important role for the FATC domain*

atm^8 is unique amongst the *atm* alleles in that it is temperature sensitive. When sequenced, atm^8 was shown to have a single missense mutation in the final amino acid of the protein (Fig. 2-2A). This region of the protein corresponds to the FATC domain, which is poorly understood but may play a role in regulating the activity of the kinase domain in response to DNA binding. This idea is based on 3D modeling of the homologous protein DNA-PKcs (Rivera-Calzada et. al., 2005). In this model, the FATC domain is thought to be repositioned when DNA-PKcs binds DNA at double strand breaks (Rivera-Calzada et. al., 2005). The conformational change in FATC is thought to somehow result in the activation of the PI(3)K-like kinase domain. Essentially, this links the binding of DNA to activation of the kinase domain. Although, there are differences between the structures of DNA-PKcs and ATM, the regions corresponding to the FAT, PI(3)K-like, and FATC domains seem to be well conserved with regards to both sequence and protein structure (Llorca et. al., 2003). Therefore, it is possible that FATC plays a similar role in stabilizing a kinase-active form of ATM. This model would require a repositioning of the FATC domain during which it may need to contact other regions of the protein. It is feasible that the missense mutation in atm^8 interferes with these intramolecular interactions and therefore the proper 3D restructuring of the FATC domain. This would in turn affect ATM activation and function of the kinase domain. This model could also explain the temperature sensitivity of atm^8. At lower temperatures, the atm^8 gene product might be able to make these contacts and remain at least partly functional despite the missense mutation. Higher temperatures could make a

thermodynamically unstable interaction less energetically favorable and render the protein non-functional. There are also other ways to explain the temperature sensitivity of atm^{8}. If the FATC domain makes contacts with other proteins, the missense mutation might affect such interactions in a temperature sensitive manner. It is also possible that changing this amino acid results in misfolding of the protein during its synthesis, a process which could conceivable be affected by temperature. Regardless of the exact mechanism for how the atm^{8} mutation affects the activity of ATM, this molecular data demonstrates that changing a single amino acid at the C-terminal end of the FATC domain has a substantial effect on the function of ATM. Based on this observation, we conclude that the FATC region of the protein is of major importance for the *in vivo* function of *Drosophila* ATM.

Chapter 3: *atm* mutants have defects in the cellular response to DSBs and exhibit ectopic apoptosis during eye development

Section 3.1 – Introduction

Section 3.1.1 – Drosophila *genes involved in the cellular response to DSBs*

In humans, ATM is thought to act as a sensor that can transduce information about DNA damage into distinct cellular responses (Kastan and Lim, 2000). These responses include both the activation of proteins involved in DSB repair (Baskaran et. al., 1997; Lee et. al., 2000; Li et. al., 2000) and the activation of cell cycle checkpoints that prevent progression through the cell cycle as long as damage is present (Abraham, 2001; Rudolph and Latt, 1989; Beamish and Lavin, 1994). Because of the critical importance of these regulatory mechanisms, ATM and other proteins involved in the DSB response have been extensively studied in a variety of organisms. A common method used to study the response to DSBs is to expose cells or organisms to a dose of gamma rays or x-rays, two types of ionizing radiation (IR) that induce DSBs in the cell. Following this treatment, the ability of mutants to carry out specific responses to DSBs, such as the recruitment of repair proteins or cell cycle checkpoint activation, can be examined. In *Drosophila*, genes involved in somatic DSB repair have been identified based on the sensitivity of mutants to IR treatments or MMS (methyl methanesulfonate), a chemical which induces DSBs in genomic DNA. Mutations affecting *Drosophila* genes involved directly in repairing DSBs or the recruitment of repair proteins are sensitive to these treatments and therefore show a much greater reduction in survival rates after these treatments, compared with controls. Genes found to be involved in the DSB repair process in *Drosophila* include *mei-41* (Boyd et. al., 1976; Baker et. al., 1978; Hari et. al., 1995; Jaklevic and Su, 2004), *okra* (Ghabrial et. al, 1998; Jaklevic and Su, 2004), *spnA* (Staeva-Vieira et. al., 2003), and *chk2* (Xu et. al., 2001; Brodsky et. al., 2004). *okra* and *spnA* encode homologs of Rad54 and Rad51 respectively (Staeva-Vieira, 2003; Ghabrial et. al, 1998), which are key components of DSB repair by homologous recombination in all organisms studied. In contrast, mutations affecting *Drosophila* genes involved solely in the G2/M checkpoint aspect of the DSB response but not the repair process are not sensitive to IR in terms of survival rates (Jaklevic and Su, 2004). For example, the Chk1 homolog *grp* is involved solely in the G2/M checkpoint response to DSBs, not repair, and

shows no decrease in survival after exposure to IR (Jaklevic and Su, 2004). Collectively, these data suggest that IR sensitivity is indicative of a role in the repair process itself.

In other organisms such as *S. cerevisiae* and humans, ATM homologs have been implicated in the recruitment and activation of DNA repair machinery (Kastan and Lim, 2000). Therefore, we expected that *Drosophila* ATM would also play a role in regulating the DSB repair process. Chk2 is a well documented target of ATM in other organisms, that may also be involved in this mechanism (Matsuoka et. al., 2000). To test this hypothesis we undertook IR-sensitivity experiments with *atm* mutant larvae to determine whether the mutants are sensitive to this treatment, relative to controls. If so, it would be consistent with a role for *Drosophila* ATM in somatic DSB repair similar to that seen in humans, where both ATM deficient cell lines and individuals suffering from ataxia telangiectasia have been shown to be extremely sensitive to IR (Arlett and Priestly, 1985; Taylor et. al., 1975).

Mutants with defective responses to DSBs have been identified in *Drosophila* that affect the G2-M checkpoint, which prevents cells with damaged DNA from entering mitosis before repair is complete. The established method for assaying the G2-M checkpoint response in *Drosophila* is to expose larvae to IR and then to dissect and stain larval wing discs or brains with antibodies to phospho-histone H3 (PH3), a marker of mitotic cells. Normally the wing disc and brain display a large number of PH3-positive foci, that are essentially eliminated following the IR exposure (Hari et. al., 1995; Xu et. al., 2001; Brodsky et. al., 2000). This reflects activation of the G2-M checkpoint that prevents entry into mitosis, by inhibitory phosphorylation of Cdk1 (Su et. al., 2000). In mutants with a defective G2-M checkpoint response, PH3 staining persists despite the presence of DSBs. Genes known to be required for the G2-M IR-induced checkpoint include *mei-41* (Hari et. al., 1995), *chk2* (Xu et. al., 2001), and *grp* (Brodsky et. al., 2000). *grp* encodes a homolog of Chk1, a Chk2 paralog that is traditionally thought of as a target of *mei-41*/ATR (Fogarty et. al., 1997; Brodsky et. al., 2000). Although Chk2 is traditionally thought of as a target of ATM and not Mei-41/ATR, Mei-41/ATR appears to be capable of activating either Grp or Chk2 during the G2/M checkpoint, implying that there is functional redundancy between the ATM/Chk2 and ATR/Chk1 pathways. When active, Grp and Chk2 are assumed to interact with the direct Cdk1 regulatory proteins to

establish the G2-M checkpoint (Xu et. al., 2001; Brodsky et. al., 2000; Hari et. al., 1995). In ATM deficient human cells lines, IR induced G2-M checkpoint responses are abnormal (Scott et. al., 1994; Beamish and Lavin, 1994, Brown and Baltimore, 2003). Therefore, work from human samples has established a precedent for a role for *Drosophila* ATM in the G2-M checkpoint. To examine this hypothesis we have performed irradiation experiments on *atm* mutant wing discs, to test the G2-M checkpoint response. The major goals of this section of the project were to determine whether the DNA repair and checkpoint aspects of the DSB response are compromised in *atm* mutants. One major conclusion from these experiments is that a role for *atm* in the somatic repair of DSBs seems to be conserved in *Drosophila*. Another major conclusion from data presented here is that *Drosophila* ATM is not required for the "late" phase of the G2-M checkpoint response, measured at 1 hour after exposure to IR. However, results from one of our competitors working on ATM suggest that it is required for the "early" phase of the checkpoint response (Song et. al., 2004). These results indicate that temporal differences in requirements for ATM and ATR in the G2-M checkpoint response to DSBs are conserved in *Drosophila*.

Section 3.1.2 – Development of the Drosophila *eye*

One of the defining features of the *Drosophila atm* mutant phenotype is a small, rough eye. A major goal of this section of the project was to analyze eye development, to determine what aspect of ATM's function is important during this process. In *Drosophila* eye development, cell fate determination and patterning occurs during the 3rd larval instar, in the eye-antennal imaginal discs. The anterior portion of the disc is composed of cells that will give rise to the antennae, whereas the posterior end of the disc gives rise to the compound eye, composed of approximately 700 identical ommatidia. During the first and second larval stages the eye portion of the disc proliferates rapidly, to provide the cells required for forming the eye. During the third instar, these cells begin the process of differentiating into the neuronal cells that make up the adult eye. This differentiation process does not happen in all cells simultaneously, but rather accompanies unique developmental events initiated by a cellular constriction called the morphogenic furrow, that sweeps across the disc from posterior to anterior (Fig. 3-1, green wave). In the wake

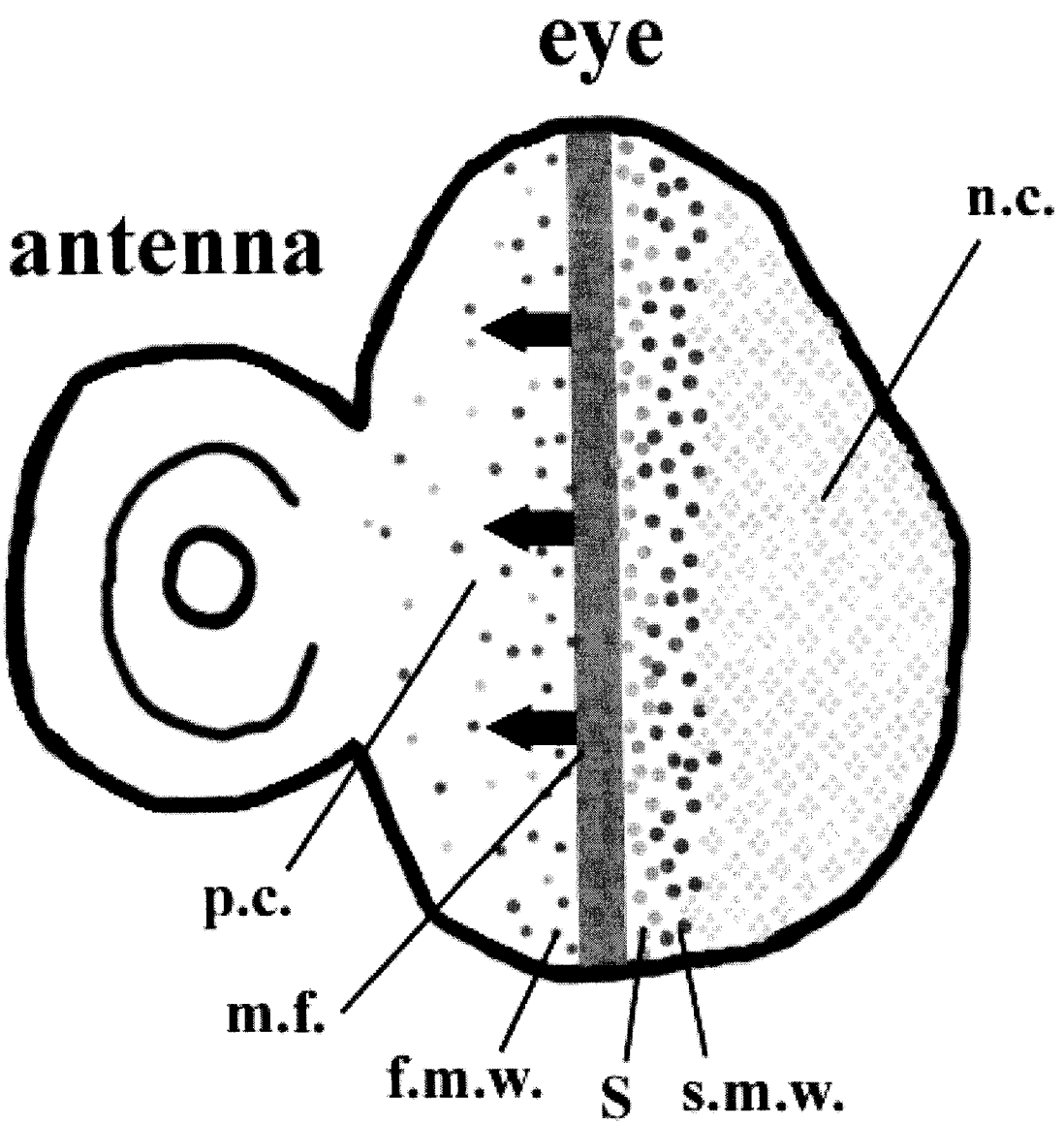

Fig. 3-1 – Development of eye imaginal discs in 3rd instar larvae. During the 3rd instar, the morphogenic furrow (green, m.f.) sweeps across the eye portion of the eye-antennal disc, posterior (right) to anterior (left). Anterior to the morphogenic furrow, the disc is composed of proliferating cells (p.c.) that have independently regulated cell cycles (blue=S-phase, red=mitosis). As cells enter the morphogenic furrow, they become synchronized in G1 phase, a process preceded by a wave of semi-synchronized mitosis referred to as the first mitotic wave (f.m.w.). In the wake of the furrow, cells proceed through a synchronized S-phase (blue cells, S) and mitosis, termed the second mitotic wave (red cells, s.m.w.). Following these synchronized cell cycle events, cells begin to form clusters of ELAV positive neuronal cells (gold cells, n.c.) that will later define individual ommatidia.

of its passage, groups of cells initiate a process of differentiation resulting in formation of clusters of eight distinct neuronal sub-types (R1 to R8) that form the individual rhabdomeres in each ommatidia, in addition to pigment cells and bristle-producing cells (Fig. 3-1). The morphogenic furrow is a physical indentation in the disc that contains cells which have been synchronized in the G1 stage of the cell cycle. This stage is preceded by the first mitotic wave (FMW), a wave of semi-synchronized mitosis that occurs when cells are forced through the cell cycle so they can be synchronized in G1 (Fig. 3-1) (Baker, 2001). Following synchronization in G1, the cells in the morphogenetic furrow enter S-phase and replicate their DNA, followed immediately by a round of mitosis that is termed the second mitotic wave (SMW) (Fig. 3-1) (Baker, 2001). In the wake of the SMW, cells begin to organize into cell clusters, each of which constitutes an ommatidial precursor (Fig.3-1, gold cells) (Wolff and Ready, 1991). The progression of the morphogenic furrow across the disc can be visualized by a variety of staining methods. The physical indentation within the disc can be seen by light microscopy with Nomarski optics. Coordinated cells cycle events such as the synchronized S-phase and mitotic divisions can be visualized by staining with BrdU and PH3 antibodies, as markers of S-phase and mitosis, respectively. BrdU is a nucleotide analog that is incorporated into DNA during DNA replication and therefore can be used to mark S phase cells. PH3 is a phosphorylated histone that is found only during mitosis, allowing anti PH3 antibodies to be used to mark mitotic cells. Cells in the wake of the second mitotic wave can be marked with antibodies to ELAV, a protein expressed in cells which have been specified for neuronal fate, in this developmental context (Robinow and White, 1991). At this point, cell proliferation has ceased and the ommatidial array has begun to form.

The rough eye phenotype of adult *atm* mutants suggest that there may be defects in some aspect of eye development during the 3rd larval instar. The goal of this aspect of the project was to determine the cause of the *atm* rough eye phenotype and establish connections between these developmental defects and the cellular roles of ATM, in DNA repair, checkpoint control and, in hindsight, telomere maintenance. We have determined that the *atm* mutant rough eye phenotype is due to ectopic p53 dependent apoptosis in the proliferating cells of the eye disc, prior to the morphogenic furrow. Although the trigger for this ectopic apoptosis is not known with certainty, our results are consistent with a

model in which genomic instability results from telomere fusion events in *atm* mutants. Such events can result in chromosome bridges and breakage during mitosis, when dicentric chromosomes are captured by opposite spindle poles (McClintock, 1939). These events have previously been shown to act as a trigger for cell death by apoptosis, in *Drosophila* (Ahmad and Golic, 1999).

Section 3.2 – Materials and Methods

Ionizing Radiation Sensitivity Assays

Crosses were setup between p^p atm^8 *e / TM6b* females and *Ki* p^p *Df(3R)PG4 / TM6b* males. The atm^8 allele is temperature sensitive; at 24°C the mutant protein has reduced function, indicated by reduced viability and developmental defects, whereas at 22°C, atm^8 mutants have relatively wild type levels of viability and are developmentally normal. 40 vials of crosses were setup altogether with each containing 5 males and 6 virgin females. Two days after the cross was set up, the flies were transferred into fresh vials. The old vials were moved to room temperatures (22°C). These vials provided the atm^8/Df mutant progeny raised at permissive temperatures that were used for a wild type control. The parent flies were left on the fresh food for another two days, before being removed. This second set of vials was then transferred to 24°C to provide the experimental group (atm^8/Df flies raised at restrictive temperatures). The larvae produced from both sets of these crosses were irradiated during the mid to late third larval instar. This corresponded to day 5 for the larvae grown at 24°C and day 8 for those at 22°C. The vials were divided into nine groups and exposed to different doses of IR. These groups include 1, 2, 3, 4, 5, 6, 8, and 10 Gy treatments, plus one unirradiated control. Each group included four of the vials of larvae from both 24°C and 22°C. Following irradiation the vials were returned to the appropriate temperature and scored after eclosion. If there was no effect on viability, either due to irradiation or the *atm* mutations, the atm^8/Df class would be expected to make up approximately one third of the total progeny. The raw scoring data is presented in Appendix C-1.

G2-M Checkpoint Assays

atm mutant (p^p atm^2 *e / Ki* p^p *Df(3R)PG4*) and control ($p^p e$) larvae were irradiated during the late third instar. *atm* mutant progeny were obtained by crossing p^p atm^2 *e / TM6b* and *Ki* p^p *Df(3R)PG4 / TM6b* flies and selecting non-Tb progeny that lack the TM6b balancer chromosome. Larvae were exposed to 40 Gy of IR. Following irradiation, progeny were left at 25°C for 1 hour prior to dissection. Dissection and staining with PH3 antibodies was then performed as outlined below.

Immunofluorescence

Larvae heads were dissected in PBS (137 mM NaCl, 2.68 mM KCl, 10.14 mM Na_2HPO_4, 1.76 mM KH_2PO_4). The anterior one third of the larvae were dissected, inverted, and teased open to allow fix and antibody solutions to access the imaginal discs. Fixation was performed in 4% Formaldehyde / PBS for 5 minutes, followed by three 5 minute washes with PBS. Discs were permeabilized by incubation in 0.5% triton-X 100 / PBS for 15 minutes. Next, pre-absorption was performed by incubation for 15 minutes in blocking buffer (PBS with normal goat serum and 0.2% triton-X 100). Following this incubation, old solution was removed and the primary antibody was added in fresh blocking buffer. See Appendix B for details on antibodies used and their appropriate dilutions. Incubation with primary antibodies was performed on a shaker overnight at 4°C. Following this incubation, three 5 minute washes were performed with PBS-Tx (PBS, 0.2% triton X-100). Pre-absorption was performed for 15 minutes with blocking buffer followed by a 1-2 hour incubation with the appropriate secondary antibodies on a shaker. All secondary antibodies were used at a 1:1000 dilution in blocking buffer. Secondary antibodies used were Alexa Fluor 488 and 568, purchased from Molecular Probes. Following secondary antibody staining, one last set of three 5 minute washes were performed with PBS. Discs were then removed from the rest of the tissue present in the anterior one third of the larvae and mounted in anti-fade reagent (1 mg/ml 1,4-phenylenediamine, 137 mM NaCl, 2.68 mM KCl, 10.14 mM Na_2HPO_4, 1.76 mM KH_2PO_4 in 90% glycerol). Pictures were taken using confocal microscopy (Leica TCS SP2) or a conventional fluorescent microscope (Zeiss Axioscope 2).

BrdU Staining

BrdU (Bromodeoxyuridine) is a thymidine analog that is incorporated into DNA of proliferating cells, during DNA replication. To mark S-phase cells in imaginal discs using BrdU, dissected larval heads with attached discs were incubated in 75 μg/ml BrdU in PBS for 20 minutes. Fixation was then performed in 5% formaldehyde for 45 minutes. Next, the DNA was denatured to allow antibodies to access the incorporated BrdU in subsequent steps. Denaturing was achieved by treating the tissue with 3M freshly diluted HCl for 30 minutes. Next, three 30 minute washes were done to ensure neutralization of the acid. Antibody staining was then performed to allow visualization of incorporated BrdU. This was done using same procedure described above for immunofluorescence staining.

Construction of *p53 atm* double mutants

p53 and *atm* are both located on the third chromosome, at positions 94D10 and 88E3-4, respectively. In order to make a stock containing both *p53* and *atm* mutations, recombinant chromosomes were generated by meiotic recombination. Because the *p53* gene lies quite close to *ebony* (*e*), which is at position 93C7-D1, recombinants were selected for by the loss of the *ebony* marker from the p^p atm^X *e* chromosome, where "X" refers to the allele designation of the different *atm* alleles used. Potential recombinants were tested for the presence of the *atm* mutation by crossing them to *Ki* p^p *Df(3R)PG4 / TM6b* flies and examining the progeny for the recessive *atm* rough eye phenotype in pharate adults. Because there is no visible phenotype associated with *p53* null mutants, the presence of the *p53* mutation on the same chromosome as the *atm* mutations had to be determined by PCR. The allele of *p53* used was $p53^{5A\text{-}1\text{-}4}$, which contains a 3.3 kb deletion that results in a non-functional protein (Rong et. al., 2002). Primers have been designed by members of Kent Golic's laboratory that selectively amplify a 4 kb product from the $p53^{5A\text{-}1\text{-}4}$ allele and a 7.3 kb product from the wild type allele (Golic, 2002). PCR was performed with these primers to ensure that suspected recombinant chromosomes possessed the $p53^{5A\text{-}1\text{-}4}$ allele (data not shown). Primer details are included in Appendix A. Three recombinant chromosomes were made in this way; p^p atm^1 $p53^{5A\text{-}1\text{-}4}$, p^p atm^2 $p53^{5A\text{-}1\text{-}4}$, and p^p atm^8 $p53^{5A\text{-}1\text{-}4}$. All three chromosomes were balanced with the TM6b

balancer chromosome. However, when working with these lines it is important to recognize that the loss of a functional *p53* from an atm^X chromosome suppresses the lethality associated with *atm* mutations, therefore the *atm p53* double mutant chromosomes are all homozygous viable to some extent.

Fly crosses to examine *p53 atm* double mutant phenotype

To examine the effect of loss of p53 function on *atm* mutant phenotypes, crosses were set up between $p^p\ atm^8\ p53^{5A\text{-}1\text{-}4}$ / TM6b flies and $p^p\ atm^1\ p53^{5A\text{-}1\text{-}4}$ / TM6b or $p^p\ atm^2\ p53^{5A\text{-}1\text{-}4}$ / TM6b flies. These crosses were setup at 24°C, which results in a rough eye phenotype in atm^8 mutants alone. Control crosses to produce *atm/atm* and *atm p53/atm* flies were also setup in parallel, as controls. *atm p53 / atm p53*, *atm p53 / atm*, and *atm / atm* progeny were identified by scoring for the absence of Hu (a dominant marker associated with the TM6b chromosome). Mendelian inheritance predicts that one third of progeny from these crosses should be *atm p53 / atm p53*, *atm p53 / atm*, or *atm / atm*, depending on the specific cross. From day 10 forward, progeny from these crosses were scored every day, so that delays in eclosion associated with the mutant genotypes or an effect on viability could be analyzed. The raw data from these experiments is presented in Appendix C-2. Data showing suppression of the rough eye phenotype in *atm p53 / atm p53* and *atm p53 / atm* flies relative to *atm / atm* flies was analyzed with scanning electron microscopy (see below).

Environmental scanning electron microscopy (ESEM)

ESEM was performed on fly eyes, to visualize the eye phenotypes associated with different genotypes. ESEM allows fly specimens to be examined with high magnification and resolution, without the labor intensive protocols normally associated with scanning electron microscopy. To prepare eyes for ESEM, a series of five incubations in increasing concentrations of ethanol were performed. These incubations began with 20% ethanol and increased in 20% increments to 100% ethanol. Each incubation was performed for 24 hours. Following this treatment, flies can be kept in 100% ethanol at -20°C indefinitely, before being examined with ESEM.

Section 3.3 – Results

Section 3.3.1 – affect of IR on atm *mutants*

In tissue culture of human cells, ATM is important for the "early" G2-M checkpoint response to ionizing radiation (Scott et. al., 1994; Beamish and Lavin, 2004; Brown and Baltimore, 2003). Furthermore, ATM deficient cell lines and individuals with ataxia telangiectasia are extremely sensitive to IR (Arlett and Priestly, 1985; Taylor et. al., 1975). In flies, mutants affecting the ATR kinase encoded by *mei-41* result in a defective G2-M checkpoint response and in sensitivity to IR (Boyd et. al., 1976; Baker et. al., 1978; Hari et. al., 1995). Sensitivity to IR in flies is indicative of a defect in the DNA repair pathway (Jacklevic and Su, 2004). Therefore, *mei-41* seems to be involved in different aspects of the DSB response, including checkpoint activation and the recruitment and/or activation of DNA repair machinery. To determine if *atm* plays similar roles in *Drosophila* DNA damage responses, sensitivity to IR and the G2/M checkpoint response were examined in *atm* mutants. To test sensitivity to IR, atm^{8}/Df flies were exposed to various amounts of IR during the 3rd larval instar. The eclosion rates of the mutant larvae grown at 24°C (restrictive temperature) and 22°C (permissive temperature) were compared to determine if lacking functional *atm* affected the survival rates of the irradiated larvae. For the flies that were kept at 24°C, atm^{8} behaves essentially as a hypomorph, with reduced gene function. In flies raised at 22°C, atm^{8} is sufficiently functional for viability comparable to wild type. At the restrictive temperature (24°C) even the unirradiated atm^{8}/Df class of progeny had reduced survival (Fig. 3-2E). However, with even very small doses of IR that have no effect on controls, the survival rates of atm^{8}/Df flies are dramatically decreased even further, to near zero (Fig. 3-2E). This was true with all irradiated groups, ranging from 1 Gy to 10 Gy. None of these doses affected the survival rates of the atm^{8}/Df flies grown at the permissive temperature of 22°C (Fig. 3-2E). In comparison, previous studies have shown that wild type flies can be irradiated with up to 30 Gy of IR before there is any significant effect on survival rates (Xu et. al., 2001; Baker et. al., 1978). A lower limit was not determined for what dosage *atm* mutants can tolerate. However, these results do indicate that atm^{8} mutants raised at restrictive temperatures are sensitive to IR doses as low as 1 Gy.

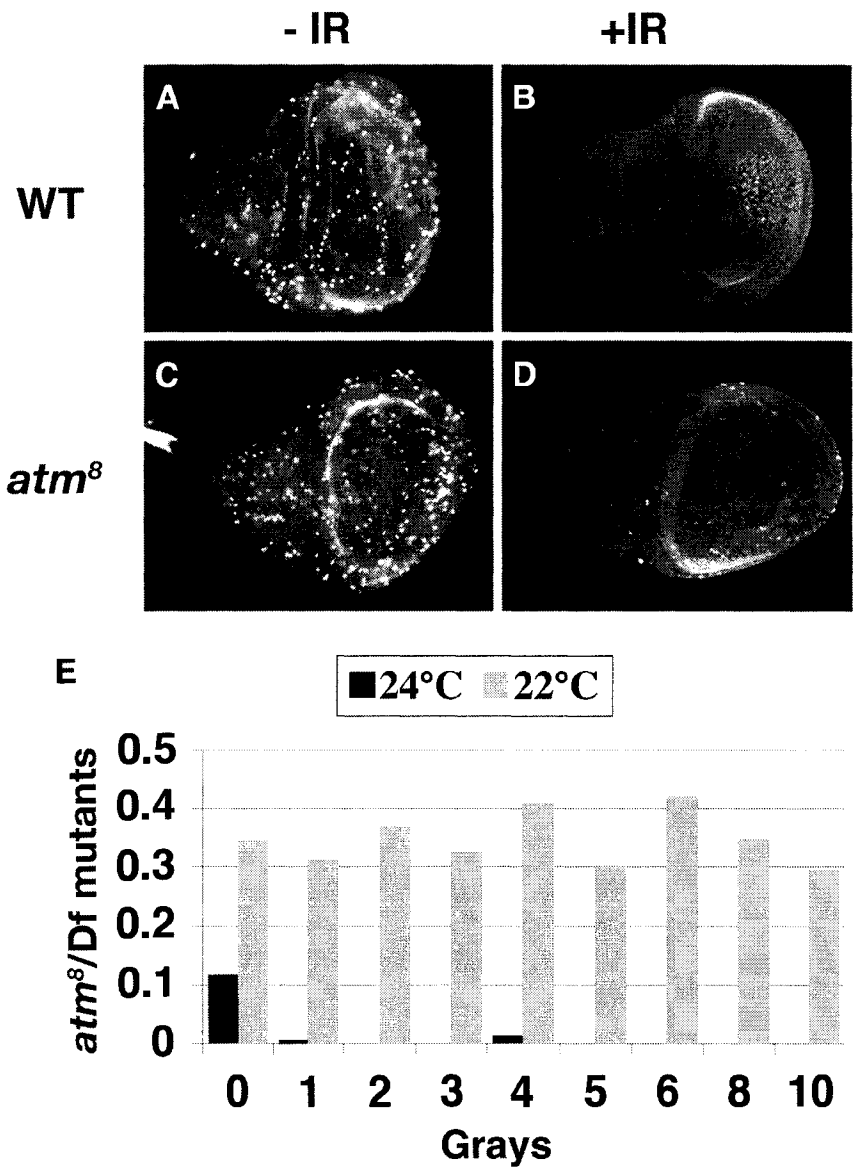

Fig. 3-2 – *atm*^{8} mutants have a functional G2/M checkpoint but are extremely sensitive to ionizing radiaition. (A-D) Third larval instar wing discs stained with antibodies to PH3, a marker of mitotic cells. (A) Unirradiated wild type control disc. (B) Irradiated control disc one hour following exposure to 40 Gy of IR. (C) Unirradiated *atm*^{8}*/Df* mutant disc from larvae raised at restrictive temperatures (24°C or 25°C). (D) Irradiated *atm*^{8}*/Df* mutant disc from larvae raised at restrictive temperatures, one hour following exposure to 40 Gy of IR. (E) Crosses were set up that are predicted to generate hemizygotes in one third of the progeny if not for effect of *atm* mutations on viability. This graph shows the survival frequency of hemizygous *atm*^{8}*/Df* progeny that are raised at either permissive (22°C, grey bars) or restrictive (24°C, black bars) temperatures when exposed to varying doses of ionizing radiation. The data from this figure was presented in a publication (Silva et. al., 2004)

We also examined the fidelity of the G2-M checkpoint response in atm^8 mutants. In this experiment, atm^8/Df and wild type control larvae from the wandering third instar stage were exposed to 40 Gy of IR, sufficient to induce large amounts of DSBs in the cells. After 1 - 4 hours, wing discs were dissected and fixed. PH3 staining was performed to mark the presence of mitotic cells in the wing disc. In wild type discs there are normally many PH3 positive foci throughout the wing disc (Fig. 3-2A). Following irradiation, the G2-M checkpoint is activated and PH3 staining disappears in the controls (Fig. 3-2B). In atm^8/Df mutants there was no discernable effect on checkpoint activation at these time points (Fig. 3-2C and D). PH3 staining disappears in atm^8 mutants following irradiation, as it does in wild type. This suggests that in *Drosophila* ATM is dispensable for checkpoint maintenance, by 1- 4 hours following irradiation.

Section 3.3.2 - atm *mutants exhibit ectopic p53 dependent apoptosis of proliferating eye disc cells*

To investigate the cause of the *atm* mutant rough eye phenotype, eye-antennal imaginal discs from 3rd instar *atm* hemizygous larvae were dissected and examined. Initial experiments were first conducted to determine if the organization or progression of the morphogenic furrow is disrupted. To examine this, eye-antennal discs were dissected and stained with antibodies to PH3 (a mitotic marker) or BrdU (incorporated into S-phase cells). In wild type discs, the morphogenic furrow sweeps across the eye portion of the disc and a series of synchronized cell cycle events occur (Fig. 3-3A and C). The organization of these events results in distinctive PH3 and BrdU staining patterns in the disc (Fig. 3-3A and C). In *atm* mutant discs these patterns appear to be disrupted (Fig. 3-3B and D). Furthermore, the size of the *atm* seems to be abnormally small compared to wild type (Fig. 3-3).

One possible explanation for the abnormal PH3 and BrdU staining patterns in *atm* mutants is that ectopic cell death is occurring in the disc, which prevents proper differentiation or organization of developing ommatidial cells. This would also explain the abnormally small discs we have observed. To determine if there is ectopic cell death in the eye-antennal discs, staining was performed with antibodies to activated caspase-3, which is an established marker for apoptotic cells (Yu et. al., 2002). We observed large

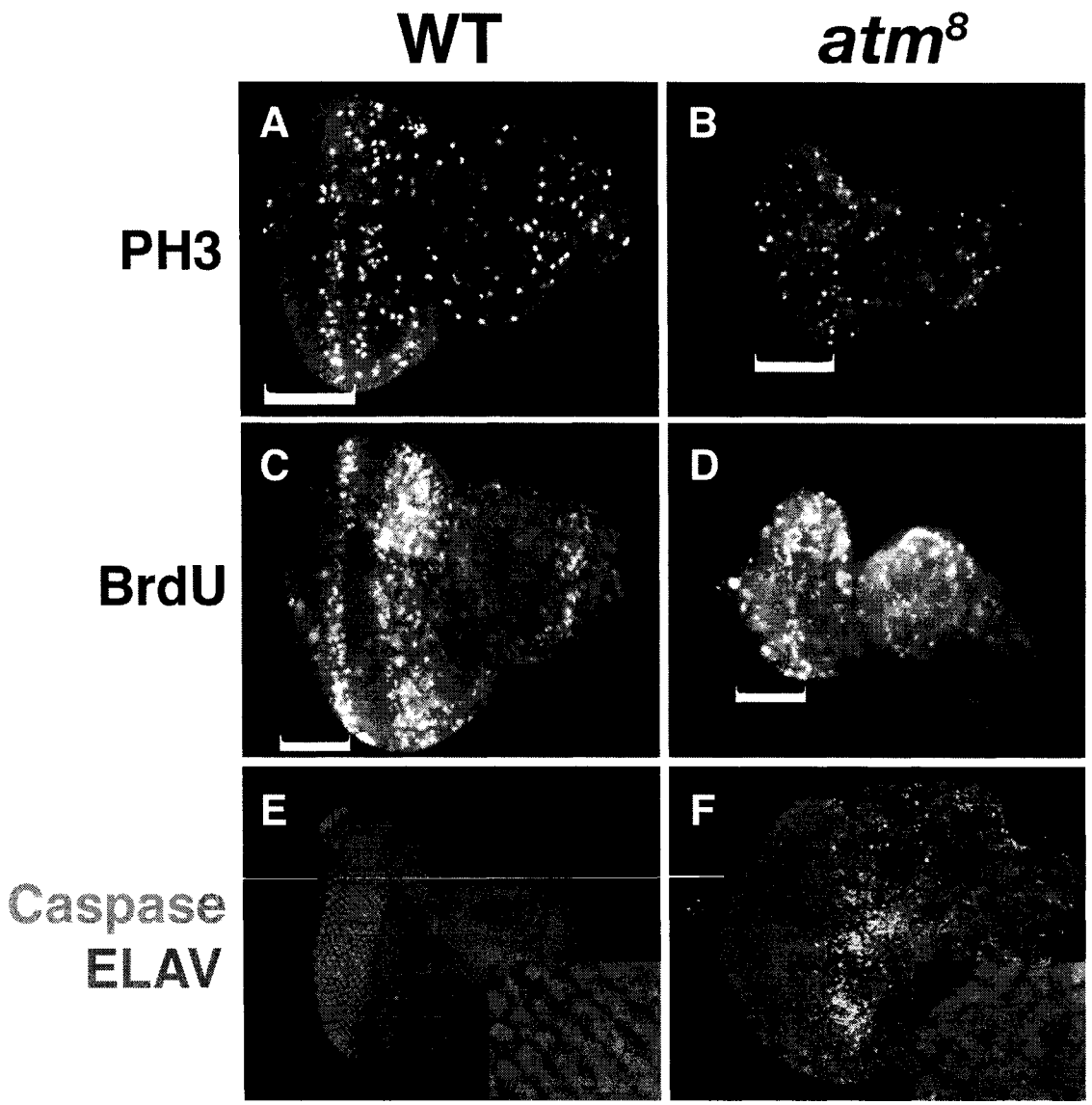

Fig. 3-3 – Eye developmental defects observed in *atm* mutant larvae. (A-D) Staining with antibodies to PH3 and BrdU demonstrates that the progression of the morphogenic furrow is disorganized in atm^{8}/Df mutant eye-antennal discs from larvae raised at restrictive temperatures (24°C or 25°C) (B and D) compared to wild type (A and C). Portion of the discs posterior to the morphogenic furrow are bracketed. (E) Wild type eye-antennal discs stained with antibodies to activated caspase-3, a marker of apoptosis, and ELAV, a marker of differentiated cells. Following the morphogenic furrow ELAV staining visualizes the arrangement cells into clusters of ommatidial precursors (inset). (F) atm^{8}/Df mutant eye antennal discs from larvae raised at restrictive temperatures stained with antibodies to activate caspase-3 and ELAV, demonstrating the apoptosis of cells ahead of the furrow and subsequent disorganization of the ommatidial precursors (inset). The data in this figure was presented in a publication (Silva et. al., 2004)

numbers of caspase-3 positive foci in the *atm* mutants, that were rarely seen in wild type discs (Fig. 3-3E vs. F). This result supported the idea that ectopic apoptosis is occurring in *atm* mutants eye discs. Furthermore, co-staining with antibodies to activated caspase-3 and ELAV (a marker for differentiating neuronal cells) indicated that this apoptosis is largely restricted to ELAV-negative proliferating cells, ahead of the morphogenic furrow (Fig. 3-3F). ELAV positive cells have ceased proliferation and are in the process of differentiating. Since ELAV staining rarely overlaps with caspase-3 staining in the *atm* mutants, these results suggested that only the proliferating cells ahead of the furrow are undergoing ectopic apoptotic cell death (Fig. 3-3F). ELAV staining also revealed that the ommatidial precursor cells that normally form tight clusters following the morphogenic furrow (Fig. 3-3E inset) are obviously disorganized in *atm* mutants (Fig. 3-3F inset). This likely reflects the loss of cells due to apoptosis prior to the furrow, resulting in a insufficient number of cells to properly establish the ommatidial array.

The p53 protein is involved in the induction of apoptosis in *Drosophila* and other eukaryotes (Jin et. al., 2000; Brodsky et. al., 2000; Ollmann et. al., 2000). To determine if the apoptosis we have observed in *atm* mutants involves a p53 dependent process, *p53 atm* double mutants were constructed. If the apoptosis in the eye disc requires p53, we expected that the double mutant would have reduced apoptosis, resulting in suppression of the rough eye phenotype. Adult eyes from atm^{8}/atm^{1}, atm^{8} *p53*/atm^{1}, and atm^{8} *p53*/atm^{1} *p53* flies grown at 24°C were examined with scanning electron microscopy (SEM). In atm^{8} *p53*/atm^{1} flies there is a slight suppression of the rough eye phenotype present in atm^{8}/atm^{1} flies (Fig. 3-4A vs. B). When both copies of *p53* were removed (atm^{8} *p53*/atm^{1} *p53*) the suppression of the rough eye phenotype became more evident, although the eye was still slightly rough (Fig. 3-4C). These observations suggest that ectopic apoptosis observed in *atm* mutant eye discs involves a p53 dependent pathway. The viability of the *p53 atm* double mutants was also investigated. Because these flies were grown at 24°C, atm^{8}/atm^{1} flies have reduced viability relative to controls, as well as delayed eclosion (Fig. 3-4D). atm^{8} *p53*/atm^{1} flies have slightly increased viability compared to atm^{8}/atm^{1} flies (Fig. 3-4D, compare red line with blue line). This suppression was much more evident in atm^{8} *p53*/atm^{1} *p53* flies, which exhibited a dramatic restoration of viability and begin eclosing on day 10, similar to heterozygous

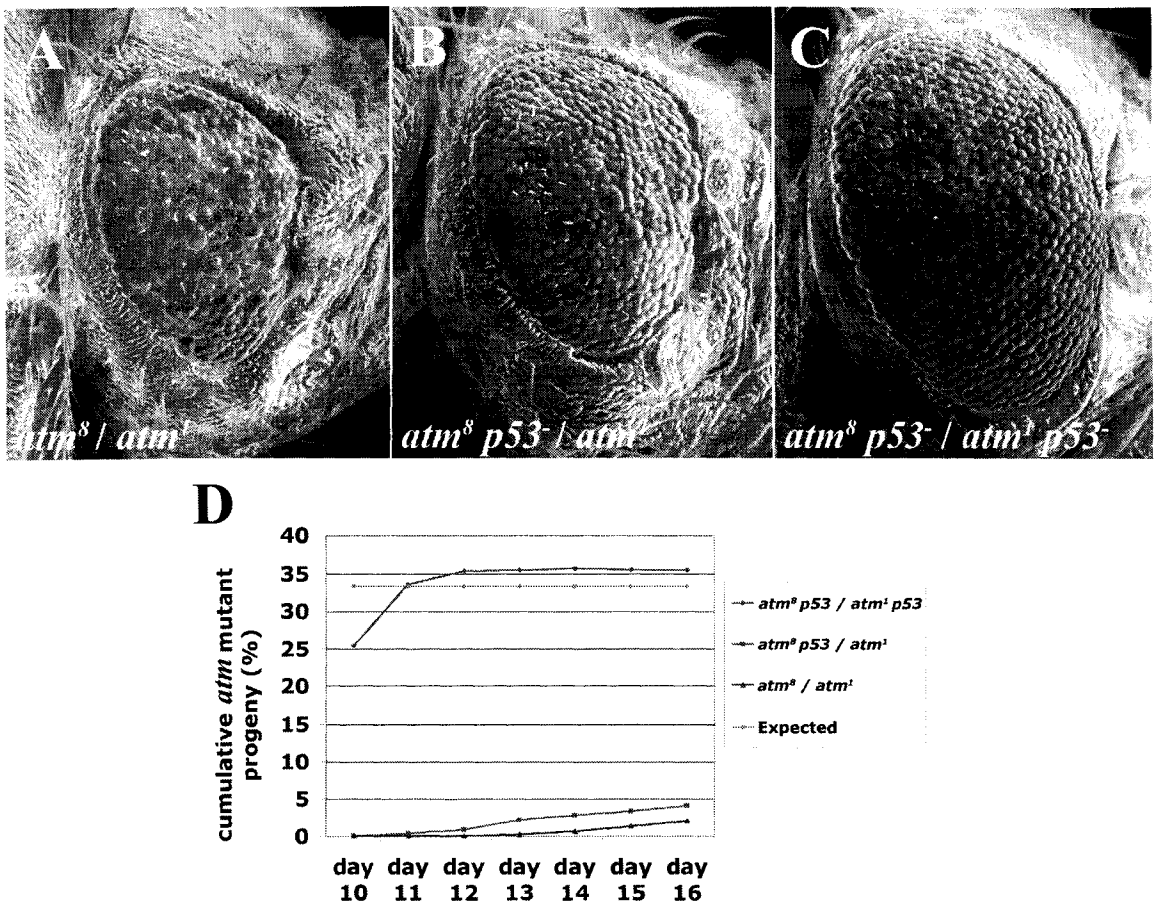

Fig. 3-4 – Removal of *p53* suppresses both the rough eye phenotype and lethality normally associated with mutations in *atm*. (A-C) SEM photographs of eyes from *atm* mutants and *atm p53* double mutants. (A) atm^{8}/atm^{1} rough eye phenotype. (B) atm^{8} *p53* / atm^{1} eye phenotype. (C) atm^{8} *p53* / atm^{1}*p53* eye phenotype. (D) Crosses were setup that are predicted to produce *atm* mutant at a frequency of one third the total progeny. This graph shows the delay and reduced viability normally associated with mutants in *atm* (blue bar) and the suppression observed by removing one copy (red bar) or both copies (purple bar) of *p53*.

controls (Fig. 3-4D, purple line). This result shows that removing both copies of *p53* suppresses the lethality and delayed eclosion aspects of the *atm* phenotype, in addition to suppressing the eye phenotype. These results lead us to conclude that the lethality and rough eye in *atm* mutants are both largely a consequence of p53-dependent apoptosis.

Section 3.4 – Discussion

Section 3.4.1 – Drosophila ATM *plays a role in somatic DSB repair*

We have demonstrated that *Drosophila atm* mutants exhibit an extreme sensitivity to IR. After exposure to as little as 1 Gy of IR, the viability of atm^{8}/Df adult flies raised at 24°C drops significantly. Previous studies by other groups demonstrated that in *Drosophila*, sensitivity to IR is indicative of a defect in the repair of DSBs (Jacklevic and Su, 2004). This link is based on the observations that mutants for genes known to be involved in DSB repair, such as *spnA*, *okr*, *chk2*, and *mei-41,* exhibit reduced viability when exposed to IR (Hari et. al., 1995; Baker et. al., 1978; Boyd et. al., 1976; Ghabrial et. al, 1998; Staeva-Vieira et. al., 2003; Xu et. al., 2001; Brodsky et. al., 2004; Jacklevic and Su, 2004). Mutations affecting genes involved solely in another aspect of the DSB response, such as induction of the G2/M cell cycle checkpoint (*grp* mutants) or apoptosis (*p53* mutants) do not show similar decreases in viability after exposure to IR (Jacklevic and Su, 2004). This suggests that in *Drosophila*, the repair of induced DSBs is critical for survival after IR treatments whereas other aspects of the DNA damage response, such as cell cycle checkpoints or apoptosis induction, are dispensable. These experiments demonstrate that *atm* is required for survival after exposure to IR, a result that is consistent with a role for ATM in the repair of DSBs. This was not unexpected, since in all organisms studied, it has been demonstrated that ATM is involved in the repair of DSBs (Kastan and Lim, 2000, Abraham, 2001).

There are two respects in which our results for *atm* are different from those previously described *Drosophila* DSB repair genes. First, unlike other mutants discovered thus far, *atm* null mutants are lethal, even without exposure to IR. Therefore, this experiment could only be carried out by using the temperature sensitive allele (atm^{8}) at semi-restrictive temperatures (24°C). This aspect of the *atm* phenotype will be discussed later in the Discussion. The second way in which the sensitivity to IR is

different in *atm* mutants, is that the sensitivity is much more extreme. The viability of atm^{8}/Df flies drops off to near zero with only 1 Gy of IR. In other mutants known to be involved in DSB repair the amount of IR needed to reduce viability is much higher. In *chk2* and *mei-41* mutants, for example, a significant decrease in viability is not seen until the mutant larvae are exposed to 10-20 Gy of X-rays (Xu et. al., 2001; Baker et. al., 1978). There are several possible explanations for why *atm* mutants are more sensitive to IR. One is that *Drosophila* ATM might play a key role in coordinating different aspects of the repair of DSBs. Alternatively, other genes implicated in DSB repair thus far may play redundant or dispensable roles in the repair process. Evidence supporting any of these ideas is currently lacking. Another possible explanation for the extreme sensitivity of *atm* mutants is that ATM might play a unique function required for recovery from low doses of IR. Typically in these assays, IR sensitivity is assayed by exposure to very high doses of IR, upwards of 40 Gy. This produces a highly artificial situation where the cells are exposed to more DSBs than they would ever encounter under normal circumstances. Perhaps some of the genes implicated in DSB repair, such as *mei-41*, are required for extensive repair only when there are an exceptionally large number of breaks present. In contrast, *mei-41* is not required for survival after exposure to low doses (1 Gy) of ionizing radiation (Baker et. al., 1978). It could be that at these lower doses, which are closer to physiological conditions, Mei-41 is not needed and/or active and only ATM is involved in activating the repair response. In support of these ideas, in human tissue culture cells there are significant differences in the responses induced by low and high doses of IR (Amundson et. al., 2003). It is possible that in *Drosophila*, similar differences exist in the requirements for survival after exposure to different amounts of IR.

Section 3.4.2 – Drosophila *ATM is dispensable for the late G2-M checkpoint response*

In organisms ranging from yeast to humans, ATM has been implicated in cell cycle checkpoint responses to DSBs (Kastan and Lim, 2000). One such checkpoint is the G2/M checkpoint, which prevents entry into mitosis until the DNA damage has been repaired. In *Drosophila*, the G2/M checkpoint response can be induced by exposing flies to IR. In the wing disc, this checkpoint has been shown to involve *mei-41*, encoding the ATR ortholog, as well as *grp* and *chk2* (Brodsky et. al., 2000; Xu et. al., 2001). Mei-41 is

thought to become activated when DSBs are present and then proceed to activate Grp and Chk2 by phosphorylation (Brodsky et. al., 2000; Xu et. al., 2001). When active, Grp and Chk2 regulate the Cdk1 regulatory mechanism responsible for maintaining the G2/M checkpoint. Because ATM is known to phosphorylate Chk2 during the G2/M checkpoint in mammals (Kastan and Lim, 2000; Abraham, 2001), we examined whether ATM also functions in controlling the G2-M checkpoint in *Drosophila*. We interpreted our results as suggesting that ATM is dispensable for the checkpoint response (Silva et. al, 2004). In these experiments, the checkpoint response was examined one or more hours following IR, therefore we could not make conclusions about requirements for ATM prior to this point. Another group found that ATM does play a role in this checkpoint response (Song et. al., 2004). Although they confirmed our results that ATM is dispensable for the checkpoint response by one hour following irradiation, they also found that ATM is required for the earlier checkpoint response (Song et. al., 2004). This suggests that regulation of the checkpoint response by ATM varies with time. Immediately following irradiation ATM is apparently required to establish the early checkpoint response. However, to maintain this checkpoint response for extended periods of time (i.e. one hour post-IR), ATM is not necessary. During this stage of the response, the G2/M checkpoint is reliant on the Mei-41 kinase (Brodsky et. al., 2000). These temporal differences in the requirement for ATM and ATR in the G2-M checkpoint have precedence in human tissue culture cells (Brown and Baltimore, 2003). If ATM deficient cell lines are irradiated while in G2 phase, they have a defective checkpoint response (Beamish and Lavin, 1994; Rudolph and Latt, 1989, Scott et. al., 1994). However, if the same cells are irradiated in G1 or S-phase, there is an intact, and in fact prolonged, G2 arrest (Scott et. al., 1994). This means that if you examined the cells soon after irradiation there would be a defective checkpoint, since the ATM deficient cells that were in G2 during irradiation do not have ATM to halt the cell cycle and will proceed into mitosis shortly after irradiation. However, the later checkpoint response is still intact, since the cells irradiated in G1 or S-phase will be arrested once they make it to G2 phase in a ATM-independent fashion. These conclusions were corroborated by direct comparisons of ATM and ATR-dependent checkpoint responses, as a function of time (Brown and Baltimore, 2003). Other data supporting the idea that ATR is responsible for late checkpoint responses involve

observations that ATR phosphorylates Chk1 following irradiation, and Chk1 is required for the G2-M checkpoint response (Liu et. al., 2000). These data, as well as in studies in *Drosophila* (Oikemus et. al., 2004; Song et. al., 2004), are consistent with a model in which the cell cycle stage of cells exposed to irradiation determines specific requirements for activation of specific checkpoint mechanisms. According to this model, we predict that cells irradiated in G2 phase of the cell cycle require ATM activity for G2-M checkpoint regulation but that cells in G1 or S-phase at the time of irradiation would only require ATR (Mei-41).

Section 3.4.3 – The rough eye phenotype and lethality associated with Drosophila atm *mutations are caused by p53-dependent apoptosis in the proliferating eye disc*

The results presented here have demonstrated that *atm* mutant eye-antennal discs exhibit significant levels of ectopic apoptosis. This apoptosis primarily affects proliferating cells, before the morphogenic furrow. It is likely that this apoptosis is directly responsible for the rough eye phenotype, consistent with previous studies showing that inducing ectopic apoptosis in the eye-disc results in a rough eye phenotype (Jin et. al., 2000). This work has also demonstrated that the observed apoptosis in *atm* mutants is dependent on *p53*, since removing both copies of *p53* suppresses the *atm* rough eye phenotype. This explanation raises another question: what is the trigger for this apoptosis? An attractive model has emerged from work done on *atm* mutants by our collaborators at the University of California, Santa Cruz and by 3 other groups working on this problem. They have all noted that *atm* mutant neuroblasts exhibit extraordinarily high rates of spontaneous telomere fusions and other major chromosome re-arrangements (Silva et. al., 2004; Song et. al., 2004; Bi et. al., 2004; Oikemus et. al., 2004). A role for *Drosophila* ATM in telomere maintenance makes sense since a telomere is a chromosome end, which is essentially a type of DSB. ATM seems to have a role in recognizing chromosome ends as being different from normal DSBs, and preventing ectopic repair mechanisms and subsequent telomere fusion. If telomeres are not properly protected and fuse, dicentric chromosomes will be created that can result cause chromosome bridges during mitosis, when the kinetochores are captured by opposite spindle poles. This can then result in random breakage along the dicentric chromosome,

producing a DSB (Ahmad and Golic, 1999, McClintock, 1939). Since these breakage events are apparently quite common in *atm* mutants (Bi et. al., 2004), these observations suggest that the number of DSBs in these cells is much higher than would normally be encountered due to other processes or spontaneous DSBs formation. The most direct interpretation of our results is that DSBs formed in this manner in *atm* mutants are triggering apoptosis, in a *p53* dependent fashion. Consistent with this conclusion, p53 has previously been implicated in the induction of apoptosis in response to DSBs in *Drosophila* (Peters et. al., 2002; Brodsky et. al., 2000; Ollmann et. al., 2000; Jin et. al., 2000). Furthermore, the induction of a single telomere fusion event and subsequent breakage has been shown to be sufficient to induce apoptosis in cells of the *Drosophila* eye disc (Ahmad and Golic, 1999), implying that *Drosophila* eye cells are exquisitely sensitive to even small amounts of chromosome breakage. In mice and humans, *p53* dependent apoptosis in response to DSBs is thought to require ATM (Kastan et. al., 1992; Lu and Lane, 1993; Khanna and Lavin, 1993; Xu and Baltimore, 1996; Barlow et. al., 1996). Our data demonstrating that p53-dependent apoptosis occurs in *atm* mutants indicates that the fly *atm* model differs in this regard .

Recent reports of *Drosophila* mutants for *mre11* and *rad50* also describe a rough eye phenotype and telomere fusion defects similar to *atm* mutant phenotypes (Bi et. al., 2004; Ciapponi et. al., 2004, Oikemus et. al., 2004). In humans, Mre11 and Rad50 have been suggested to interact with ATM during the activation of DNA repair proteins (Kastan and Lim, 2000). The presence of telomere fusions in *Drosophila atm, mre11* and *rad50* mutants suggests that these genes may be cooperating in *Drosophila* to maintain telomeres, in addition to their roles in DNA DSB repair. One current model proposes that ATM, Mre11, and Rad50 are involved in recognizing chromosome ends as being telomeres, and not simply DSBs, and are required for the localization of telomere specific "capping" proteins, such as HP1 and HOAP, which prevent ectopic telomere fusions (Bi et. al., 2004; Oikemus et. al., 2004). These data are also consistent with the model that telomere fusion and subsequent chromosome breakage during mitosis are the most proximate trigger for apoptosis in developing *atm* mutant eye cells. This model also provides an explanation for our observation that it is primarily proliferating cells that undergo spontaneous apoptosis in the *atm* mutants.

Another question that these experiments raise is what the sensor for spontaneous DSBs is in an *atm* mutant. Mei-41 would be a obvious candidate, however we have excluded this possibility based on the observation that *mei-41; atm* double mutants still exhibit elevated levels of spontaneous apoptosis in the eye discs (Tiong S., unpublished result). This result suggests that other proteins may be involved in the detection of broken chromosomes and the activation of the apoptotic response in this situation. There are currently no obvious candidates for what these proteins might be.

Analysis of the *atm p53* double mutants has also revealed that the lethality of *atm* mutants is dramatically suppressed by removing *p53*. Furthermore, while the eclosion of *atm* mutants is normally delayed by several days, *atm p53* double mutants eclose normally, ten days after egg laying. This suggests that whatever is killing the *atm* mutants is also dependent on an apoptotic pathway that requires *p53*. Although this result was not explored further, it does provide clues as to what might be causing the delay in eclosion or death of *atm* flies. It has been demonstrated that ectopic apoptosis in imaginal discs induces compensatory proliferation in surrounding cells (Huh et. al., 2004; Ryoo et. al., 2004). Furthermore, eclosion is regulated by hormonal mechanisms (Ashburner, 1989) that have been suggested to be sensitive to excessive proliferation in the larval discs and brain (Abbott and Natzle, 1992). Since *atm* mutants have ectopic apoptosis in the eye disc, there may be compensatory proliferation which is inhibiting eclosion. Because the apoptosis exceeds cell proliferation in these mutants, the discs are small, since they can not replenish the dying cells. Therefore, it can take extended periods of time for the *atm* mutants to eclose and if they do eclose they exhibit a rough eye phenotype, a consequence of defects during eye differentiation likely resulting from previous loss of cells. In *p53 atm* double mutants this apoptosis is prevented, allowing flies to develop and eclose in a timely fashion.

It is very interesting that removing *p53* also suppresses lethality in *atm* mutants. This may be due to *p53* dependent apoptosis in a vital tissue, such as the brain, in *atm* mutants. The brain makes a tempting candidate tissue given that we have already observed apoptosis in the eye disc and both the brain and eye are neural tissues. Furthermore, we have observed telomere fusion and breakage in the *atm* larval brain (Silva et. al., 2004) which could be a trigger for apoptosis. The atm^{8}/Df adults that were

raised at 24°C also display climbing defects, suggesting that there may also be defects in the pharate adult / adult brain that could conceivably be caused by apoptosis (Silva et. al., 2004). It is also possible that the delay in eclosion results in death of the *atm* mutant pharate adults. If constant proliferation in the pharate adult inhibits eclosion for too long, the pharate adult may simply die in the pupal case. Consistent with this idea is our observation that *atm* mutants tend to die during the pharate adult stage.

Regardless of the exact mechanism for the lethality, these experiments have clearly demonstrated that in addition to suppressing apoptosis in the eye, removing *p53* can suppress the delay and lethality associated with *atm* mutations. This suggests that *p53* dependent apoptosis is likely responsible for the delay and death of *atm* mutants. These results are consistent with a model that links a known cellular role of *Drosophila* ATM (telomere maintenance) to several aspects of the *atm* phenotype including the rough eye, wing notching, eclosion delay, and lethality.

Chapter 4 : *Drosophila atm* is required for follicle cell survival during oogenesis and for double strand break repair during meiotic recombination

Section 4.1 – Introduction

Drosophila females have two ovaries, each of which is composed of about 16 ovarioles. Each ovariole consists of two regions, the germarium and the vitellarium (Fig. 4-1B). Within the germarium there are two populations of stem cells which give rise to the somatic and germline components of the egg chambers, respectively. These stem cells give rise to cells that divide mitotically to form cysts of germline cells. When the cysts have formed, they bud off from the germarium to form egg chambers. The vitellarium is composed of a chain of these egg chambers, which develop into maturity as they move towards the posterior end of the ovariole (Fig. 4-1B).

The germarium is subdivided into three regions (Fig. 4-1A). Region 1 is the anterior end of the germarium, where the germline stem cells are located. The germline stem cells divide asymmetrically to give rise to a new stem cell and a cystoblast. The cystoblast then undergoes exactly four synchronous divisions to produce 16 cell cysts (Fig. 4-1A). The 16 cells remain interconnected because of a specialized incomplete cytokinesis that leaves a structure called a ring canal between two dividing cells. Later in oogenesis these ring canals will provide a channel through which RNAs and proteins can be shuttled from the nurse cells into the developing oocyte.

The middle of the germarium is termed region 2 and is subdivided into region 2a and region 2b (Fig. 4-1A). It is in this region that somatically derived follicle cells divide and envelope the cysts and where the process of meiotic recombination occurs. Also in region 2, one of the 16 cyst cells is specified as the oocyte. The other 15 cells are destined to become nurse cells which will eventually endoreplicate their genomes and mass produce RNAs and proteins which will be pumped into the oocyte for use during early embryogenesis. In region 2b the oocyte can be identified based on Orb immunofluorescence (Fig. 4-1A, Orb marked as blue) (Lantz et. al., 1992). Orb is an RNA binding protein required for establishing egg polarity and oocyte differentiation (Lantz et. al., 1992; Lantz et. al., 1994) In region 2a, Orb staining can be seen in all cells of the cyst (Fig. 4-1A). However, by region 2b the amount of Orb protein has decreased in the pro-nurse cells and is selectively enriched in the oocyte (Fig. 4-1A).

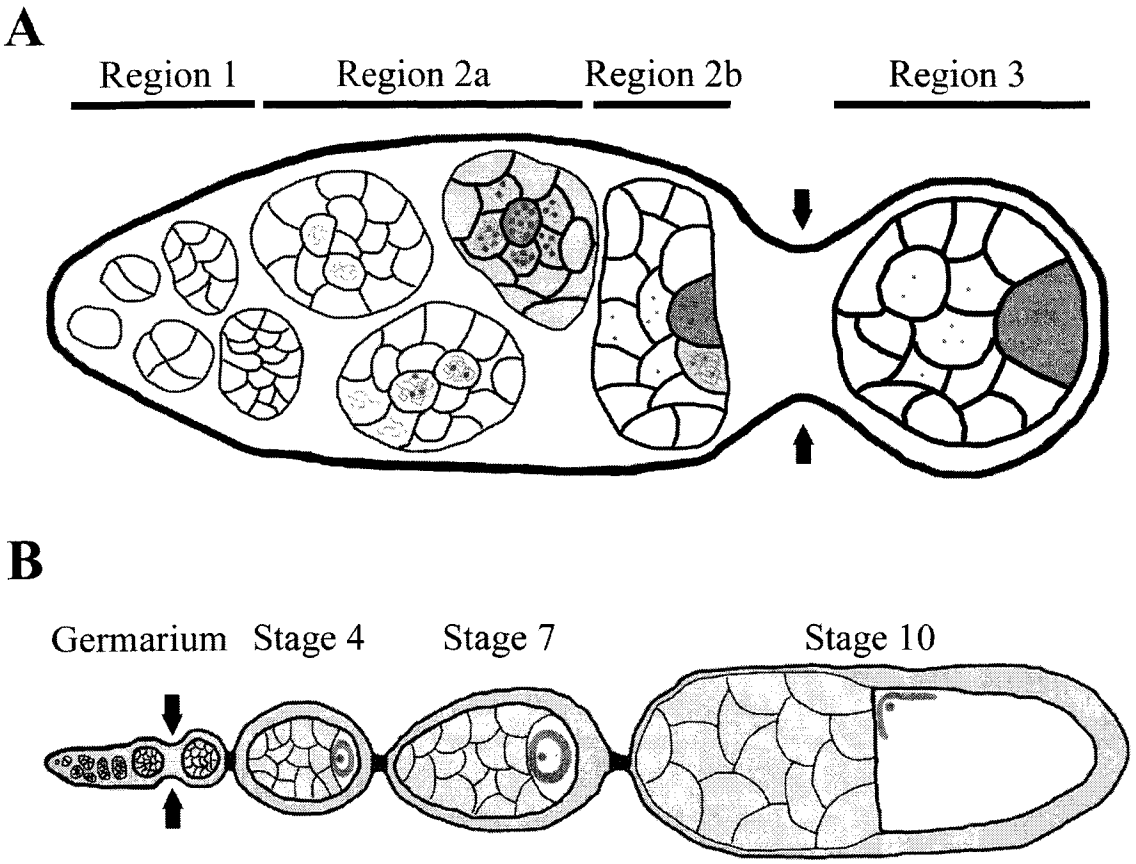

Fig. 4-1 – Oogenesis in *Drosophila melanogaster*. (A) In region 1 of the germarium, a single cystoblast divides four times to give rise to a 16 cell cyst. Within region 2a, the process of meiotic recombination will begin in the oocyte and a subset of nurse cells, marked by formation of the synaptonemal complex (S.C., green). Following formation of the S.C., DNA DSBs are induced by the *mei-W68* gene product in the oocyte and some nurse cells (red foci). Also in region 2a, the oocyte marker Orb appears, first in all germline cells, then selectively enriched within the oocyte (blue). In region 2b, the induced breaks are rapidly repaired. Within the oocyte, a subset of these breaks can be repaired in such a way as to allow crossing over. In region 3, the cyst becomes rounded as it is surrounded by follicle cells. As follicle cells surround the cyst, they pinch inwards and cause the cyst to begin budding off (black arrows) from the germarium, thus forming an egg chamber. (B) Following budding (black arrows), egg chambers are formed, composed of an oocyte (white), 15 nurse cells (gold), and a layer of follicle cells (light blue). Egg chambers form a chain, connected to one another by specialized follicle cells termed stalk cells (dark blue). As new egg chambers are made, older egg chambers move down the ovariole and develop. In stage 4 of oogenesis, the oocyte nucleus forms the karyosome (red), which is surrounded by Grk protein (green). By stage 10, the karyosome has repositioned itself to the dorsal anterior corner of the oocyte. At this point, Grk is also re-localized to a patch on the dorsal anterior side of the karyosome, adjacent to the nearby follicle cells. Communication between the oocyte and the adjacent follicle cells, via Grk, are critical for establishing egg polarities.

Early in region 2a, two of the cyst cells will begin to form synaptonemal complexes (Fig. 4-1A, SC marked with green) (Page and Hawley, 2001). These two cells are referred to as pro-oocytes since one of them will go on to become the true oocyte while the other will revert to a nurse cell. The synaptonemal complex (SC) is a proteinacious structure which forms between homologous chromosomes and causes them to associate tightly along their entire length (Walker and Hawley, 2000; Page and Hawley, 2001; von Wettstein et. al., 1984). This is an important first step in homologous recombination in *Drosophila* (Page and Hawley, 2001). The next step in the recombination process occurs later in region 2a, with the production of DNA double strand breaks (DSBs) (Fig. 4-1A, DSBs marked with red) (Jang et. al., 2003; McKim et. al., 2002). It is important to note that even in cells destined to become nurse cells (pro-nurse cells at this point) the SC structure begins to form between homologous chromosomes and DSBs are made, although this occurs later in the pro-nurse cells than in the two pro-oocytes (Fig. 4-1A) (Carpenter, 1994; Liu et. al., 2002; McKim et. al. 2002). Although this step constitutes the beginning of meiotic recombination, all cells except the oocyte will abort this process before it is complete and the DSBs will be repaired. Only in the true oocyte can the DSBs repaired in such as way as to result in cross-over events (McKim et. al., 2002).

The repair of DSBs occurs in region 2b of the germarium (Fig. 4-1A) (Jang et. al., 2003, McKim, 2002). The pro-oocyte destined to become the oocyte will induce crossing-over at certain DSBs present along the chromosome. Not all DSBs are repaired in such a way as to allow crossing-over. Although the distribution of DSBs is thought to be random, the distribution of cross-over sites is not, owing to the existence of "hotspots" where cross-overs are more frequent (McKim et. al., 2002). A specialized DSB repair pathway is used at recombination sites that results in crossing-over between the paired homologs. The remaining DSBs are repaired through a process called gene conversion that does not result in crossing-over. How the decision is made between repair resulting in crossing-over and gene conversion is not entirely understood, but seems to involve the *mei-9* and *mei-218* gene products (McKim et. al., 1996; Sekelsky et. al., 1995; McKim et. al., 2002). Thus far, genes known to be involved in the DSB repair in oogenesis include a family of Rad51-like genes (*spnA*, *spnB*, *spnD*), as well as the *Drosophila* Rad54

homolog *okr* and the ATR homolog *mei-41* (Ghabrial et. al., 1998; Ghabrial and Schupbach, 1999; Abdu et. al., 2002; Staeva-Vieira et. al., 2003; Jang et. al., 2003; Hari et. al., 1995; Baker and Carpenter, 1972). The Rad51 family of gene products all possess a conserved recA recombinase domain that is thought to be involved in strand invasion, the process by which one strand of a chromosome forms a heteroduplex with a homologous strand in the sister chromosome (Baumann and West, 1998). Rad54 is a versatile protein that seems to have multiple distinct roles during recombination (Tan et. al., 2003). Disruption of *spnB, spnD,* or *ork* prevents timely repair of DSBs in oogenesis, regardless if that break was destined to become a recombination event or not (Jang et. al., 2003; Ghabrial et. al., 1998; Abdu et. al., 2002). Interestingly, of the five *Drosophila* Rad-51-like genes, only *spnD* and *rad51D* are germline specific (Staeva-Vieira et. al., 2003, Abdu et. al., 2003). The others, as well as *okr,* are also expressed in the soma. In fact, *spnA* and *okr* mutants are both sensitive to DSB inducing agents such as ionizing radiation and MMS (methyl methanesulphonate), implying a role in normal somatic DSB repair (Staeva-Vieira et. al., 2003; Jaklevic and Su, 2004). This result confirms that the mechanism used to repair DSBs in *Drosophila* oogenesis is conserved with traditional somatic DSB homologous repair pathways. Current data suggests that only a handful of unique genes are involved in resolving the DSB repair intermediate into an actual cross-over event during oogenesis (McKim et. al., 2002). However, despite the similarities between meiotic recombination and somatic DSB repair, meiotic recombination has some important modifications. One unique aspect of meiotic DSB repair is that the homologous chromosomes involved in the cross-over event remain connected after DNA repair, forming what are called chiasmata. These chiasmata are of critical importance later in meiosis to ensure proper segregation of the chromosomes (McKim et. al., 2002). In the *spnB, spnD,* and *okr* mutants, chromosome non-disjunction increases dramatically (Ghabrial et. al., 1998), as DSBs are not properly repaired to allow recombination and therefore do not form chiasmata.

All DSBs in the oocyte will normally be repaired prior to region 3 of the germarium (Jang et. al., 2003). The DSBs in the nurse cells will sometimes persist longer than those in the oocyte, but they will also be repaired either in region 2b or 3 (Fig. 4-1A). Region 3 is usually composed of a single stage 1 egg chamber that is about to bud

off and enter the vitellarium (Fig. 4-1A). By this point, the oocyte has been determined and is arrested in prophase of meiosis I. The remaining 15 cells in the cyst are specified as nurse cells. By region 3, somatically derived follicle cells have divided multiple times to provide enough follicle cells to entirely envelope the cyst. The final step required to allow budding off of the egg chamber is the migration of inter-follicular stalk cells between the new egg chamber and the posterior tip of the germarium (Spradling, 1993). Inter-follicular stalk cells are terminally differentiated, specialized follicle cells that are responsible for connecting egg chambers in the vitellarium. As they form between the region 3 cyst and the germarium, budding off occurs to form a new stage 1 egg chamber (Fig. 4-1A and B, arrows). When a subsequent egg chamber is made it will be connected to this egg chamber by these stalk cells. That new egg chamber will in turn have it's own stalk cells connecting it to the germarium. In this way, all egg chambers in the vitellarium form a "chain" where each egg chamber is connected to the previous one by stalk cells (Fig. 4-1B).

As an egg chamber moves through the vitellarium, it get progressively larger and its various cell populations go through several developmental changes (Fig. 4-1B). The developmental progression of the egg chamber has been subdivided into 14 stages based on size, morphology, and developmental progression of the follicle cells, nurse cells, and oocyte. At stage 3, the nurse cells begin endoreplication (Spradling, 1993). This is important since it generates multiple genome equivalents in each cell, allowing for mass transcription and production of RNAs and proteins which will later be transferred into the oocyte. Also in stage 3, the oocyte nuclei undergoes a unique morphological change. The chromosomes condense, but not in such a way that the individual chromosomes are recognizable (as is the case later, in metaphase). Instead, the DNA condenses into a round structure referred to as a "karyosome" (Fig. 4-1B, karyosome marked with red). At later stages of oogenesis the follicle cells also undergo further developmental changes. These changes occur in order to allow the follicle cells to deposit the eggshell. The eggshell in *Drosophila* is composed of multiple layers including the vitelline membrane and the chorion (Spradling, 1993). Depositing this complex structure requires the production of many proteins and it must be completed in a relatively short period of time. The follicle cells cease proliferating and begin endoreplication, thereby providing enough genetic

material to quickly produce the proteins required for the vitelline membrane and chorion. This endoreplication happened in two steps. First, the follicle cells switch to endoreplication of the entire genome during stage 6. Then, during stage 10B, the follicle cells stop endoreplicating the entire genome and begin the selective amplification of specific chorion gene loci (Orr-Weaver, 1991; Calvi and Spradling, 1999).

During oogenesis, the growing oocyte begins to establish polarities which will persist to define the dorsal/ventral (D/V) axis and anterior/posterior (A/P) axis of the egg. In the mature egg, specialized structures called the dorsal appendages are present on the anterior dorsal end of the egg, whereas a micropyle, which serves as an entry point for sperm, is present on the anterior tip. The precise positioning of these structures reflects the D/V and A/P boundaries that have previously been defined. The processes used to establish D/V and A/P asymmetry during oogenesis have been extensively studied in *Drosophila* and are known to involved a Grk/Egfr signal transduction system (van Eeden and St Johnston, 1999; Riechmann and Ephrussi, 2001). The *grk* locus encodes a TGF-(alpha)-like protein which is a ligand for the *egfr* encoded receptor (Neuman-Silberberg and Schupbach, 1993; Sapir et. al., 1998). Activation of Egfr by Grk binding sets off a signaling cascade which is thought to act through the *ras* pathway (Ruohola-Baker et. al., 1994). Mutations affecting either *grk* or *egfr* result in improper axis determination and a loss of dorsal appendage material; termed a "ventralized" phenotype (Schupbach, 1987). Establishing the A/P axis begins early in oogenesis with communication between the oocyte and the dorsal follicle cells via the Grk ligand and Egfr receptor (Ray and Schupbach, 1996). This in turn induces a reorganization of a microtubule network in the oocyte, which will be used to establish the A/P axis by shuttling anterior or posterior determinants to the appropriate end of the oocyte (Ray and Schupbach, 1996, Riechmann and Ephrussi, 2001). Later in oogenesis, a second Grk/Egfr mediated signaling event between the oocyte and dorsal follicle cells allows the establishment of the D/V axis (Ray and Schupbach, 1996). During this second signaling event the oocyte nucleus is repositioned to the anterior/dorsal region of the oocyte. Throughout oogenesis, the Grk protein can be visualized with immunofluorescence and is localized to the oocyte cytoplasm surrounding the nucleus (Fig. 4-1B, Grk marked with green). As the oocyte nucleus is repositioned during the second Grk/Egfr signaling event Grk localization

changes as well (Fig. 4-1B). Rather than surrounding the entire nucleus Grk becomes localized to a patch at the anterior/dorsal corner of the oocyte (Fig. 4-1B) (Ray and Schupbach, 1996).

Screens for mutants that affect patterning of the oocyte like *grk* and *egfr* mutants have revealed a surprising connection to the repair of meiotic DSBs. In fact, mutations in the Rad51 DNA repair genes *spnA, spnB, spnD,* and *okr* were all initially recovered as mutations affecting D/V and A/P patterning in the egg (Gonzalez-Reyes et. al., 1997; Schupbach and Wieschaus, 1991). Mutant mothers defective in for any of these genes lay eggs with fused dorsal appendages and duplicated microphyles, similar to what is seen in *grk* and *egfr* mutants. Only later when they were molecularly characterized were these genes found to encode homologs of DSB repair pathway components that are critical for repairing meiotic DSBs and allowing proper recombination (Ghabrial et. al., 1998). Although it might seem difficult to explain how two apparently different processes like meiotic recombination and oocyte axis patterning could be related, the connection is starting to become understood. Initial clues arose from an examination of oogenesis itself in *spnB, spnD,* and *okr* mutants. Grk mRNA and protein localization was found to be mislocalized or absent altogether and the normal spherical and condensed morphology of the oocyte karyosome was disrupted (Ghabrial et. al., 1998). Removing both copies of another gene called *mei-W68* in a *spnA, spnB, spnD,* or *okr* mutant background was found to suppress this mislocalization of Grk, as well as the karyosome defects (Staeva-Vieira et. al., 2003; Ghabrial and Schupbach, 1999). *mei-W68* is the *Drosophila* spo-11 homolog that is required for inducing the DSBs at the onset of meiotic recombination. Without *mei-W68* activity, no DSBs are induced, no repair can take place (nor does it need to), and no recombination occurs. The fact that removing *mei-W68* suppressed the mislocalization of Grk in these mutants showed that the axis patterning defects were indeed related to an inability to repair DSBs and not to some novel function of these genes.

Similar experiments with *mei-41* and *chk2* mutants revealed that these checkpoint genes are also required for both the mislocalization of Grk and abnormal karyosome in *spnA, spnB, spnD,* and *okr* mutants (Ghabrial and Schupbach, 1999; Abdu et. al., 2002; Staeva-Vieira et. al., 2003). The *mei-41* gene encodes the ATR kinase that is thought to

be involved not only in the detection and repair of DSBs, but also in this context in a checkpoint response which signals through Chk2 to downstream targets. The current hypothesis to explain this data assumes that Mei-41 activates a checkpoint in response to DSBs, that persist in the DNA repair mutants. Indeed, immunofluorescence studies have shown that in *spnB* and *okr* mutants DSBs persist past region 2b of the germarium where they are normally repaired, even into the vitellarium (Jang et. al., 2003). In response to these DSBs, Mei-41 is thought to signal through Chk2 to activate what is being called a "meiotic checkpoint" (Fig. 4-2A) (Ghabrial et. al., 1998; Ghabrial and Schupbach, 1999; Abdu et. al., 2002). This checkpoint is unlike a typical cell cycle checkpoint, in that there is no evidence for cell cycle arrest (McKim et. al., 2002). Instead, it is thought that activation of this checkpoint prevents the normal progression of developmental events in oogenesis. Such a checkpoint makes sense, since it prevents the female from investing resources in eggs that have compromised genomic stability due to unrepaired DSBs. These events include translation and localization of the Grk protein, and establishment of proper spherical karyosome morphology (Fig. 4-2A). In *mei-41 spnB* double mutants, the checkpoint cannot respond to the unrepaired DSBs and as a result, the oocyte proceeds normally through events of oogenesis that would normally be halted if *mei-41* was functional. A similar result is observed when *chk2* is removed in a *spnB* background, implying that Chk2 is required to transmit the DSB signal from Mei-41 to downstream targets (Fig. 4-2A). Currently, targets of the Chk2 kinase in this process, which are presumably phosphorylated to regulate the checkpoint, remain unclear. It is known that somewhere downstream of Chk2 in the pathway, the translation initiation factor Vasa is required to carry out the checkpoint (Ghabrial and Schupbach, 1999; Abdu et. al., 2002). One idea is that Vasa might be involved in the proper translation of Grk, which is disrupted when the checkpoint is active (Fig. 4-2A). Vasa is also known to be involved somehow in modifying the oocyte nucleus into the karyosome, during stage 3 (Styhler et. al., 1998; Tomancak et. al., 1998). There are also likely to be still other players that connect Chk2 to Vasa, whose identities are not yet known.

Drosophila atm mutants that are able to reach adulthood are female sterile, suggesting that they also have defects during oogenesis. Germline clones made by Stanley Tiong, in which the whole organism is wild type except for the germline, allowed

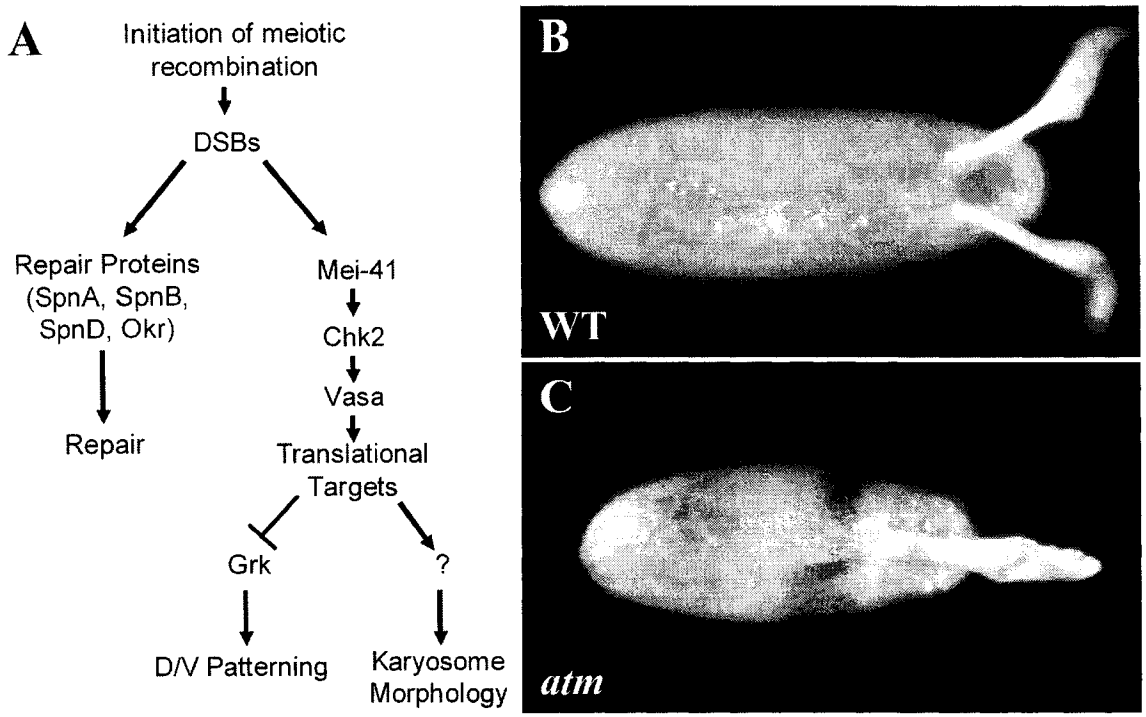

Fig. 4-2 – Activation of meiotic checkpoint leads to D/V patterning defect, a phenotype observed in eggs laid by *atm* mutant females. (A) In oogenesis, DSBs are induced at the onset of meiotic recombination. Normally these breaks will be repaired rapidly through recombination repair pathways (left branch of pathway in A). If repair mechanisms are compromised, a Mei-41 and Chk2 dependent checkpoint is activated (termed the meiotic checkpoint, right branch of the pathway in A), which results in improper Grk localization and an abnormal karyosome morphology. The checkpoint is thought to involve Vasa, a translational regulator, and may interfere with Grk translation, resulting in the localization defect. Grk mislocalization ultimately leads to a failure to properly pattern the D/V axis of the egg. (B) Wild type eggs are surrounded by a eggshell, deposited by follicle cells during oogenesis, and contain two appendages on the dorsal posterior end of the egg. (C) In eggs laid by *atm* mothers (*atm*^{2} germline clones in B), the eggs display two distinct defects. First, the eggshell is thin in places. Second, the dorsal appendages are often fused (as in B), or absent altogether, suggestive of a failure to properly pattern the D/V axis of the egg.

some eggs to be laid by mothers with *atm* mutant germlines. These eggs showed two obvious defects: a thin and patchy eggshell and the fusion or absence of dorsal appendages (Fig. 4-2B vs. C). This dorsal appendage phenotype is remarkably similar to the ventralized phenotype of eggs laid by *spnB* mutants, or other mutants with defects in meiotic DSB repair. In these repair mutants, the ventralized phenotype is thought to be a consequence of meiotic checkpoint activation. Since *atm* is well known to be involved in somatic DSB repair, we have undertaken experiments to address whether *atm* might also be involved in repairing DSBs produced during meiotic recombination, as is the case in *spnB* mutants. A precedent for this possibility is based on data from the mouse ATM model. It has been shown that *Atm-/-* mouse oocytes undergo degenerative apoptosis that is a result of unrepaired DSBs produced during prophase by Spo11 (Barlow et. al., 1998; Di Giacomo et. al., 2005). Despite the differences between mouse and fly oogenesis these similarities suggest that the mechanism of DSB repair during recombination is fairly well conserved. Therefore, there was good reason to think *atm* might also be involved in meiotic recombination in *Drosophila.* The thin eggshell of eggs laid by *Drosophila atm* mothers on the other hand is unlike anything seen in *spnB* or related mutants. Because the follicle cells are responsible for laying down the vitelline membrane and chorion that make up the eggshell it seemed plausible that there might be defects in these somatic cells, as well. In order to investigate this possibility, and to examine the role of ATM in repairing meiotic DSBs, we undertook a thorough investigation of oogenesis in *atm* mutants. Our results suggest that the thin eggshell defect is caused by ectopic apoptosis of the follicle cells during early oogenesis. Furthermore, we have demonstrated that the fused dorsal appendage phenotype is caused by the activation of the meiotic checkpoint response to unrepaired DSBs, suggesting a role for *atm* in the timely repair of DSBs during meiotic recombination.

Section 4.2 – Materials and Methods

Dissection of *Drosophila* Ovaries:

Drosophila females were collected within 24 hours of eclosion and transferred to a fresh vial. Females were mated to wild type males and aged for 3-4 days a 25°C prior to dissection. During dissection, ovaries were removed with forceps and then ovarioles were

teased apart at the tip and base of the ovary using tungsten needles. This separation was done to allow access of the fixative and antibodies to the egg chambers within the ovaries. To obtain *atm* mutant females, p^p atm^8 *e/Ki* p^p *Df(3R)PG4* larvae were raised at 24°C. At these semi-restrictive temperatures, p^p atm^8 *e/Ki* p^p *Df(3R)PG4* flies are partially viable but display the various *atm* morphological phenotypes, including sterility. After collection the females were up-shifted to 25°C for mating and aging.

Immunofluorescence:

Following dissection, ovaries were incubated in fixative for 20 minutes on a rotator. Fixative was composed of 200µl of 2% formaldehyde in PBS (137 mM NaCl, 2.68 mM KCl, 10.14 mM Na_2HPO_4, 1.76 mM KH_2PO_4), 600µl heptane, and 5µl of 20% NP-40. Following fixation the solution was removed, ovaries were rinsed three times in PBS-Tx (PBS with 0.3% Triton-X), then washed three times 5 minutes in PBS-Tx. After washing, ovaries were incubated in blocking solution (PBS-Tx with 1% BSA) for 1 hour. Blocking solution was removed and fresh blocking solution containing an appropriate concentration of primary antibody was added (see Appendix B for antibody dilutions and other details). Incubation with primary antibodies was performed overnight at 4°C on a rotator. After incubation with primary antibodies, the ovaries were rinsed three times and then washed three times for 5 minutes each, with PBS-Tx. Next, secondary antibodies were added, diluted in blocking buffer 1:1000. Secondary antibodies used were conjugated with Alexa Fluor 488 or 568, purchased from Molecular Probes. Incubation with secondary antibodies was performed at room temperature for one hour. After staining with the secondary antibodies, ovaries were rinsed three times in PBS-Tx. If DNA staining was performed, it was carried out at this point (see next section). Following rinsing or DNA staining, ovaries were washed a final three times for 5 minutes each, in straight PBS. Ovaries were mounted in anti-fade reagent (1 mg/ml 1,4-phenylenediamine, 137 mM NaCl, 2.68 mM KCl, 10.14 mM Na_2HPO_4, 1.76 mM KH_2PO_4 in 90% glycerol). Slide were sealed with nail polish following mounting, to prevent the coverslip from shifting. All ovary pictures were taken with a confocal microscope (Leica TCS SP2).

DNA Staining:

DNA staining was performed in conjunction with immunofluorescence following the secondary antibody step (see above). DNA staining was performed with propidium iodide staining whenever possible. However, because propidium iodide and the Alexa 568 secondary antibody emit light of similar wavelengths, Hoechst 33258 stain was used to stain DNA whenever Alexa 568-conjugated secondary antibodies were used. Staining with Hoechst 33258 was performed by incubating in PBS with 5 μg/ml of Hoechst for 10 minutes. Propidium iodide stains all nucleic acids, including RNA. Therefore, propidium iodide staining was preceded by incubation in 1 mg/ml RNaseA at 37°C for 1 hour. Following this treatment, ovaries were incubated in PBS with 20 μg/ml propidium iodide at room temperature for 20 minutes.

Acridine Orange Staining:

Acridine orange is a nucleic acid stain that is actively removed from living cells. Because it is removed quickly, normal viable cells will not stain strongly with acridine orange. In dying cells however, acridine orange will accumulate and stain the cells brightly. Therefore, acridine orange can be used to mark cell death, including apoptotic cells. Because this application relies on acridine orange being actively removed from living cells, ovaries can not be fixed prior to staining. This means that the whole procedure must be carried out under near-physiological conditions (in Ringer's buffer) and pictures must be taken immediately after staining and mounting. Acridine staining procedure for ovaries was carried out as previously described (Smith et. al., 2002), with minor variations. Ovaries were dissected in *Drosophila* Ringer's solution (182 mM KCl, 46 mM NaCl, 3 mM $CaCl_2$, 10 mM Tris-Cl, adjusted to pH 7.2 with HCl) and immediately placed in acridine orange stain (5 μg/ml acridine orange diluted in Ringer's solution). Acridine orange was obtained from Molecular Probes, as a 10 mg/ml solution in water. Incubation with acridine orange was performed on a rotator at room temperature for 15 minutes. Following incubation, ovaries acquire an orange and green colouration that can be seen with the naked eye. Ovaries were rinsed briefly and washed two times for 5 minutes each with Ringer's solution, before being mounted on a slide with about 40 μl of Ringer's solution. A 18X18 coverslip was then placed on top of the samples. To avoid

crushing the samples it is of critical importance that no pressure is placed on the coverslip, the surface tension of the 40 µl of Ringer's should be adequate to hold the coverslip in place. Following mounting there is a 15-20 minute window where pictures can be taken before the samples dry out. This window can be expanded by adding more Ringer's solution, however the sample may start to undergo ectopic apoptosis after dissection so care should be taken to minimize the time spent taking pictures. All pictures were taken with the Leica TCS TSP2 confocal microscope.

Genetic Clones:

There are methods of producing homozygous clones of cells in organisms that are otherwise heterozygous. This allows the cell autonomous effects of a given mutant to be examined and compared with the phenotype of neighbouring non-mutant cells. Clones were made using the atm^2 allele and the FRT/FLP system (Xu and Rubin, 1993). The FRT/FLP system uses the FLP recombinase to induce mitotic recombination between FRT sequences on the chromosome of interest. Clones were marked by making the FRT atm^2 chromosome heterozygous with another FRT chromosome that bears an *arm-LacZ* construct on chromosome 3R. This construct expresses ß-galactosidase in both follicle cells and germline cells of the ovaries. In clonal cell populations that have been made homozygous for the atm^2 mutation through FLP-induced somatic recombination, the *arm-LacZ* chromosome will not be present and ß-galactosidase will not be produced. Therefore, when immunofluorescence is performed with antibodies to ß-galactosidase, clonal cells that are *atm* homozygous will not stain. Cells that are still heterozygous, or that have been made homozygous for the FRT *arm-LacZ* chromosome, will stain with antibodies to ß-galactosidase.

The cell autonomy of the follicle cell defect was examined by making atm^2 homozygous clones in populations of follicle cells or germ line cells, using slightly different methods. In follicle cells, the FLP recombinase that induces clones was expressed in follicle cells using a UAS/Gal4 system and a follicle cell-specific promoter called *e22c*. This results in patches of *atm* homozygous follicle cells of various sizes in growing egg chambers. The ß-galactosidase positive cells outside of this patch were still heterozygous for atm^2 and a wild type copy of the gene. Clones were produced in germ

line cells by using a heat shock promoter to ubiquitously drive the FLP recombinase to induce clones. Heat shock was performed at a time when germ line stem cells are dividing, during days 4 and 5 of larval development. Heat shocks were performed on both days, 1 hour each time, at 37°C. The result is germ line stem cell clones that produce egg chambers whose entire complement of nurse cells and oocyte are homozygous for atm^2. The follicle cells in such clones however are still heterozygous for atm^2 and a wild type allele.

Analysis of Double Mutants:

Double mutants were made with *atm* and several other genes by myself and Stanley Tiong, who was a research associate in our laboratory. Double mutants included combinations of *atm* with *mei-41* on the X chromosome, *chk2*, *grp*, and *mei-W68* on the 2nd chromosome, and *p53* on the 3rd chromosome. Double mutant genotypes included *w* $mei\text{-}41^{D3}/w\ mei\text{-}41^{D3}$; $p^p\ atm^8\ e/Ki\ p^p\ Df(3R)PG4$ for the *mei-41 atm* double mutant, *w;* $chk2^{P1}/chk2^{P1}$; $p^p\ atm^8\ e/Ki\ p^p\ Df(3R)PG4$ for the *chk2 atm* double mutant, grp^1/grp^1; $p^p\ atm^8\ e/Ki\ p^p\ Df(3R)PG4$ for the *grp atm* double mutant; $mei\text{-}W68^1$ / $mei\text{-}W68^{2\text{-}4472}$ *cn bw;* $p^p\ atm^8\ e/Ki\ p^p\ Df(3R)PG4$ for the *mei-W68 atm* double mutant, and $p^p\ atm^8\ p53^{5A\text{-}1\text{-}4}$ / $p^p\ atm^8\ p53^{5A\text{-}1\text{-}4}$ for the *atm p53* double mutant. The *atm p53* double mutant required the creation of a recombinant chromosomes since both genes are located on chromosome arm 3R. The generation of these recombinants is described in the materials and methods section of chapter 3.

Some of these double mutants have difficulty eclosing when raised at 24°C, the normal temperature under which atm^8 / *Df* females were raised. To increase viability, these double mutants were raised at 18°C or 22°C, which is a more permissive temperature for atm^8. The adult females were then up-shifted to 25°C after collection and incubated at that temperature with males for 3-4 days. This is sufficient time to disrupt the function of the temperature sensitive ATM and cause sterility. To confirm that any suppression results in the double mutants were not due to residual ATM activity caused by differences in temperatures during larval development, side by side controls were performed where $p^p\ atm^8\ e/Ki\ p^p\ Df(3R)PG4$ larvae were also grown at 18°C-22°C and up-shifted to 25°C as adults. After 3-4 days, the ovaries of $p^p\ atm^8\ e/Ki\ p^p\ Df(3R)PG4$

females treated in such a way are indistinguishable from those of p^p atm^8 *e/Ki* p^p *Df(3R)PG4* females raised at 24°C during larval development.

Analysis of the Chromosome Segregation Defect:

To test atm^8/Df females for chromosome non-disjunction during meiosis, virgin females raised at 22°C were crossed to males from a special stock, referred to as G035, that is designed to allow progeny from non-disjunction events to survive and be scored. All crosses were carried out at 22°C, allowing the atm^8/Df females to remain fertile. p^pe females were used as a negative control in the experiment. The exact genotype of G035 is *C(1;Y)1, y v f B:* y^+ */ C(1)RM, y v; C(4)RM, ci* ey^R. This stock is special because males possess attached XY chromosomes and attached 4th chromosomes. The inheritance patterns of the X and 4th chromosomes during the cross between G035 males and atm^8/Df or p^pe females is outlined in Table 4-1. Non-disjunction events for the X chromosome were recognized as males with the dominant *Bar* phenotype or females without the *Bar* phenotype. Note that one half of all the non-disjunction events for the X chromosome are lethal because they contain zero or three copies of the X-chromosome, therefore the observed non-disjunction rate was multiplied by two to get the actual rate (Table 4-1). Non-disjunction events for the 4th chromosome were recognized as flies expressing the recessive *ci* phenotype. For the 4th chromosome, the observed non-disjunction rate was multiplied by 4 to get the actual rate because half of all non-disjunction events for the 4th are lethal, because they possess zero or four copes of the 4th chromosome, and one quarter are indistinguishable from normal flies (Table 4-1).

Section 4.3 – Results

Section 4.3.1 – atm *mutant egg chambers display ectopic* p53 *independent apoptosis of follicle cells*

To determine the cause of female sterility in the *atm* mutants, ovaries from atm^8/Df females were dissected and examined. Immunofluorescent staining of ovaries with antibodies to Hts, a marker of follicle cell membranes, suggested that there is a defect in *atm* mutant follicle cells during oogenesis. In *atm* mutants, gaps form in the follicle cell layer that normally surrounds the egg chamber. These gaps have been

X Chromosome Inheritance	♀ atm^8/Df or $p^p e$			
	X (one normal X)	X (one normal X)	O (non-disjunction)	XX (non-disjunction)
♂ G035 $X^{Bar\wedge Y}$ (attached XY)	X $X^{Bar\wedge Y}$ Bar Female	X $X^{Bar\wedge Y}$ Bar Female	$X^{Bar\wedge Y}$ Bar Male	XX $X^{Bar\wedge Y}$ Lethal
♂ G035 O (no X or Y)	XO Non-Bar Male	XO Non-Bar Male	OO Lethal	XX Non-Bar Female

4th Chromosome Inheritance	♀ atm^8/Df or $p^p e$			
	4 (one normal 4)	4 (one normal 4)	O (non-disjunction)	44 (non-disjunction)
♂ G035 $4^{ci\wedge ci}$ (attached 4's)	4 $4^{ci\wedge ci}$ Non-ci Wings	4 $4^{ci\wedge ci}$ Non-ci Wings	$4^{ci\wedge ci}$ ci Wings	44 $4^{ci\wedge ci}$ Lethal
♂ G035 O (no 4's)	4 O Non-ci Wings	4 O Non-ci Wings	OO Lethal	44 Non-ci Wings

Table 4-1 – Genetic assay for chromosome non-disjunction during female meiosis. G035 males were mated to *atm*^{8} or *p*^{p}*e* females to test non-disjunction rates during meiosis in these females. This cross allows non-disjunction events effecting chromosomes X and 4 to produce viable, scorable progeny. G035 males have attached X and Y chromosomes as well as attached 4th chromosomes. Therefore, normal segregation of the sex chromosomes result in either both an X and a Y being passed on or nothing at all. Likewise, normal segregation of the 4th chromosomes will result in inheritance of either two paternal copies or no paternal copies. Both these attached chromosomes have scorable markers, *Bar* for the attached XY and *ci* for the attached 4th chromosomes. In the above tables, progeny with blue text are a result of normal chromosome segregation patterns. Progeny marked with green text are exceptional progeny that are a result of non-disjunction events and can be scored. For chromosome X, exceptional progeny include Bar males and Non-Bar females. For chromosome 4, exceptional progeny include flies with the *ci* wing phenotype. Non-disjunction events that result in lethality are marked with red text and cannot be scored. Progeny marked with orange text are viable, but can not be scored because they are indistinguishable from normal progeny. For chromosome X, one half of non-disjunction events produce progeny that can be scored. With chromosome 4, a quarter of non-disjunction events produce progeny that can be scored.

observed as early as stage 4 (compare Fig. 4-3A with Fig. 4-3D) of oogenesis and get progressively worse (Fig. 4-3B vs. E). By stage 9, the majority of egg chambers abort, apparently because of wholesale apoptosis of the remaining follicle cells and nurse cells. To determine if the follicle cell gaps are due to ectopic cell death, acridine orange staining, used as a marker for dying cells, was performed on wild type and *atm* ovaries. There is some normal developmentally programmed cell death present in the germarium regions of both WT and *atm* mutants (Fig. 4-3C vs. F). Therefore, it is difficult to determine if there is increased cell death in the germarium region of *atm* mutants. In the vitellarium however, the region of the ovary where egg chambers are located, there is a significant increase in dying cells in *atm* egg chambers compared to wild type (Fig. 4-3C vs. F). This abnormal cell death can be recognized as early as the stage 2. Staining with DNA dyes has shown that some follicle cells in *atm* mutants display a apoptotic morphology, characterized by a small, hypercondensed nucleus (Fig. 4-3G). Follicle cells with apoptotic morphology were not observed in wild type vitellaria. Therefore, these results are consistent with the ectopic cell death being due to apoptosis. In eye-antennal discs of *atm* mutants, we also observed significant amounts of ectopic apoptosis (see chapter 3). This apoptosis was found to require the pro-apoptotic gene, *p53*. To determine if the apoptosis observed in follicle cells is also dependent on *p53*, ovaries from *atm p53* females were examined with DNA dyes and Hts staining to mark follicle cell membranes. The gaps that are normally present in *atm* mutants are still observed in *atm p53* double mutants (Fig. 4-3H). Furthermore, follicle cells with a hypercondensed, apoptotic morphology were also still present in the double mutant (Fig. 4-3I). These results suggest that the follicle cell death does not require *p53*, unlike the situation in the eye.

Section 4.3.2 – atm *mutant ovarioles are unable to properly translate or localize Grk and display karyosome abnormalities*

Eggs laid by *atm* mutant mothers show a ventralized phenotype characterized by fused or absent dorsal appendages. In other DSB repair mutants that show this phenotype (*spnB*, *okr*, etc.), the defect is due to improper translation and localization of Grk, an important signaling molecule used for establishing polarity in the developing egg (Ghabrial et. al., 1998). To determine if this is also the case in *atm* mutants,

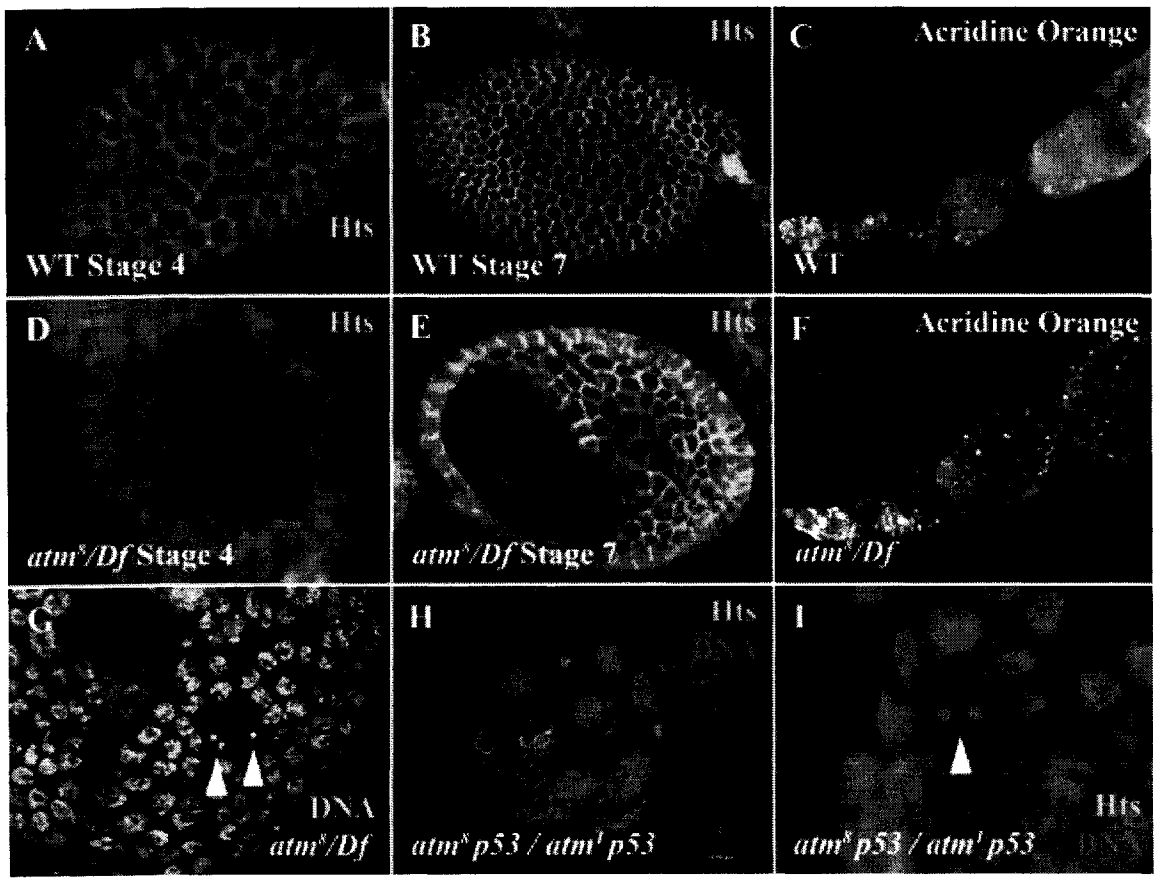

Fig. 4-3 – *atm* mutant follicle cells undergo spontaneous *p53* independent apoptosis. (A-B) During oogenesis, egg chambers are normally surrounded by an even layer of somatic follicle cells. Follicle cell membranes can be marked with antibodies to Hts. (C) Cell death, marked with acridine orange, is uncommon in wild type ovarioles except for developmental programmed apoptosis within the germarium. (D) Gaps in the follicle cell layer are first apparent in *atm* mutant egg chambers during stage 4 of oogenesis. The gaps can be visualized when staining is performed using antibodies to Hts. (E) These gaps get progressively worse, growing large by stage 7. (F) Staining with acridine orange suggests that there is abnormal cell death in follicle cells of *atm* mutants. (G) DNA stains suggest that this cell death may be apoptotic, based on the presence of follicle cell nuclei with a hypercondensed appearance (arrowheads), typical of apoptotic cells. (H-I) In *atm p53* double mutants the gaps are still present, as are cells with apoptotic morphology (arrowhead in I). All atm^{8}/Df females were raised at restrictive temperatures (24°C-25°C).

immunolocalization studies were carried out with anti-Grk antibodies. During early-mid oogenesis, Grk protein normally localizes in a ring surrounding the karyosome (oocyte nucleus) (Fig. 4-4A and B). This pattern persist until mid-late oogenesis, when the karyosome moves to the dorsal anterior corner of the oocyte. At this point, Grk becomes localized to a patch on the anterior dorsal side of the karyosome, adjacent to the nearby follicle cells (Fig. 4-4 C). In *atm* mutants there were errors in Grk localization; 87% of the time Grk is mislocalized or absent altogether, n=38 (Fig. 4-4D and E). Occasionally Grk will localize more normally by mid-late oogenesis in approximately half of atm^{8} mutants, when Grk becomes localized to the dorsal anterior patch (Fig. 4-4F). However, even in these egg chambers there are still abnormalities in the Grk pattern, such as residual Grk staining on the ventral side of the karyosome. The *spnB* and *okr* phenotypes are also characterized by errors in karyosome morphology. To determine if *atm* mutants also share this defect, the karyosome was visualized with a DNA dye and marked with antibodies to Orb, a protein that is found specifically in oocyte cytoplasm. The karyosome is normally compact and spherical until very late in oogenesis (Fig. 4-4G). In *atm* mutants, the karyosome morphology is often abnormal, becoming flattened or fragmented 80% of the time (n=40) (Fig. 4-4H). Occasionally, the DNA from the karyosome is extremely fragmented and forms a ring around the inside of the nuclear membrane (Fig. 4-4I). Such karyosome morphologies were never seen in wild type ovaries.

Section 4.3.3 – atm *mutant ovarioles display errors in repairing meiotic DSBs and in homologous chromosome segregation*

The *spnB* class of mutants are involved in repairing DSBs produced during meiotic recombination in the oocyte and some nurse cells (Ghabrial et. al., 1998; Jang et. al., 2003). Since *atm* and *spnB* mutants both show Grk mislocalization and karyosome defects, our observations suggest that *atm* might also be involved in repairing meiotic DSBs, in addition to it's DNA repair role in the soma. To address this question, staining was performed with antibodies to phospho-His2AV. His2AV is a histone variant that is phosphorylated during the initial response to DSBs (Madigan et. al., 2002). Therefore, phospho-His2AV (hereafter referred to as "His2AV") can be used as a marker of DSBs.

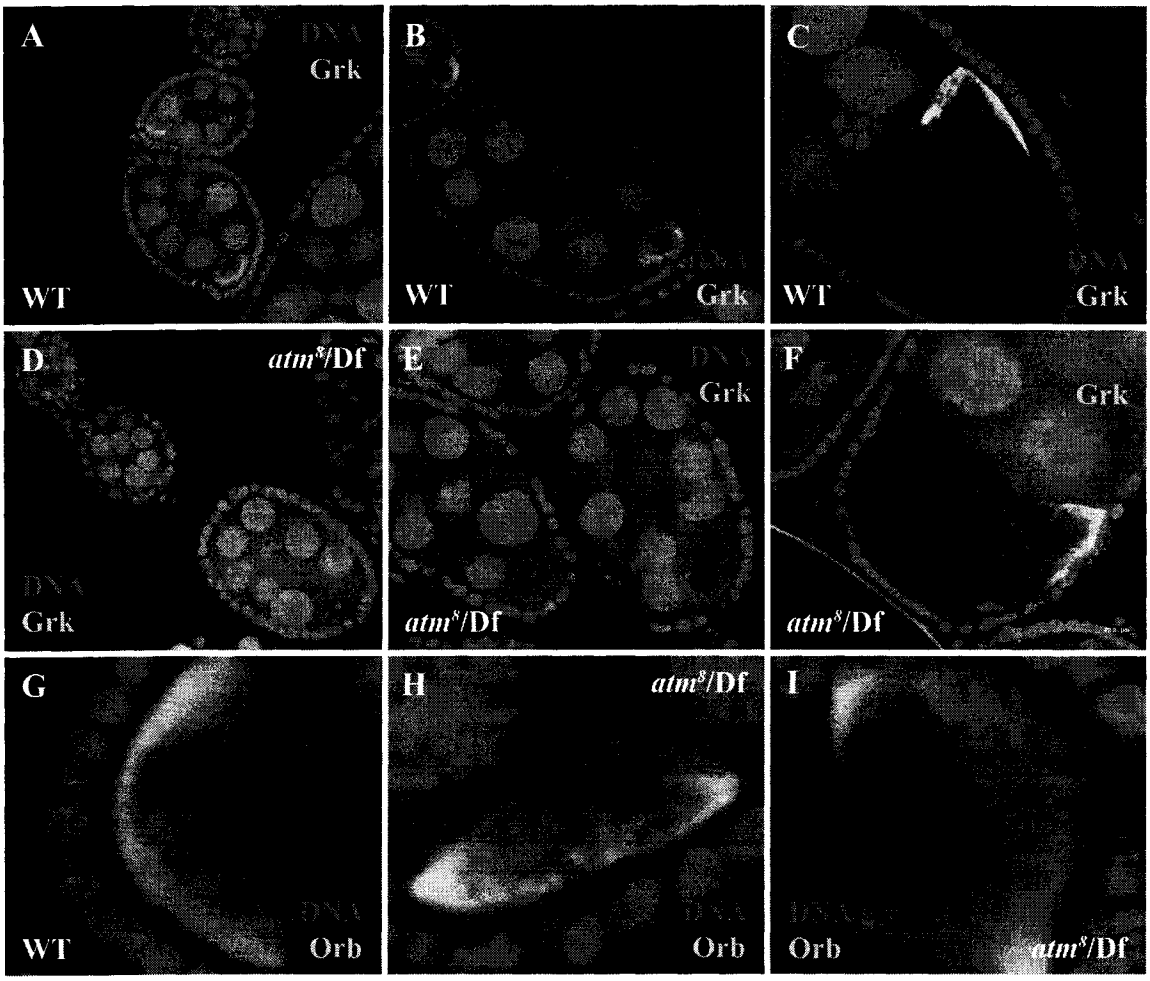

Fig. 4-4 – *atm* mutant egg chambers exhibit defective Grk localization and karyosome morphology. (A-B) During early oogenesis, Grk protein (green) localizes in a ring pattern around the oocyte nucleus (karyosome). (C) During mid oogenesis, the karyosome becomes relocalized to the anterior dorsal corner of the oocyte. At this point, Grk protein is also relocalized to a dorsal anterior patch between the karyosome and the nearby follicle cells. (D-E) In *atm* mutants, Grk localization is abnormal during early oogenesis. Grk staining is very weak or absent altogether. (F) In later oogenesis, *atm* mutant egg chambers will occasionally recover and exhibit enriched Grk staining at the anterior dorsal patch. However, localization is rarely perfect and residual Grk protein can be observed on the ventral side of the karyosome. (G) In wild type egg chambers, oocyte DNA becomes hypercondensed during stage 4 of oogenesis, into a spherical structure termed karyosome. Antibodies to Orb, a protein that localizes to the oocyte cytoplasm, were used to conclusively identify the oocyte nucleus and karyosome. (H-I) In *atm* mutant egg chambers the karyosome is often misshapen or fragmented. The karyosome will often be found in a "stretched out" confirmation (H) or become fragmented and form a "ring" around the inside edge of the nucleus (I). All atm^{8}/Df mutant females were raised at restrictive temperatures (24°C-25°C).

Normally, DSBs are induced early in oogenesis in region 2a of the germarium. Breaks are induced both in the oocyte and in some of the nurse cells (Jang et. al., 2003). These breaks are normally repaired very rapidly however, so that His2AV signal is no longer present in the oocyte by region 3 (Fig. 4-5A, Jang et. al., 2003). His2AV staining is not present in significant levels within egg chambers of the vitellarium (Fig. 4-5C). In *atm* mutants, the His2AV signal persists longer than normal, into region 3 of the germarium and the vitellarium (Fig. 4-5B and D). This abnormally persistent staining is present in both the oocyte and some nurse cells (Fig. 4-5B and D). In early oogenesis (germarium to stage 4), some nurse cells in *atm* mutants have strong His2AV staining throughout the nucleus, while others lack staining altogether (Fig. 4-5B). At stage 5-6, some of the His2AV positive nurse will begin to display a weaker, more punctate staining pattern (Fig. 4-5D). The abnormal oocyte His2AV staining does eventually disappear from *atm* mutant egg chambers by around stage 3, whereas the nurse cell staining tends to persist until stage 5-6. To confirm that the oocyte has persistent DSBs in *atm* mutants, cysts from region 3 were stained with antibodies to Orb, to mark the oocyte, and His2AV to mark DSBs. Normally, no staining is seen within the oocyte at this point of oogenesis since the DSBs have already been repaired (Fig. 4-5E). In *atm* mutant germariums however, oocytes are frequently seen in region 3 that staining strongly with His2AV (Fig. 4-5F).

During recombination, DSBs are repaired to form heteroduplex DNA and chiasma, which are covalent connections between homologous chromosomes. These chiasma persist until chromosome segregation during metaphase I of meiosis, where they play a important role in ensuring proper chromosome disjunction. Thus, mutants affecting meiotic DSB repair also affect chromosome segregation, presumably because the chiasma do not properly form. Since *atm* mutants seem to have defects repairing meiotic DSBs, *atm* mutants were examined for defects in chromosome segregation during meiosis, characterized by elevated rates of chromosome non-disjunction. To measure non-disjunction rates, females from wild type and *atm* mutants were crossed to males from a special strain, termed G035. If non-disjunction occurs during meiosis in these females, this cross will result in exceptional progeny that can be recognized and scored (see Materials and Methods). A caveat to this experiment is that it required us to examine the

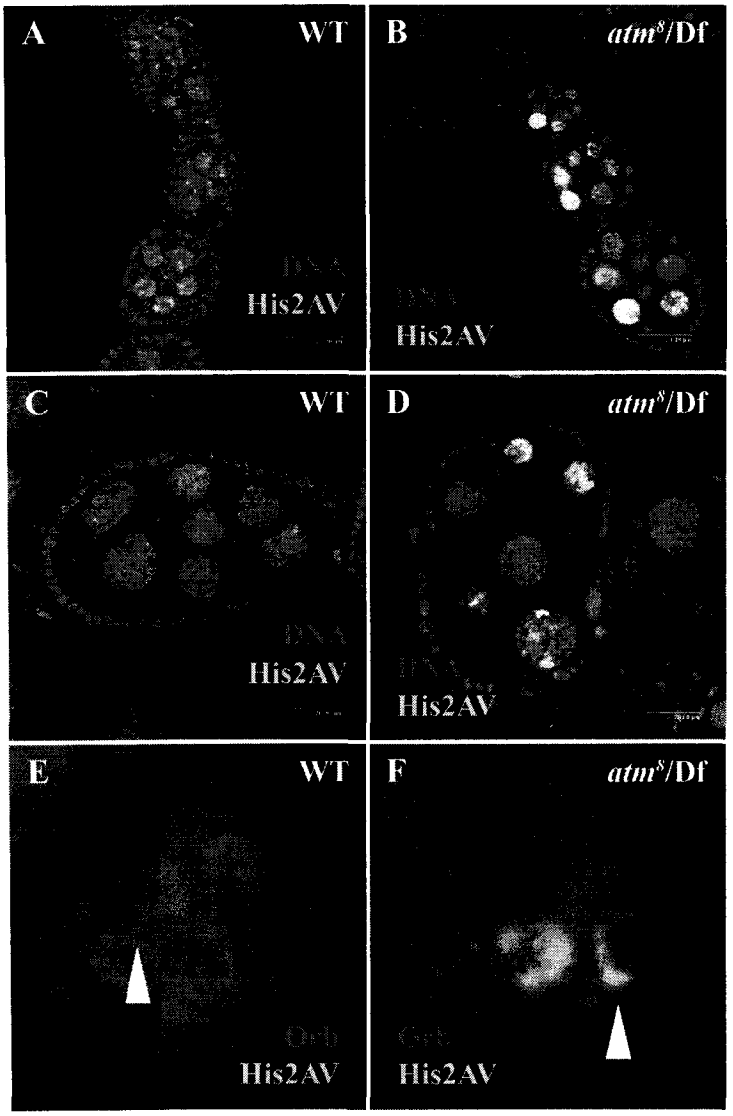

Fig. 4-5 – *atm* mutants exhibit ectopic His2AV staining past region 2 of the germarium. Antibodies to His2AV (green) were used to mark the presence of DNA DSBs during oogenesis. In wild type ovaries, DSBs are restricted to region 2a of the germarium (fig 3-10). (A and C) No strong His2AV staining is seen in wild type vitellariums.(B and D) in *atm* mutant vitellariums however, strong and persistent His2AV staining is observed in nurse cells and the oocyte. (E-F) To confirm that His2AV staining was persistent in the oocyte, cysts from region 3 of the germarium were co-stained with antibodies to Orb and His2AV. By region 3, Orb has become selectively enriched within the oocyte cytoplasm and can be used as a oocyte marker. In wild type region 3 cysts, the oocyte (arrowhead) does not show His2AV staining as all DSBs have been repaired (E). In *atm* mutant cysts, His2AV staining persists within the oocyte at this stage (arrowhead, F). All atm^{8}/Df mutant females were raised at restrictive temperatures (24°C-25°C).

progeny of *atm* females, which are normally sterile. To circumvent this problem, temperature sensitive atm^8/Df females were grown at 22°C, a permissive temperature where the atm^8 gene product is partially functional and the females are partially fertile. All of the crosses for the non-disjunction test were also carried out at 22°C, to prevent the *atm* mutant females from subsequently becoming sterile. Despite the partially functional atm^8 gene product, atm^8/Df females still display reduced fertility at 22°C, producing about half as many progeny as their wild type counterparts. Therefore, we thought we might be able to see an effect on non-disjunction at 22°C, even though there is some functional ATM present. Because we cannot examine an *atm* null allele, any increases in non-disjunction we observe are likely to be an underestimate of what we would see under actual null conditions. This makes it difficult to accurately quantify the effect that losing ATM function has on chromosome segregation, but allows us to simply determine whether or not there is any effect. When these crosses were performed, a 1.8% rate of X chromosome non-disjunction was observed in atm^8/Df females, compared to 0.48% in wild type, roughly a 3.5 fold increase (Fig. 4-6). For chromosome 4, a 0.93% rate of non-disjunction was observed, compared to 0.26% in wild type, also an approximate 3.5 fold increase (Fig. 4-6). Statistical analysis was performed on the data, using chi squared tests. The difference between the atm^8/Df and wild type non-disjunction rates were significant for both the X chromosome ($p=1.77 \times 10^{-10}$) and 4th chromosome ($p=0.0153$). In total, 6205 progeny from wild type flies and 5531 progeny from *atm* mutant flies were scored.

Section 4.3.4 – Repair defects and Grk mislocalization in atm *mutants are suppressible by removing* mei-W68

In *Drosophila*, the nuclease encoded by *mei-W68* is involved in inducing DSBs during meiotic recombination (McKim and Hayashi-Hagihara, 1998). Mutants for *mei-W68* are not capable of inducing these DSBs in the first place and therefore do not require repair pathways to fix the breaks. As a result, removing both copies of *mei-W68* in *spnB* and *okr* mutants prevents the accumulation of unrepaired DSBs which normally occurs in these mutants (Ghabrial and Schupbach, 1998). Unrepaired DSBs in oogenesis are thought to trigger a "meiotic checkpoint", which halts progression through oogenesis when genomic stability is compromised. Activation of the meiotic checkpoint results in

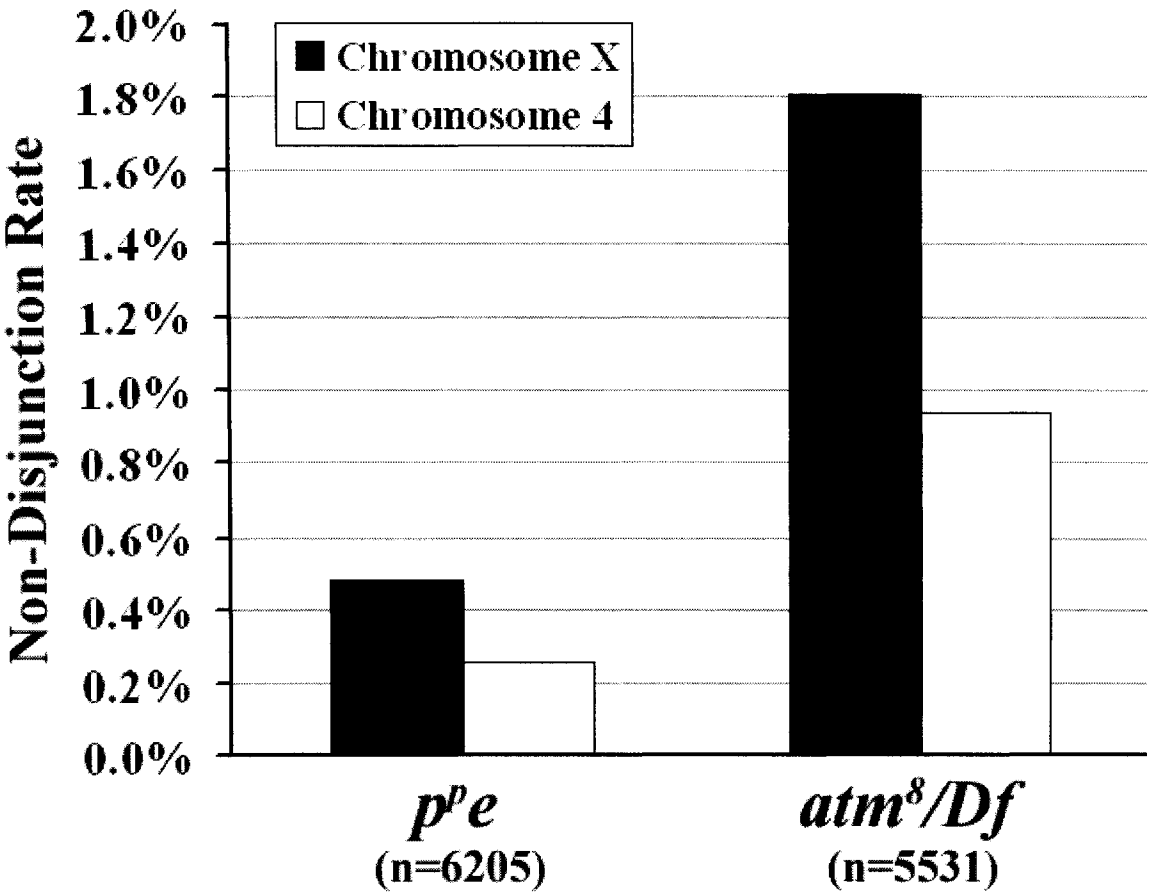

Fig 4-6 – *atm* mutant females exhibit increased rates of chromosome non-disjunction during meiosis. To test for chromosome non-disjunction, $p^p e$ or atm^8/Df females raised at 22°C were crossed to G035 males and the progeny were scored for non-disjunction events involving chromosomes X and 4. atm^8/Df females exhibit a 3.7 fold increase in non-disjunction of the X-chromosome compared to $p^p e$ females (black bars). Furthermore, atm^8/Df females exhibit a 3.6 fold increase in non-disjunction of the 4th chromosome compared to $p^p e$ females (white bars).

Grk mislocalization and abnormal karyosome phenotypes of *spnB* and *okr* mutants. Because removing *mei-W68* prevents the induction of breaks, *mei-W68; spnB* and *mei-W68; okr* double mutants do not exhibit these oogenesis defects, indicating suppression. We reasoned that if the persistent His2AV staining observed in *atm* mutants is also due to a defect in the repair of meiotic DSBs, and these breaks are activating the meiotic checkpoint, then removing *mei-W68* in an *atm* mutant background should also restore normal Grk localization and karyosome morphology (which is otherwise defective in *atm* mutants). This experiment had two goals: 1) To show that the persistent DSBs observed in *atm* mutants are due specifically to unrepaired meiotic DSBs, which removing *mei-W68* should selectively eliminate. 2) To show that the mislocalization of Grk and karyosome defects observed in *atm* mutants are a due to a response to these unrepaired DSBs, and not some other novel role of *atm.* Ovaries from *mei-W68$^{2-4472}$/mei-W68^{1}; atm^{8}/Df* females were dissected and compared to both wild type and *atm^{8}/Df.* After staining with antibodies to Grk, *mei-W68$^{2-4472}$/mei-W68^{1}; atm^{8}/Df* egg chambers displayed a restoration of both Grk localization and normal karyosome morphology, similar to wild type (Fig. 4-7A). The follicle cell defect however, was equally severe in *mei-W68$^{2-4472}$/mei-W68^{1}; atm^{8}/Df* (Fig. 4-7A and B) and *atm^{8}/Df* (same as Fig. 4-3B and E) egg chambers. Staining with antibodies to H2AV confirmed a lack of normal recombination breaks in *mei-W68$^{2-4472}$/mei-W68^{1}; atm^{8}/Df* germariums (Fig. 4-7C vs. D), as would be expected since *mei-W68* is required to induce these breaks. Furthermore, the persistent and strong staining of the oocyte and nurse cells, which is characteristic of *atm* mutants, is absent in *mei-W68; atm* double mutants (Fig. 4-7C).

Section 4.3.5 – Removing mei-41 *suppresses the developmental defects in* atm *mutant oocyte but enhances the follicle cell defect*

If activation of the meiotic checkpoint in response to unrepaired DSBs is responsible for the abnormal Grk localization and karyosome morphology in *atm* mutants, then mutating components of the checkpoint should suppress these phenotypes. Work from other labs has suggested that the ATM paralog, Mei-41, is the protein kinase responsible for detecting unrepaired meiotic DSBs and activating the meiotic checkpoint. A prediction of the hypothesis stated above is that *mei-41; atm* double mutants would

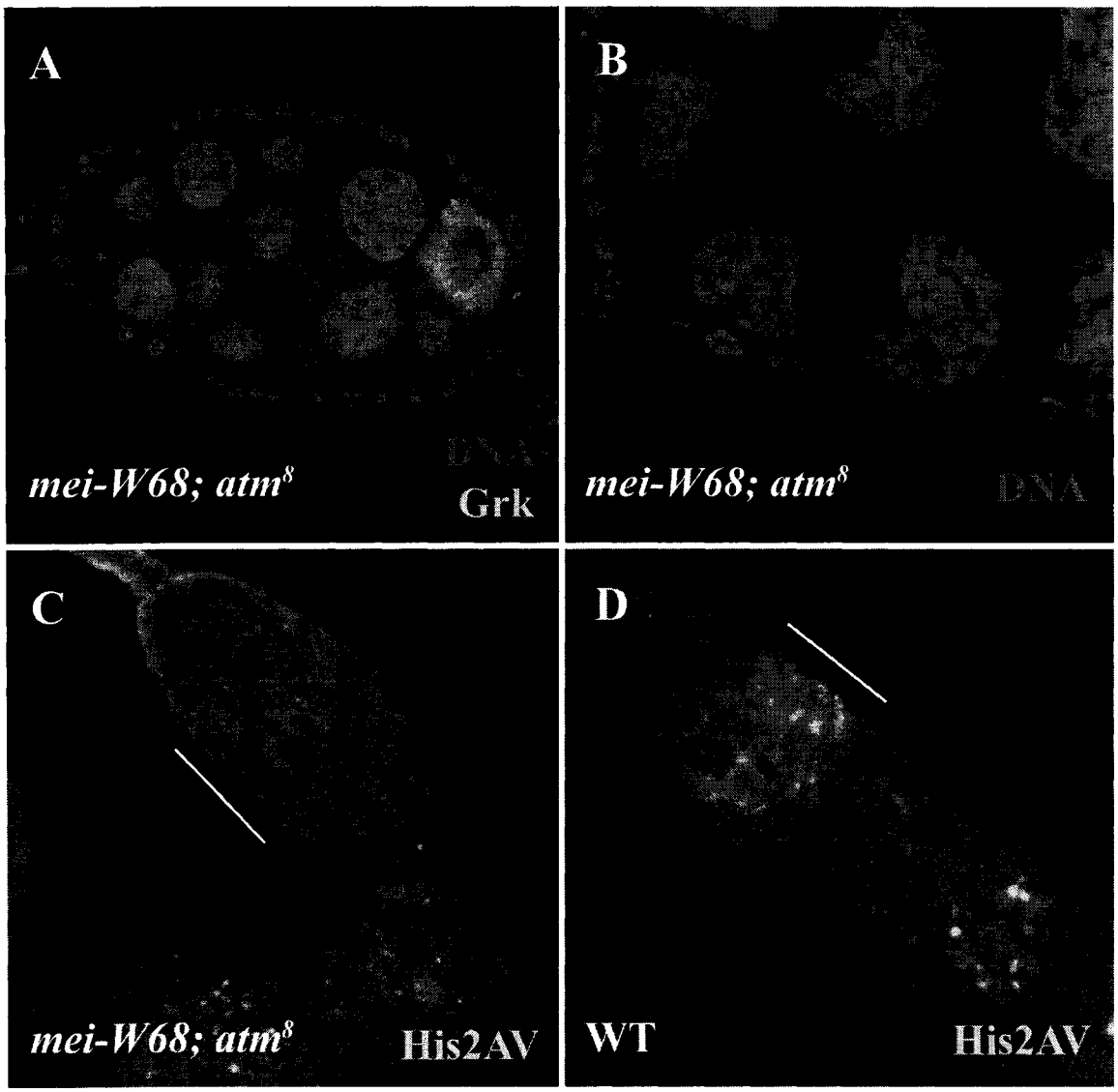

Fig. 4-7 – Mutations in *mei-W68* suppress the Grk localization and karyosome defects of *atm* mutants. (A-B) *mei-W68; atm^{8}/Df* double mutants were stained with DNA stains and antibodies to Grk. (A) These double mutants exhibit a marked restoration of both normal Grk localization (green) and normal karyosome morphology, which are normally disrupted in *atm* mutants (Fig. 3-4). (B) The follicle cell defect however, is not suppressed in *mei-W68; atm^{8}/Df* double mutants, as gaps are still present in the follicle cell layer. (C-D) *mei-W68; atm^{8}/Df* double mutants also exhibit an absence of the His2AV staining (green) that is normally observed in region 2a (outlined region) of wild type germariums. All *atm^{8}/Df* mutant females were raised at restrictive temperatures (24°C-25°C).

have normal Grk localization, because although there are unrepaired DSBs present in these flies, the meiotic checkpoint cannot be activated due to the absence of functional Mei-41. To investigate this possibility, ovaries from *mei-41; atm* double mutants were dissected and stained with DNA dyes and antibodies to Grk. atm^{8}/Df mutants were used for a positive control to ensure that these conditions were sufficient to perturb the temperature sensitive function of ATM and cause the full range of ATM phenotypes, including Grk mislocalization (Fig. 4-8A). As predicted, *mei-41; atm* ovaries exhibited a restoration of both normal Grk localization and the proper karyosome morphology (Fig. 4-8B, C, and D). Normal Grk staining was observed in 72% of $mei\text{-}41^{D3}$; atm^{8}/Df egg chambers examined (n=36), compared to only 13% in atm^{8}/Df egg chambers (n=38). Although this aspect of the *atm* phenotype is suppressed by removing both copies of *mei-41*, a contradictory enhancement of other aspects of the *atm* phenotype was also observed in these double mutants. When *mei-41; atm* egg chambers were examined with antibodies to the follicle cell membrane marker, Hts, the follicle cell gaps that are typical of *atm* mutants were found to be significantly enhanced in the *mei-41; atm* double mutants (Fig. 4-8F). Optical cross-sections of *mei-41; atm* egg chambers that lacked normal follicle cells altogether were frequent (Fig. 4-8C). The result of the enhanced follicle cell loss is striking. Many egg chambers are abnormally large and contain multiple oocytes that stain with Grk, as well as many (greater than the normal number of 15) nurse cells (Fig. 4-8E). In general, nurse cells are significantly larger towards the posterior end of these large egg chambers, suggesting that they represent multiple cysts that are in different stages of oogenesis. Furthermore, germariums from *mei-41; atm* double mutants are often longer than normal and contain nurse cells from egg chambers that should have already formed egg chambers (Fig. 4-8I). These large egg chambers and long germariums could be explained if the enhanced follicle cell defect is interfering with the budding off of cysts from the germarium to form distinct egg chambers. To investigate this possibility, germariums from *mei-41; atm* double mutants were stained with antibodies to Hts, a marker for follicle cell membranes. In wild type ovaries, follicle cells proliferate in the germarium and envelope the cyst in region 3, just prior to budding (Fig. 4-8G). In *mei-41; atm* double mutants, a significantly smaller numbers of follicle cells in region 3 of the germarium was observed and the envelopment of cysts was not complete (Fig. 4-8H).

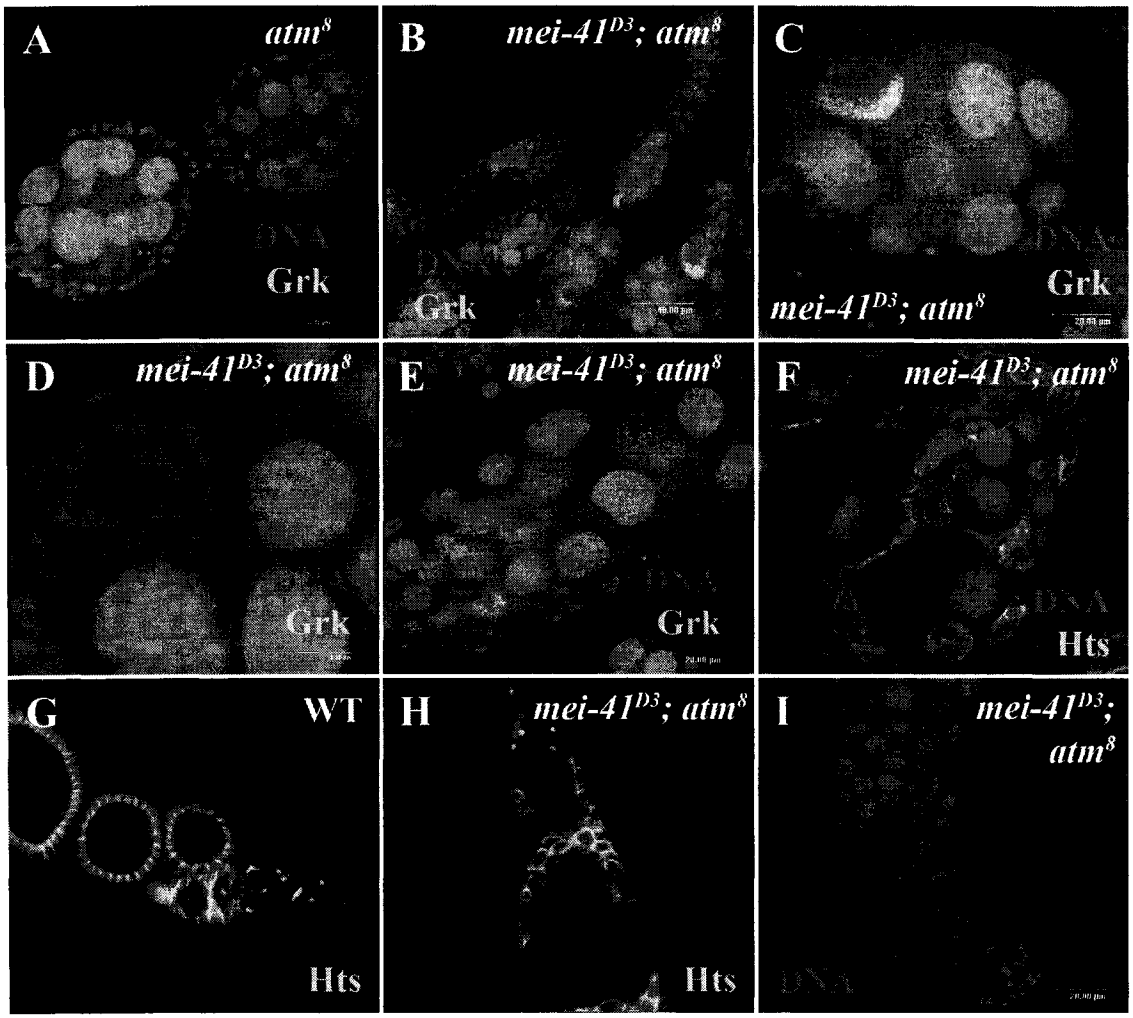

Fig. 4-8 – Mutations in *mei-41* suppress Grk mislocalization and karyosome abnormalities in *atm* mutants, but enhance the follicle cell defect. (A) The *atm* mutant phenotype is characterized by abnormal karyosome morphology, failure to properly localize Grk, and a severe follicle cell defect (B-D) *mei-41; atm* mutants exhibit a restoration of both normal Grk localization (B-C) and normal karyosome morphology (D). (C, E, and F) The follicle cell defect however, is enhanced in *mei-41; atm* double mutants compared to *atm* mutants. (F) Staining with antibodies to Hts, a marker of follicle cell membranes, was performed to visualize follicle cells in *mei-41, atm* double mutants. (E) Concurrent with the enhanced follicle cell defect, abnormally large egg chambers have been observed that contain multiple karyosomes, each with Grk staining, and a large number of nurse cells. The nurse cells towards the posterior end of such egg chambers (right side in E) tend to be larger than those on the anterior end. (G-I) *mei-41; atm* germariums are also abnormally long compared to wild type. (G-H) Staining of germariums with antibodies to Hts was performed in order to investigate the envelopment of cysts by follicle cells during this stage of oogenesis. (G) In wild type germariums, region 3 cysts are enveloped by follicle cells and bud off shortly thereafter to form egg chambers. (H) In *mei-41; atm* germariums there appear to be insufficient follicle cells for proper budding. atm^8 mutants used here are all atm^8/Df hemizygotes and are raised at restrictive temperatures (24°C-25°C).

Section 4.3.6 – atm *has genetic interactions with both* chk2 *and* grp

Chk2 and Grp are checkpoint kinases that are activated by ATM/ATR kinases in response to checkpoint stimuli (Abraham, 2001). They proceed to phosphorylate their own downstream targets to carry out the checkpoint response. In the meiotic checkpoint, it has been demonstrated that Mei-41 and Chk2 are involved in carrying out the meiotic checkpoint response (Ghabrial and Schupbach, 1999; Abdu et. al., 2002). If the meiotic checkpoint is triggered by the unrepaired recombinational DSBs in *atm* mutants, then we would predict that mutating *chk2* would suppress the Grk mislocalization and karyosome defects, as is seen in *mei-41; atm* double mutants. To test this hypothesis, ovaries from *chk2; atm* and *grp; atm* double mutants were dissected and stained with antibodies to Grk. A strong restoration of Grk localization and karyosome morphology was observed in *chk2; atm* double mutants (Fig. 4-9A, B and G). 60% of *chk2; atm* egg chambers possess normal Grk staining (n=30), compared to 13% in *atm* mutants alone (n=38) (Fig. 4-9A and G). Furthermore, 88% of *chk2; atm* egg chambers had a normal karyosome (n=40), compared to only 20% in *atm* mutants (n=40) (Fig. 4-9B and G). To confirm that this suppression was due to a defective meiotic checkpoint response and not to a reduction in the amount of DSBs, *chk2; atm* ovaries were also stained with antibodies to His2AV. *chk2; atm* ovarioles exhibit the abnormally strong and persistent His2AV staining in the oocytes and nurse cells that is characteristic of *atm* mutants (Fig. 4-9C). There was also a less pronounced suppression of the oocyte defects in *grp; atm* double mutants. 27% of *grp; atm* egg chambers have a normal Grk staining pattern (n=30) and 51% had normal karyosome morphology (n=41) (Fig. 4-9D, E, and G). In addition to suppressing the Grk and karyosome phenotypes, *chk2; atm* double mutants displayed an enhanced follicle cell defect, similar to what is seen in *mei-41; atm* double mutants. These *chk2; atm* mutant ovarioles often contain long germariums with cysts that have failed to bud off, as well as large egg chambers with multiple Grk positive oocytes and abnormally large numbers of nurse cells (Fig. 4-9F).

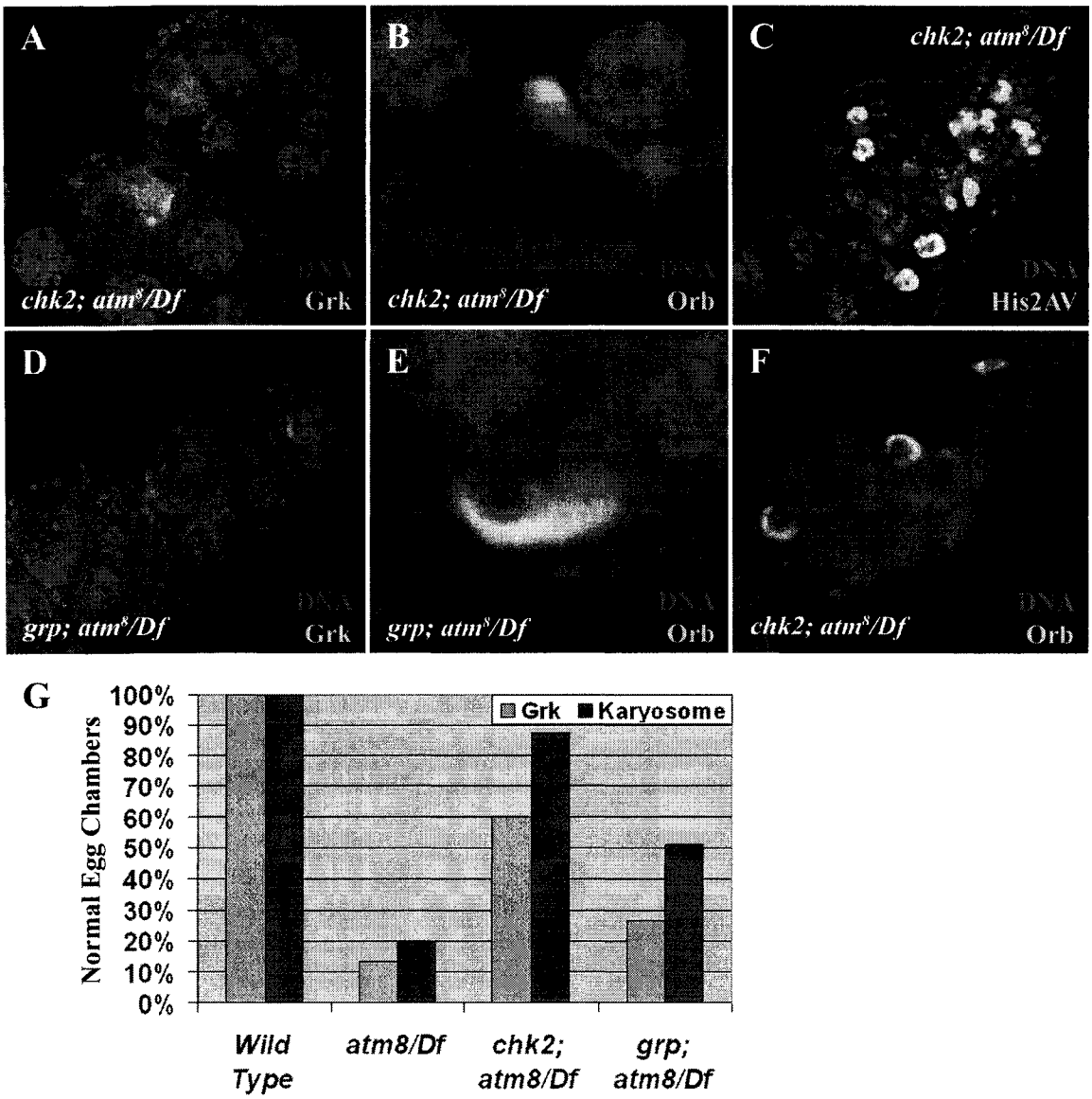

Fig 4-9 – Mutations in *grp* and *chk2* suppress the Grk mislocalization and karyosome abnormalities associated with mutations in *atm*. (A) Staining of *chk2; atm* ovaries with antibodies to Grk. These double mutants exhibit a restoration of normal Grk localization. (B) Staining with antibodies to Orb allow the karyosome to be recognized and demonstrates a restoration of normal karyosome morphology in *chk2, atm* double mutants. (D-E) This suppression is also seen in *grp; atm* double mutants, but to a lesser extent. (C) His2AV staining persists in *chk2; atm* double mutants, similar to *atm* mutants, indicating that this suppression is not due to a decrease in DSB formation. (F) *chk2; atm* mutants also exhibit a enhancement of the follicle cell defect, characterized by large egg chambers with multiple oocytes, each with Grk staining, and a large number of egg chambers. (G) Comparison of suppression of *atm* karyosome and Grk mislocalization phenotypes by mutation of *chk2* or *grp*. All atm^{8}/Df mutants were raised at restrictive temperatures (24°C-25°C).

Section 4.3.7 – mei-41 *and* atm *are redundantly required to phosphorylate His2AV in ovaries*

Phosphorylation of His2AV is a early event following the induction of DSBs (Jang et. al., 2003). A similar phenomena occurs in human tissue culture cells, where ATM is known to phosphorylate His2AX (His2AV in *Drosophila*) when DSBs are present (Burma et. al., 2001), however ATM function is not required for this phosphorylation to occur (Stiff et. al., 2004; Wang et. al., 2005). This observation suggests that another kinase, possibly ATR, can also phosphorylate His2AX. In *Drosophila*, abnormally strong phospho-His2AV staining is present in *atm* mutants, also suggesting that another kinase is able to phosphorylate His2AV in response to DSBs in *Drosophila* ovaries. To determine the relative roles of ATM and Mei-41 (ATR) in the phosphorylation of His2AV, *mei-41; atm* double mutant egg chambers were stained with antibodies to phospo-His2AV and compared to the wild type and *atm* mutant patterns. In wild type germariums, His2AV staining can be seen in region 2a of the germarium, but disappears soon after, before the end of region 2b (Fig. 4-10A). *atm* mutants, however, exhibit strong and persistent phospho-His2AV staining past region 2 (Fig. 4-10B). Furthermore, when His2AV staining is first observed in region 2, it is more intense in *atm* mutants compared to wild type (Fig. 4-10A vs. B). *mei-41; atm* double mutants display no phospho-His2AV staining whatsoever (Fig. 4-10C). The normal phospho-His2AV staining that appears and disappears within region 2 of wild type germariums is also absent from these double mutants, as is the persistent staining otherwise seen in *atm* mutants.

Section 4.3.8 –The atm *mutant follicle cell defect is a cell autonomous phenotype*

Because there is significant communication between the follicle cells and the underlying germline cells (Van Buskirk and Schupbach, 1999), we thought it might be possible that the follicle cell apoptosis could be triggered cell non-autonomously by unrepaired DSBs in the oocyte and nurse cells. To address this possibility, clonal analysis was performed to generate populations of *atm* mutant follicle cells or germline cells in a otherwise heterozygous background. The e22c gal4 driver was used to specifically express the FLP recombinase in follicle cells to generate follicle cell clones. *atm* mutant

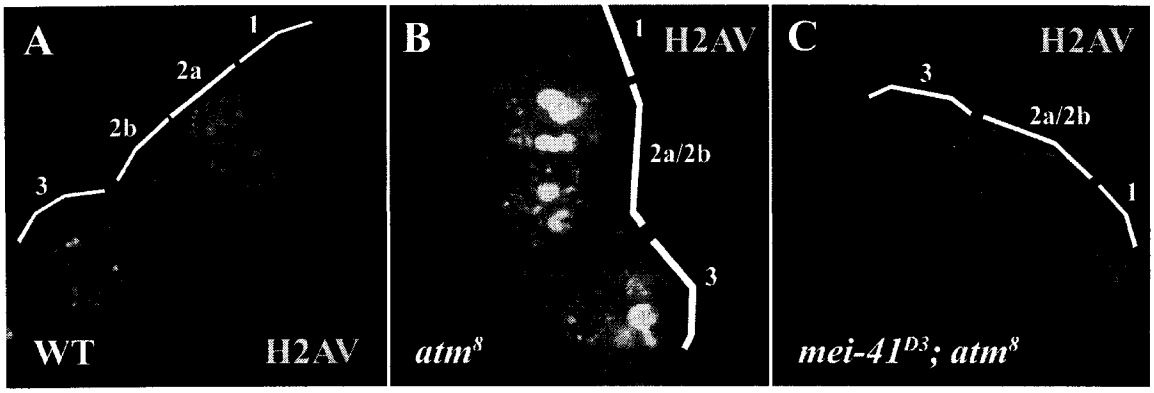

Fig. 4-10 – *mei-41* and *atm* are redundantly required for the phosphorylation of His2AV in response to DSBs. (A) Wild type ovaries exhibit developmentally timed DSBs in region 2a of the germarium. These breaks induce the phosphorylation of His2AV (green), allowing it to be used as a marker for DSBs. (B) *atm* mutants exhibit abnormally strong, and persistent His2AV phosphorylation. (C) *mei-41; atm* double mutants lack not only the strong His2AV signal typical of *atm* mutants, but also the normal His2AV signal in region 2a of the germarium, suggesting a inability to phosphorylate His2AV. atm^{8} mutants used here are all atm^{8}/Df hemizygotes and were raised at restrictive temperatures (24°C-25°C).

clones were marked by the loss of *arm-LacZ*, which expresses throughout somatic and germline components of the ovaries. The *atm* mutant clones contained a significant number of follicle cells with apoptotic morphology, suggesting that the defect is cell autonomous (Fig. 4-11C and D). To confirm that the nurse cell and oocyte defects were not inducing apoptosis in the surrounding follicle cells, the reciprocal experiment was also done, using heat shock induction of the FLP recombinase to induce clones in the germline. Results from this experiment confirmed that egg chambers with entirely *atm* mutant germline cells have perfectly normal follicle cells (Fig. 4-11A and B). The abnormal karyosome phenotype was present in these clones however (Fig. 4-11B, arrow), suggesting that the activation of the meiotic checkpoint in *atm* mutants did not require mutant follicle cells. Taken together, these data suggest that the follicle cell death is cell autonomous and not triggered by problems in the underlying germline cells.

Section 4.4 – Discussion

Eggs laid by *atm* females exhibit two defects, including a thin eggshell and a ventralized phenotype, characterized by fusion of the dorsal appendages. These experiments have provided data that explain both of these defects, based on events that occur during oogenesis. Our results suggest that *atm* mutant follicle cells undergo ectopic apoptosis during oogenesis in a *p53* independent fashion, resulting in the formation of gaps in the follicle cell layer that surrounds each egg chamber. Because the follicle cells are responsible for laying down the eggshell during late oogenesis, these follicle cell gaps can explain the thin eggshell phenotype of eggs laid by *atm* mothers. The follicle cell death is different from the ectopic apoptosis that has been observed in *atm* mutant eye tissue which was shown to be largely dependent on *p53*. The common theme that links the apoptosis observed in these different tissues is that they both occur in proliferating somatic cells. In the eye-antennal discs, only proliferating cells that are ahead of the morphogenic furrow exhibit spontaneous apoptosis. Follicle cells continue to divide up to stage 7 of oogenesis. Although we have not determined if endoreplicating follicle cells from stage 7 forward are protected from apoptosis, we have observed apoptosis early in oogenesis when follicle cells are known to be proliferating. This is consistent with a hypothesis where proliferating cells are particularly sensitive to loss of ATM function.

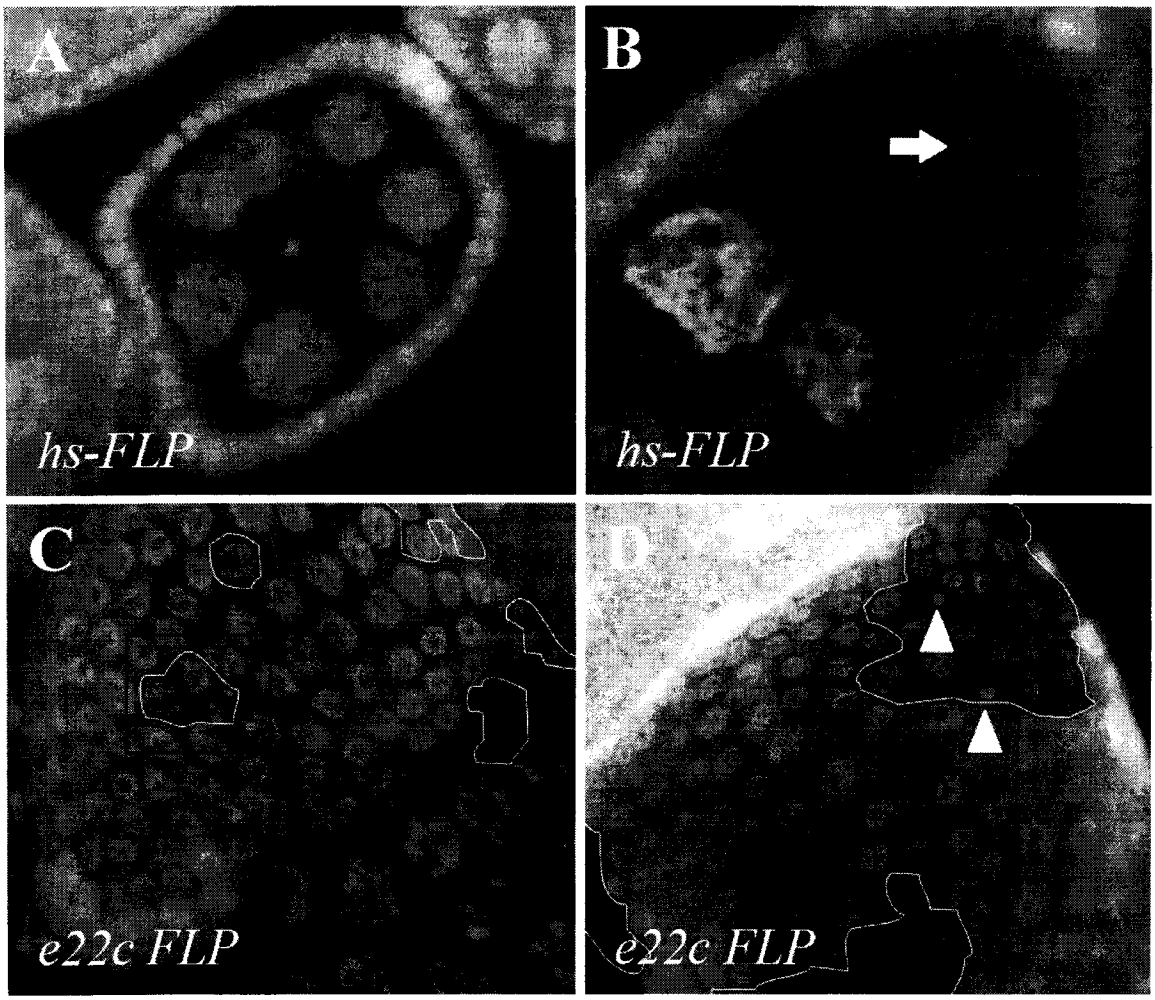

Fig. 4-11 – *atm* follicle cell and oocyte morphology defects are cell autonomous. (A-B) Genetic mosaics made using the hs-FLP / FRT system and stained for DNA (red) and with antibodies to LacZ (green). Follicle cells stain with antibodies to LacZ (green), indicating that they are heterozygous for the atm^2. Nurse cells and oocytes are LacZ negative, indicating that are homozygous for this same allele. In these mosaics, the mutant oocyte often exhibits the abnormal oocyte morphology characteristic of *atm* mutants (arrow in B), however the follicle cells are normal (A and B). (C-D) Genetic mosaics were also made using a follicle cell specific Gal4 to drive expression of the FLP recombinase. Some follicle cells and all nurse cells and oocytes stain strongly with antibodies to LacZ (green), indicating that they are heterozygous for the atm^2. Patches of follicle cells are LacZ negative, indicating that are homozygous for this same allele. Patches of homozygous mutant cells are outlined in white. These patches often contain follicle cells with apoptotic morphologies (inset in C, arrowheads in D)

A major question that remains is to determine what the trigger is for this apoptosis. A tempting hypothesis is that spontaneous, unrepaired somatic DSBs are inducing apoptosis. This hypothesis is based on ATM's known role in the repair of somatic DSBs in the cell. However, when His2AV staining was performed, no evidence was found for DSBs in the follicle cells. Since there is inappropriate staining in the nurse cells and oocyte, we thought that this damage might be inducing apoptosis in the surrounding follicle cells. Since there is so much known communication between the follicle cells and the underlying germline cells (Van Buskirk and Schupbach, 1999), this seemed like a very real possibility. However, clonal analysis refuted this hypothesis, demonstrating that whatever is triggering the apoptosis of the follicle cells is cell autonomous and therefore present in the follicle cells. Despite the absence of His2AV in the follicle cells, there still might be breaks present which are not detectable for some reason. First of all, if breaks were present we expect that they would be spontaneous breaks rather than Mei-W68 induced breaks, as seen in the germline cells. Therefore, there may be far fewer foci and consequently less signal, making detection an issue. Perhaps the His2AV antibody is not sensitive enough to detect a few, rare unrepaired DSBs. This is a very real possibility, since the antibody is associated with considerable background, non-specific staining. Another possible explanation is that perhaps Mei-41 cannot phosphorylate His2AV in the follicle cells, as it can in the germline. Although *atm* and *mei-41* appear to be redundantly required to phosphorylate His2AV in germline cells, perhaps in follicle cells there is a strict requirement for ATM to phosphorylate His2AV. Thus, *atm* mutants might not show phospho-His2AV staining in the follicle cells, even if DSBs are present. One problem with this idea is that it assumes that Mei-41 cannot phosphorylate His2AV in follicle cells, yet we have also demonstrated that Mei-41 is present and active in these cells, since removing it enhances the follicle cell defect of *atm* mutants.

Another possible trigger for the follicle cell apoptosis is telomere fusion events. Experiments in larval neuroblast cells have demonstrated that ATM plays a role in the proper maintenance of telomeres, because *atm* mutants display abnormally high rates of telomere end to end fusions (Silva et. al., 2004; Song et. al., 2004; Bi et. al., 2004; Oikemus et. al., 2004). If the kinetochores of fused chromosomes are captured by

opposite spindle poles during mitosis, these fusion events can lead to chromosome bridges, and subsequent breakage during anaphase/telophase (McClintock, 1939). Such events could also be occurring in the follicle cells meaning that either the telomere fusions themselves, or the subsequent breakages, could be triggering ectopic apoptosis. The problem with this explanation is that it does not explain the lack of phospho-His2AV staining in the follicle cells, which should lead to inappropriate levels of double strand breaks that should stain with phospho-His2AV antibodies.

It is interesting that removing *mei-41* enhances the follicle cell defect in the *atm* mutants. Our results suggest that there are far fewer follicle cells present in *mei-41;atm* double mutants compared to *atm* mutants. *mei-41;atm* ovaries contain egg chambers with few follicle cells, and fused egg chambers with multiple oocytes and extra nurse cells. In region 3 of the germarium, the envelopment of developing cysts by follicle cells and the formation of inter-follicular stalk cells from subpopulations of follicle cells, is critical for budding off from the germarium and the formation of egg chambers. If there is a shortage of follicle cells, budding may not always happen when it should, resulting in large egg chambers with multiple oocytes and extra nurse cells. There are two specific observations which support the failure to bud hypothesis. First, Hts/DNA staining has indicated that cysts in the germarium that are not properly enveloped by follicle cells and result in a long germarium, suggesting a problem with budding. The second observation is that the fused egg chambers show nurse cells of different developmental stages. Essentially, the groups of nurse cells get larger towards the posterior end. This supports the idea that there are actually multiple fused cysts, rather than one cyst which went through multiple extra divisions. This suggests that the large, multiple oocyte egg chambers is probably not due to a cell cycle defect and is more likely a failure to bud, resulting from increased loss of follicle cells.

Why are the gaps worse in *mei-41; atm* mutants? That is to say, why are there fewer follicle cells in *mei-41;atm* double mutants compared to *atm* mutants? There are two attractive explanations for this. If the follicle cell apoptosis is triggered by unrepaired DSBs or by improper telomere interactions, it is possible that Mei-41 might be partly able compensate for ATM in repairing these breaks or maintaining telomeres. This may be a minor role compared to ATM, which could explain why there is still apoptosis in *atm*

mutants alone but not *mei-41* mutants alone. Removing both gene functions however, aggravates the problem, resulting in more apoptosis. Another possibility is that *mei-41* has a checkpoint role in these follicle cells. For example, if telomere fusions are rampant in *atm* mutants, perhaps Mei-41 can activate a checkpoint which gives the cell a chance to resolve the fusion through a *atm*-independent mechanism. The fusion may not always be resolved, explaining why *atm* mutants still exhibit apoptosis, but it could give the cells a second chance at repair and survival. When *mei-41* is removed the cells would have no "second chance" and apoptotic cell death would be more frequent as a result. Analysis of *chk2; atm* double mutants lends support to the latter checkpoint hypothesis. *chk2* is a downstream checkpoint target of ATM kinases, including *mei-41*, but is likely not involved in DNA repair or telomere maintenance directly. Because *chk2; atm* double mutants have a similar enhancement of the follicle cell defect as *mei-41; atm* double mutants, the checkpoint involving *mei-41* and *chk2* might be at play in these cells. Although no further work has been done to characterize this checkpoint, *mei-41* and *chk2* are well known to be involved in halting cell cycle progression at different points in the cell cycle in response to different stimuli. Based on our results thus far, we propose that a *mei-41* and *chk2* dependent checkpoint is engaged in *atm* mutant follicle cells. We speculate that this checkpoint may halt cell cycle progression in response to unrepaired DSBs or fused telomeres, caused by lack of functional ATM. This would give the cell a second chance to resolve these problems and avoid apoptotic death. However, if the checkpoint is perturbed by a mutation in *mei-41* or *chk2*, cells could proceed uninhibited through the cell cycle, resulting in increased genomic instability and apoptosis.

In addition to the thin chorion phenotype, eggs laid by *atm* mutant mothers often have fused or missing dorsal appendages, suggesting a defect in dorsal/ventral patterning. This is interesting since other genes involved in the repair of DSBs during meiotic recombination also exhibit this phenotype, including *spnA*, *spnB*, and *okr*. An essential step of normal meiotic recombination is the induction, and subsequent repair, of DSBs. The absence of *spnB* or *okr* results in the persistence of breaks past region 2b of the germarium where they should normally be repaired (Jang et. al., 2003). These persistent breaks are thought to activate the so called "meiotic checkpoint" which interferes with normal progression through oogenesis, including localization of the Grk signaling protein

and formation of the karyosome (Ghabrial and Schupbach, 1999). Because Grk is involved in establishing dorsal/ventral polarities during oogenesis, a failure to localize Grk properly in these mutants could lead to a ventralized phenotype in mature eggs. Therefore, there is an established link between the repair of DSBs in oogenesis and dorsal/ventral patterning. Our experiments have demonstrated that ATM is another protein involved in the repair of DSBs during meiotic recombination and that when *atm* is mutated, this meiotic checkpoint is activated as a response to the unrepaired breaks. The established hallmarks of this checkpoint's activation are present in *atm* mutants, namely that Grk is mislocalized and the karyosome is abnormal. This abnormal Grk localization in *atm* mutants provides an explanation for the fused dorsal appendages that have been observed in eggs laid by *atm* mutant mothers.

To make the conclusion that ATM is involved in the repair of recombinational DSBs, it is important to demonstrate that *atm* mutants have unrepaired breaks that are a specific result of meiotic recombination and are not simply spontaneous or a result of some other role for ATM. Staining with antibodies to phospho-His2AV has shown that *atm* mutants have ectopic DSBs that are seen exclusively in the germline cells (nurse cells and oocyte). It is interesting that only some of the nurse cells show His2AV staining but those that do stain show a very strong signal (Fig. 4-5B and D). Although this pattern might seem odd initially, it is actually consistent with a role for *atm* in repairing DSBs produced during recombination. This is because formation of the synaptonemal complex and the induction of DSBs only occurs in some of the nurse cells (McKim et. al., 2002). Those that begin recombination would be expected to have DSBs that accumulate and show strong His2AV staining, when DSB repair is compromised. The nurse cells with no His2AV staining on the other hand, probably never initiated recombination. Recombination is always initiated in the oocyte, hence why the oocyte in *atm* mutants always shows persistent DSBs past region 2b of the germarium. There are two more observations which support the idea that the persistent breaks in *atm* mutants are a result of a meiotic repair defect and are not spontaneous. First, *atm* females which are grown at room temperature have increased frequencies of chromosome non-disjunction in their progeny. Because the formation of chiasma from recombination are critical for chromosome segregation, a non-disjunction phenotype suggests a defect in meiotic

recombination (although not necessarily DSB repair). The second piece of evidence is that the strong His2AV signal seen in *atm* females can be suppressed by removing both copies of *mei-W68*. Mei-W68 is a protein required for the formation of DSBs during meiotic recombination and would not be expected to affect the occurrence of "spontaneously" generated breaks. Therefore, this suppression result strongly suggests that the ectopic breaks in *atm* mutants are the result of a defect in the repair of DSBs induced by Mei-W68 during meiotic recombination. Removing *mei-W68* however, does not suppress the follicle cell defect in *atm* mutants. This was expected since *mei-W68* has no role in somatic cells, as they do not undergo meiotic recombination. Therefore, removing *mei-W68* would not be expected to modify the follicle cell defect. Our results also demonstrate that removing *mei-W68* restores normal Grk localization and karyosome morphology in *atm* mutants. This is likely because without *mei-W68*, no meiotic DSBs are produced and the repair process in which *atm* is involved is not needed. Without these persistent breaks, the meiotic checkpoint would not be triggered, and thus Grk localization and karyosome formation should occur normally, which is what we have demonstrated here (Fig. 4-4).

To further test the hypothesis that the oocyte defects in *atm* mutants are caused by activation of the meiotic checkpoint, we attempted to suppress the Grk and karyosome defects by removing known components of the checkpoint pathway. The sensor of persistent DSBs is thought to be Mei-41, the *Drosophila* ATR ortholog. When Mei-41 is activated by persistent meiotic DSBs, it phosphorylates Chk2, a checkpoint transducer (Abdu et. al., 2002). Although the targets of Chk2 are not well characterized in this developmental context, the checkpoint pathway is also known to require Vasa at some point (Abdu et. al., 2002). Since Vasa is involved in protein translation and karyosome formation, its involvement could explain the Grk mislocalization and karyosome defects. To test whether activation of this checkpoint is responsible for the oocyte defects seen in *atm* mutants, *mei-41; atm* and *chk2; atm* double mutants were constructed. In both of these double mutant combinations, Grk localization and karyosome morphology were restored to normal. This result supports the idea that the meiotic checkpoint is activated in the *atm* phenotype. In these double mutants, persistent DSBs would not be expected to disappear, since the DNA DSB repair process would be compromised by the absence of

ATM. What has changed in the double mutants is simply the ability of the cell to recognize that these ectopic breaks are present. In accordance with this, we have observed that DSBs, marked with antibodies to His2AV, are still present in *chk2;atm* mutants despite the restoration of Grk localization and normal karyosome morphology.

The genetic interaction of *atm* with *mei-41* is complex. On one hand, Mei-41 is responsible for detecting breaks in the oocyte that are unrepaired when *atm* is absent, and activating the meiotic checkpoint. On the other hand, we have observed situations where *mei-41* and *atm* seem to be acting together in a common process. One example of this is the phosphorylation of His2AV in response to meiotic DSBs. His2AV is a histone variant whose phosphorylated form is located around DSBs. In human tissue culture cells, the phosphorylation of His2AX (which serves a similar function as His2AV) is known to involve ATM. That being said, His2AX can be phosphorylated even without ATM, suggesting that something else can perform this role as well. Our results demonstrate that this is true in *Drosophila* as well, since phospho-His2AV staining can still been observed in *atm* mutants. In *mei-41; atm* double mutants however, there is no phospho-His2AV staining whatsoever. This suggests that either ATM or Mei-41 can phosphorylate His2AV in response to meiotic DSBs and that one of the two must be present for phosphorylation to occur. Previous reports from other labs have also suggested that there is a link between the repair of DSBs and His2AV phosphorylation (Jang et. al., 2003). This was based on the observation that repair defective mutants, such as *spnB* and *okr*, have delayed His2AV phosphorylation (Jang et. al., 2003). We postulate that this link may be due to the activity of ATM, since we have demonstrated that ATM function is required for both repair of DSBs and His2AV phosphorylation. In *spnB* and *okr* mutants it is possible that the observed delay in His2AV phosphorylation is caused by an inability to properly assemble the recombination complex around the break site, which might affect the phosphorylation of His2AV by ATM. Interestingly, there seems to be no delay in His2AV phosphorylation in *atm* mutants. Not only does phospho-His2AV appear normal in region 2a of the germarium, but this staining is significantly more intense than wild type germariums. This implies that Mei-41 is not only able to compensate for ATM's role in His2AV phosphorylation, but perhaps also overcompensates. This

abnormally intense His2AV staining is present in both nurse cells and the oocyte of *atm* mutants and continues well into the vitellarium.

The various genetic interactions reported here between *atm* and *mei-41* may seem contradictory initially, because we have observed both enhancement and suppression of different *atm* phenotypes, when *mei-41* function is also removed. However, all the results we have obtained are consistent with previously established roles for ATM/ATR kinases because they can be explained by *Drosophila* ATM and Mei-41 acting in various aspects of the cellular response to DSBs. The observed similarities and differences between ATM and Mei-41 activities in the ovaries are summarized in Fig. 4-12. In the germline cells, DSBs are induced in a developmentally regulated fashion by *mei-W68*. In response to these breaks, the histone variant His2AV is phosphorylated at sites near the DSBs. We have demonstrated that *atm* and *mei-41* are redundantly required for phospho-His2AV staining, suggesting that they both play a role in this phosphorylation event (Fig. 4-12). Next, the DSBs need to be repaired to protect genomic stability and allow meiotic recombination to occur. We have demonstrated that *atm* is required for the repair process as well, since *mei-W68* dependent breaks persist in *atm* mutant ovaries (Fig. 4-12). *Drosophila* ATM's role in the repair process is likely through phosphorylation and recruitment of repair proteins. There is evidence from human cells, which has implied that during somatic DNA repair through homologous recombination, ATM is required for the assembly of a recombination complex which includes Rad51 and Rad54 (Chen et. al., 1999; Morrison et. al., 2000). *spnA, spnB,* and *spnD* are *Drosophila* homologs of Rad51 and mutants affected in these genes display DSB repair errors during oogenesis similar to what is seen in *atm* mutants. Therefore, it is likely that *Drosophila* ATM's role in the repair process involves formation of the complex that involves Okr and the Spn class of proteins. The role of Mei-41 in oogenesis also appears to involve the cellular response to DSBs, although not in the repair process itself. Instead, Mei-41 detects DSBs that are not repaired in a timely fashion (as in *atm* mutants) and responds by activating the meiotic checkpoint that prevents progression through oogenesis (Fig. 4-12). As a result of this role, removing *mei-41* and *chk2* in an *atm* mutant background allows normal progression through events of oogenesis, including Grk localization and karyosome formation, despite the presence of unrepaired breaks.

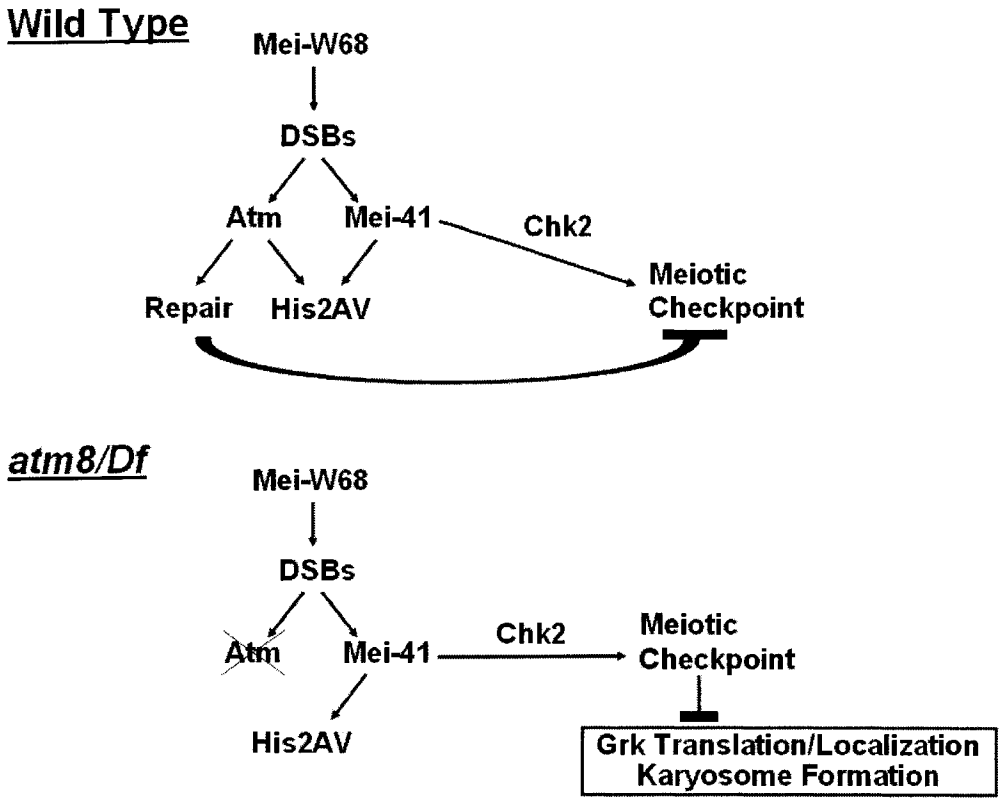

Fig. 4-12 – Model explanation of genetic interaction data between *atm* and *mei-41* in the germline. *mei-W68* is required for the induction of DNA DSBs at the onset of meiotic recombination. This study has demonstrated that *atm* is required to repair these breaks in a timely fashion. Mutation of *atm* (lower diagram), results in the persistence of DSBs and the subsequent activation of a *mei-41* and *chk2* dependent checkpoint that prevents orderly progression through oogenesis. The hallmarks of checkpoint activation, Grk mislocalization and abnormal karyosome morphology, are present in *atm* mutant ovaries. The repair of DSBs and checkpoint activation provides a context where *atm* and *mei-41* gene products can both detect DSBs, but function in temporally distinct fashions with different targets. ATM is involved in the activation or recruitment of repair proteins whereas Mei-41 activates checkpoint components if the DSBs persist past region 2 of the germarium. However, we have demonstrated that in within the same cells, *atm* and *mei-41* also have redundant roles and can function in parallel to phosphorylate His2AV in response to DSBs.

Although the events leading to the follicle cell defect in *atm* mutants are not entirely understood, it is tempting to speculate that they are also a result of ATM's involvement in the cellular response to DSBs or telomere fusion events. As mentioned, telomere fusion events can lead to chromosome breakage, implying that telomere maintenance and the prevention of DSBs are closely linked. If ectopic chromosome breaks are present in *atm* mutant follicle cells, they could be a trigger for apoptosis. The enhancement of the follicle cell defect by removing *mei-41* and *chk2*, both known checkpoint genes, suggests that engagement of a Mei-41 dependent checkpoint may help reduce the cell death in *atm* mutants. Again, this constitutes a role for *mei-41* in the cellular response to DSBs, assuming that this checkpoint is triggered by DSBs.

To summarize, the genetic interaction between *mei-41* and *atm* is complicated, but all of the results presented here are consistent with roles for both ATM and Mei-41/ATR kinases in the response to DSBs. There is evidence that ATM is involved in the phosphorylation of His2AV as well as the repair of DSBs produced during recombination. In the follicle cells, ATM might also be involved in the repair of DSBs that are produced either spontaneously and/or as a result of chromosome breakage after telomere fusions. Mei-41 seems to be also be involved in the phosphorylation of His2AV and also in the activation of the meiotic checkpoint response to DSBs in the oocyte. Mei-41 also has a role in mitotically dividing follicle cells, where it may have a role in the checkpoint response to DSBs and/or telomere fusion events.

Chapter 5: Conclusion

The initial goal of this project was to characterize the eight mutant alleles of *Drosophila atm* isolated by our laboratory. Analysis was focused on three fronts. First, the mutant alleles were sequenced in an attempt to increase our understanding of the ATM protein on a molecular level. Second, the response of *atm* mutants to DNA DSBs was examined to determine if known cellular roles of ATM that have been established in other organisms, such as somatic DNA repair and checkpoint activation, are conserved in *Drosophila*. Third, whole organism phenotypes associated with *atm* mutations, such as the rough eye phenotype and female sterility, were further investigated in an attempt to determine how known cellular roles of ATM relate to specific developmental events. Progress has been made on all three fronts that provides a basis for further studies to investigate the function of ATM in *Drosophila*. This section will attempt to summarize the most relevant results from this project and outline how they address these objectives.

Several regions of the ATM are critical for protein function:

When the eight alleles of *atm* were sequenced, the majority of the alleles were found to encode proteins with premature truncations that would result in loss of the conserved domains of the ATM protein. This result is consistent with what is already know about ATM from other organisms: namely, that these conserved domains, and in particular the kinase domain, are required for ATM function. Because these regions are relatively well conserved, it is not at all surprisingly that this is also the case in *Drosophila*. Amongst these alleles however, there are two that are of particular interest as they provide novel insight into important regions of the protein that are not well characterized. The first of these alleles is atm^4, which has a single amino acid change affecting the poorly conserved, amino terminal half of the protein. Although the nature of this part of the protein remains largely uninvestigated, recent studies have suggested that it may be important for DNA binding (Llorca et. al., 2003) and/or the formation of protein complexes (Fernandes et. al., 2005, Perry and Kleckner, 2003). Bioinformatic analysis has demonstrated that the amino terminal portion of ATM contains a large number of HEAT repeats, a protein motif with low sequence homology but a strict three dimensional conformation (Perry and Kleckner, 2003). These HEAT domains are thought

to act as protein scaffolds for the formation of large complexes. Because ATM localizes to DSBs, and interacts with many proteins at the break site, it is tempting to speculate that ATM could serve a critical role in bringing together proteins, as well as regulating their activity by phosphorylation. Such a role could be as important as the kinase function. Although it is circumstantial evidence, the fact that the *atm*^{4} mutation is located within one of these predicted HEAT repeats and behaves as a null, is consistent with these domains being present and important for ATM function.

The second mutation of particular interest is *atm*^{8}, a temperature sensitive mutation affecting the final amino acid of the protein. This region of the protein corresponds to the FATC domain, which, like most of ATM, is poorly understood. 3D modeling of ATM and the related protein DNA-PKcs has suggested that when DSBs are present, ATM directly binds DNA and undergoes a conformational change that activates the kinase domain. During this conformational change, the FATC domain seems to shift relative to the rest of the protein, a change that has been postulated to stabilize the kinase in its active conformation. If the FATC domain does play such a role, the mutation in *atm*^{8} could interfere with the re-orientation of FATC, or with subsequent stabilization of the kinase active form. The conformational change could require the FATC domain to move into close proximity to other parts of the protein. A change from a small amino acid such as leucine to a large, bulky, phenylalanine might render this interaction less favourable and thereby make it sensitive to temperature changes.

Taken together, these two alleles provide molecular data that hint at novel insights into regions of the ATM protein that are critical for function. These data have provided a starting point for subsequent experiments addressing ATM protein structure in further detail. Our laboratory is currently involved in a collaboration with Mark Glover (Biochemistry, U. Alberta), which will attempt to crystallize portions of the ATM protein. We hope to determine if conformational changes in ATM structure can be observed following the induction of DNA DSBs and if so, whether these changes are impeded in protein structures generated using *atm*^{8} mutations incorporated into peptides.

The role of Drosophila *ATM in the cellular response to DSBs*

A second major goal of this project was to investigate the cellular role of *atm* in response to DSBs. First, we attempted to determine if there was a requirement for ATM in the G2/M checkpoint response to DSBs. Our results suggested that ATM was, in fact, dispensable for this response. However, conclusions were limited in that we only examined the activation of the G2/M checkpoint in wing discs, after one hour post-irradiation. Work by other groups has demonstrated that there is apparently a requirement for ATM in an earlier G2/M checkpoint response, 25 minutes post-irradiation (Song et. al., 2004). This group also confirmed our result, namely that at one hour post-irradiation ATM is dispensable for the checkpoint response. The ATR ortholog *mei-41*, seems to play a role in both the early and late response to DSBs (Song et. al., 2004; Brodsky et. al., 2000). The current model for checkpoint activation by ATM and Mei-41 suggests that they activate the checkpoint transducer kinases Chk1 and Chk2, via phosphorylation. Chk1 and Chk2 then phosphorylate the Wee1 and Cdc25 regulators of Cdk1, resulting in a block to mitosis. Despite the similarities between how ATM and Mei-41 are thought to activate the checkpoint, results presented here and by other groups (Song et. al., 2004, Brodsky et. al., 2000) suggest that there are temporal differences in activation of ATM and Mei-41 in *Drosophila* and when they regulate the checkpoint.

In addition to activation of cell cycle checkpoints in response to DNA damage, ATM and related kinases are also traditionally thought to activate the repair process when DSBs are present. To determine if this was also the case in *Drosophila*, we examined the sensitivity of *atm* mutants to ionizing radiation, measured by adult survival rates following exposure to ionizing radiation during the 3rd larval instar. It has been suggested that in *Drosophila*, mutations affecting genes involved in the repair response directly demonstrate sensitivity to irradiation in such assays, but not genes involved in other responses to DSBs, such as checkpoint activation and apoptosis (Jaklevic and Su, 2004). The results presented in this thesis demonstrates that *atm* mutants are indeed sensitive to even low doses (1 Gy) of ionizing radiation. This sensitivity is much greater than that seen in mutants for *mei-41*, which has also been proposed to be involved in the DSB repair process (Baker et. al., 1978). One possible explanation for this difference is that the requirements for ATM and Mei-41 during DSB repair are different depending on the

amount of damage present. At lower doses, ATM may be preferentially used by the cell to activate relevant repair machinery. Perhaps at higher doses, the damage is simply too much to deal with using ATM alone, and Mei-41 becomes required as well. This is a interesting possibility since it suggests another situation where the ATM and Mei-41 are used in different ways to the same stimulus. In G2/M checkpoint regulation there is an apparent difference in the roles of ATM and Mei-41 at different time points following irradiation. In contrast, the ionizing radiation sensitivity assay suggests that ATM and Mei-41 might also behave differently depending on the amount of damage present. Together, these data have shed some light on the functions of ATM and Mei-41 during the cellular response to DSBs and provide a starting point for future experiments addressing how these two proteins work together to insure the maintenance of genomic stability.

atm *mutant lethality and rough eye phenotypes are caused by* p53 *dependent apoptosis*

One objective of this project was to analyze the rough eye phenotype of *atm* mutants and attempt to find a cause. We originally hoped that we could link the rough eye phenotype to a cellular role of ATM in the DSB response. Immunofluorescence studies in eye discs using antibodies to ELAV (a marker of differentiating neuronal cells) and activated caspase 3 (a marker of apoptosis) revealed that there is ectopic apoptosis during eye development in the proliferating cells ahead of the morphogenic furrow. Genetic interaction data has demonstrated that this apoptosis is dependent on the apoptosis-promoting factor, p53. DSBs have previously been shown to activate p53-dependent apoptosis in *Drosophila*, following exposure to ionizing radiation (Peters et. al., 2002; Jin et. al., 2000; Ollmann et. al., 2000; Brodsky et. al., 2000). However, if spontaneous DSBs alone were inducing apoptosis, why is it that only proliferating cells are affected? A possible explanation for this conundrum emerged from a collaboration with researchers at the University of California, Santa Cruz. They, as well as researchers in several other groups, observed high frequencies of telomere fusion defects in larval neuroblasts of *atm* mutants (Silva et. al., 2004; Song et. al., 2004; Bi et. al., 2004; Oikemus et. al., 2004). These telomere fusion defects can result in subsequent breakage of the dicentric chromosomes during mitosis, thereby generating large numbers of inappropriate DSBs.

Even small numbers of chromosome breaks have previously been documented to induce p53 dependent apoptosis in *Drosophila* (Ahmad and Golic, 1999). Therefore, this model can explain both the dependence of the ectopic apoptosis on *p53* in *atm* mutant eye discs as well as the preferential sensitivity of actively dividing cells ahead of the morphogenic furrow.

Another interesting aspect of the *p53* suppression data is that *p53 atm* double mutants are apparently fully viable and even eclose on time. This suggests that whatever is causing lethality in *atm* mutants is also dependent on *p53*. This suggests that there is also apoptosis in another tissue that is critical for survival, such as the brain, since eyes and wings are not essential. Although these results have not been pursued any further, they provides a framework for further study of the *atm* phenotype. The availability of the temperature sensitive allele, atm^{8}, as well as an easily scorable rough eye phenotype, also puts our laboratory in a good position for undertaking genetic modifier screens to identify ATM-interacting genes. For example, a screen for suppressors of the atm^{8} phenotype could allow us to dissect the pathway leading to the ectopic apoptosis. Suppressors might include mutations in apoptotic genes, as well as genes responsible for detecting chromosome breakage and triggering apoptosis in response. The identification of these genes would further our understanding of how DSBs are detected and communicated to the apoptotic machinery in *Drosophila.*

The role of atm *in oogenesis and meiotic recombination*

The third major goal of this project concerns how oogenesis is affected in *atm* mutants and to determine the cause of female sterility. Like the investigation of the eye phenotype, it was thought that there might be a connection between the role of ATM in the cellular response to DSBs and the female sterility. Upon examination of eggs laid by *atm* mothers, it became apparent that there were multiple defects during oogenesis, since there were multiple distinct phenotypes in these eggs (Silva et. al., 2004). Based on the results presented here, we now know that the thin eggshell defect is caused by ectopic cell death, most likely by apoptosis, in follicle cells during oogenesis. Furthermore, I have demonstrated that there is a defect in the repair of DSBs during meiotic recombination and that this leads to the activation of the meiotic checkpoint and failure to

properly pattern the anterior/posterior and dorsal/ventral axes of the egg. There are several lines of evidence that support a role for *atm* in the repair of DSBs during meiotic recombination. First, staining with antibodies to phosphorylated His2AV in the germarium revealed strong, persistent staining in *atm* mutants, suggesting that these DSBs are not being repaired in a timely fashion. Furthermore, the staining pattern in *atm* mutants is consistent with these being DSBs induced at the onset of meiotic recombination and not spontaneous breaks. The strong staining is first apparent in region 2a, at the time when meiotic recombination is initiated, and only a subset of nurse cells show the persistent staining, likely those that begin but do not follow through with meiotic recombination. The second piece of evidence that this is a meiotic recombination defect is that removing *mei-W68* in a *atm* background causes this strong His2AV staining to disappear. *mei-W68* is the *Drosophila* homolog of Spo11, which encodes a nuclease that is specifically responsible for inducing DSBs during meiotic recombination (McKim and Hayashi-Hagihara, 1998). The absence of His2AV staining in these double mutants strongly suggests that the persistent breaks in *atm* mutants are due to a failure to specifically repair meiotic DSBs. One last piece of evidence that supports a role for ATM in meiotic recombination is that *atm* mutants exhibit increased rates of chromosome non-disjunction, a phenotype that is associated with errors in meiotic recombination. Taken together, these results are interesting because they suggest that ATM is required for a specific developmental event involving the response to DNA DSBs. This is the most conclusive evidence presented to date in *Drosophila* that specifically links ATM to DSB repair and establishes a developmental context where the specific role of ATM in DSB repair can be studied further, *in vivo*.

My work on oogenesis has gone on to explain how a failure to repair DSBs during meiotic recombination can explain the patterning defect seen in mature eggs laid by *atm* mutant females. Removing *mei-41, mei-W68, chk2,* or *grp* in double mutants all result in a suppression of the Grk mislocalization and karyosome defects associated with *atm* mutant egg chambers. These results suggest that in *atm* mutants, as in other mutants affecting repair of DSBs during meiotic recombination, persistent DSBs activate a *mei-41* and *chk2*-dependent meiotic checkpoint. This checkpoint prevents normal Grk localization and karyosome formation, causing eggs to present a "ventralized" phenotype.

Comparison of the roles of *mei-41* and *atm* in this context is particularly interesting since it provides another example of *atm* and *mei-41* responding to the same stimulus in different, and temporally distinct, fashions. In this case, *atm* appears to be responsible for activating the DNA repair machinery in response to DSBs very early in oogenesis. *mei-41* can be activated later, if it detects unrepaired DSBs, and proceeds to activate the meiotic checkpoint. Another conclusion of these studies is that *mei-41* and *atm* activity are not always temporally distinct from one another during oogenesis. I have observed that *mei-41 atm* double mutants lack phospho His2AV staining, suggesting that they may have redundant roles with regards to the phosphorylation of His2AV in response to DSBs, as process which has also been shown to involve ATM and ATR in mammals (Burma et. al., 2001; Stiff et. al., 2004; Wang et. al., 2005). This result presents an apparently contradictory conclusion to the former situation, since in this context *atm* and *mei-41* apparently act in parallel, to achieve one aspect of the DSB response.

One aspect of the *atm* oogenesis phenotype that remains largely unresolved is the follicle cell defect. I have demonstrated that removing both *chk2* and *mei-41* can enhance follicle cell death in *atm* mutants and that this death is independent of p53. It is tempting to hypothesize that there may be a telomere maintenance defect in follicle cells that is triggering apoptosis, similar to what we believe is true in eye tissue. However, there is no direct evidence for this idea at this point. *chk2* is a checkpoint target of *mei-41*, and the fact that mutating either of these genes can enhance the *atm* follicle cell defect suggests that some sort of checkpoint exists which can partially protect *atm* mutant cells from ectopic death. It is possible that this checkpoint detects telomere fusion events in *atm* mutants and activates a cell cycle checkpoint that prevents cell cycle progression and subsequent chromosome breakage, until the telomere fusion can be repaired somehow. This process may be error prone, explaining why follicle cell death is still observed in *atm* mutants. Testing this hypothesis could shed more light on the role of *atm* in actively dividing somatic cells and could be studied further in conjunction with the eye disc apoptosis. However, this question will not be easy to address since detecting telomere fusion and breakage in follicle cells would be a technical challenge.

Together, this initial analysis of the follicle cell defect and the meiotic recombination repair defect has provided a basis for future studies on *atm* in oogenesis.

Oogenesis is good model system in which to further examine *atm* function for a couple of reasons. First, *atm* mutants have a somatic cell defect in the follicle cells of the ovaries which allows us to study the role of *atm* in maintaining genomic stability within a developmentally meaningful context. Whether this defect is due to a role for *atm* in telomere regulation, spontaneous DSB repair, or some other process remains an open question. The second reason oogenesis makes a good system to study *atm* is that it provides a system where DSBs are induced and repaired in a developmentally regulated fashion, during meiotic recombination. Studies in this system could allow us to uncover specific functions of ATM in developmental DSB repair and provide an opportunity to determine how it interacts with other proteins to recruit/activate components of the repair process. Oogenesis lends itself well to immunofluorescence and genetic experiments, which will help address these open questions regarding the roles of *atm* in *Drosophila*.

Literature Cited:

Abbott, L. A. and J. E. Natzle, 1992. Epithelial polarity and cell separation in the neoplastic l(1)dlg-1 mutant of Drosophila. Mech. Dev. **37**(1-2): 43-56.

Abdu, U., M. Brodsky and T. Schupbach, 2002. Activation of a meiotic checkpoint during Drosophila oogenesis regulates the translation of Gurken through Chk2/Mnk. Curr. Biol. **12**(19): 1645-51.

Abraham, R. T., 2001. Cell cycle checkpoint signaling through the ATM and ATR kinases. Genes Dev. **15**(17): 2177-96.

Abraham, R. T., 2004. PI 3-kinase related kinases: 'big' players in stress-induced signaling pathways. DNA Repair (Amst) **3**(8-9): 883-7.

Ahmad, K. and K. G. Golic, 1999. Telomere loss in somatic cells of Drosophila causes cell cycle arrest and apoptosis. Genetics **151**(3): 1041-51.

Ahn, J. Y., J. K. Schwarz, H. Piwnica-Worms and C. E. Canman, 2000. Threonine 68 phosphorylation by ataxia telangiectasia mutated is required for efficient activation of Chk2 in response to ionizing radiation. Cancer Res. **60**(21): 5934-6.

Amundson, S. A., R. A. Lee, C. A. Koch-Paiz, M. L. Bittner, P. Meltzer, et al., 2003. Differential responses of stress genes to low dose-rate gamma irradiation. Mol Cancer Res. **1**(6): 445-52.

Arlett, C. F. and A. Priestley, 1985. An assessment of the radiosensitivity of ataxia-telangiectasia heterozygotes. Kroc. Found. Ser. **19**: 101-9.

Ashburner M., 1989. *Drosophila*- A Laboratory Handbook. Cold Springs Harbor Press: Cold Springs Harbor, NY.

Baker, B. S. and A. T. Carpenter, 1972. Genetic analysis of sex chromosomal meiotic mutants in Drosophilia melanogaster. Genetics **71**(2): 255-86.

Baker, B.S., A.T. Carpenter, P. Ripoll, 1978. The utilization during mitotic cell division of loci controlling meiotic recombination in *Drosophila melanogaster*. Genetics **90**: 531-78.

Baker, N. E., 2001. Cell proliferation, survival, and death in the Drosophila eye. Semin Cell Dev. Biol. **12**(6): 499-507.

Bakkenist, C. J. and M. B. Kastan, 2003. DNA damage activates ATM through intermolecular autophosphorylation and dimer dissociation. Nature **421**(6922): 499-506.

Banin, S., L. Moyal, S. Shieh, Y. Taya, C. W. Anderson, et al., 1998. Enhanced phosphorylation of p53 by ATM in response to DNA damage. Science **281**(5383):

1674-7.

Barlow, C., S. Hirotsune, R. Paylor, M. Liyanage, M. Eckhaus, et al., 1996. Atm-deficient mice: a paradigm of ataxia telangiectasia. Cell **86**(1): 159-71.

Barlow, C., M. Liyanage, P. B. Moens, M. Tarsounas, K. Nagashima, et al., 1998. Atm deficiency results in severe meiotic disruption as early as leptonema of prophase I. Development **125**(20): 4007-17.

Baskaran, R., L. D. Wood, L. L. Whitaker, C. E. Canman, S. E. Morgan, et al., 1997. Ataxia telangiectasia mutant protein activates c-Abl tyrosine kinase in response to ionizing radiation. Nature **387**(6632): 516-9.

Baumann, P. and S. C. West, 1998. Role of the human RAD51 protein in homologous recombination and double-stranded-break repair. Trends Biochem. Sci. **23**(7): 247-51.

Beamish, H. and M. F. Lavin, 1994. Radiosensitivity in ataxia-telangiectasia: anomalies in radiation-induced cell cycle delay. Int. J. Radiat. Biol. **65**(2): 175-84.

Bi, X., S. C. Wei and Y. S. Rong, 2004. Telomere protection without a telomerase; the role of ATM and Mre11 in Drosophila telomere maintenance. Curr. Biol. **14**(15): 1348-53.

Boulton, S. J. and S. P. Jackson, 1998. Components of the Ku-dependent non-homologous end-joining pathway are involved in telomeric length maintenance and telomeric silencing. Embo J **17**(6): 1819-28.

Boyd, J. B., M. D. Golino, T. D. Nguyen and M. M. Green, 1976. Isolation and characterization of X-linked mutants of Drosophila melanogaster which are sensitive to mutagens. Genetics **84**(3): 485-506.

Bressan, D. A., B. K. Baxter and J. H. Petrini, 1999. The Mre11-Rad50-Xrs2 protein complex facilitates homologous recombination-based double-strand break repair in Saccharomyces cerevisiae. Mol. Cell. Biol. **19**(11): 7681-7.

Brodsky, M. H., W. Nordstrom, G. Tsang, E. Kwan, G. M. Rubin, et al., 2000. Drosophila p53 binds a damage response element at the reaper locus. Cell **101**(1): 103-13.

Brodsky, M. H., J. J. Sekelsky, G. Tsang, R. S. Hawley and G. M. Rubin, 2000. mus304 encodes a novel DNA damage checkpoint protein required during Drosophila development. Genes Dev. **14**(6): 666-78.

Brodsky, M. H., B. T. Weinert, G. Tsang, Y. S. Rong, N. M. McGinnis, et al., 2004. Drosophila melanogaster MNK/Chk2 and p53 regulate multiple DNA repair and apoptotic pathways following DNA damage. Mol. Cell. Biol. **24**(3): 1219-31.

Brown, E. J. and D. Baltimore, 2003. Essential and dispensable roles of ATR in cell cycle arrest and genome maintenance. Genes Dev. **17**(5): 615-28.

Burma, S., B. P. Chen, M. Murphy, A. Kurimasa and D. J. Chen, 2001. ATM phosphorylates histone H2AX in response to DNA double-strand breaks. J. Biol. Chem. **276**(45): 42462-7.

Calvi, B. R. and A. C. Spradling, 1999. Chorion gene amplification in Drosophila: A model for metazoan origins of DNA replication and S-phase control. Methods **18**(3): 407-17.

Canman, C. E., D. S. Lim, K. A. Cimprich, Y. Taya, K. Tamai, et al., 1998. Activation of the ATM kinase by ionizing radiation and phosphorylation of p53. Science **281**(5383): 1677-9.

Carpenter, A. T., 1994. Egalitarian and the choice of cell fates in Drosophila melanogaster oogenesis. Ciba Found. Symp. **182**: 223-46; discussion 246-54.

Carson, C. T., R. A. Schwartz, T. H. Stracker, C. E. Lilley, D. V. Lee, et al., 2003. The Mre11 complex is required for ATM activation and the G2/M checkpoint. Embo J **22**(24): 6610-20.

Chehab, N. H., A. Malikzay, M. Appel and T. D. Halazonetis, 2000. Chk2/hCds1 functions as a DNA damage checkpoint in G(1) by stabilizing p53. Genes Dev. **14**(3): 278-88.

Chen, G., S. S. Yuan, W. Liu, Y. Xu, K. Trujillo, et al., 1999. Radiation-induced assembly of Rad51 and Rad52 recombination complex requires ATM and c-Abl. J. Biol. Chem. **274**(18): 12748-52.

Ciapponi, L., G. Cenci, J. Ducau, C. Flores, D. Johnson-Schlitz, et al., 2004. The Drosophila Mre11/Rad50 complex is required to prevent both telomeric fusion and chromosome breakage. Curr. Biol. **14**(15): 1360-6.

Cornforth, M. N. and J. S. Bedford, 1985. On the nature of a defect in cells from individuals with ataxia-telangiectasia. Science **227**(4694): 1589-91.

D'Amours, D. and S. P. Jackson, 2002. The Mre11 complex: at the crossroads of dna repair and checkpoint signalling. Nat. Rev. Mol. Cell Biol. **3**(5): 317-27.

Di Giacomo, M., M. Barchi, F. Baudat, W. Edelmann, S. Keeney, et al., 2005. Distinct DNA-damage-dependent and -independent responses drive the loss of oocytes in recombination-defective mouse mutants. Proc. Natl. Acad. Sci. U S A **102**(3): 737-42.

Dore, A. S., A. C. Drake, S. C. Brewerton and T. L. Blundell, 2004. Identification of DNA-PK in the arthropods. Evidence for the ancient ancestry of vertebrate non-homologous end-joining. DNA Repair (Amst) **3**(1): 33-41.

Falck, J., J. H. Petrini, B. R. Williams, J. Lukas and J. Bartek, 2002. The DNA damage-dependent intra-S phase checkpoint is regulated by parallel pathways. Nat. Genet. **30**(3): 290-4.

Fernandes, N., Y. Sun, S. Chen, P. Paul, R. J. Shaw, et al., 2005. DNA damage-induced association of ATM with its target proteins requires a protein interaction domain in the N terminus of ATM. J. Biol. Chem. **280**(15): 15158-64.

Fogarty, P., S. D. Campbell, R. Abu-Shumays, B. S. Phalle, K. R. Yu, et al., 1997. The Drosophila grapes gene is related to checkpoint gene chk1/rad27 and is required for late syncytial division fidelity. Curr. Biol. **7**(6): 418-26.

Fridovich, I., 1995. Superoxide radical and superoxide dismutases. Annu. Rev. Biochem. **64**: 97-112.

Gatei, M., D. Young, K. M. Cerosaletti, A. Desai-Mehta, K. Spring, et al., 2000. ATM-dependent phosphorylation of nibrin in response to radiation exposure. Nat. Genet. **25**(1): 115-9.

Gatti, R. A., I. Berkel, E. Boder, G. Braedt, P. Charmley, et al., 1988. Localization of an ataxia-telangiectasia gene to chromosome 11q22-23. Nature **336**(6199): 577-80.

Ghabrial, A., R. P. Ray and T. Schupbach, 1998. okra and spindle-B encode components of the RAD52 DNA repair pathway and affect meiosis and patterning in Drosophila oogenesis. Genes Dev. **12**(17): 2711-23.

Ghabrial, A. and T. Schupbach, 1999. Activation of a meiotic checkpoint regulates translation of Gurken during Drosophila oogenesis. Nat. Cell Biol. **1**(6): 354-7.

Giaccia, A. J. and M. B. Kastan, 1998. The complexity of p53 modulation: emerging patterns from divergent signals. Genes Dev. **12**(19): 2973-83.

Golic, K, 2002. Personal communication to FlyBase available from http://flybase.bio.indiana.edu/.bin/fbpcq.html?FBrf0151688

Gonzalez-Reyes, A., H. Elliott and D. St Johnston, 1997. Oocyte determination and the origin of polarity in Drosophila: the role of the spindle genes. Development **124**(24): 4927-37.

Goodarzi, A. A., J. C. Jonnalagadda, P. Douglas, D. Young, R. Ye, et al., 2004. Autophosphorylation of ataxia-telangiectasia mutated is regulated by protein phosphatase 2A. Embo J **23**(22): 4451-61.

Gowen, L. C., A. V. Avrutskaya, A. M. Latour, B. H. Koller and S. A. Leadon, 1998. BRCA1 required for transcription-coupled repair of oxidative DNA damage. Science **281**(5379): 1009-12.

Greenwell, P. W., S. L. Kronmal, S. E. Porter, J. Gassenhuber, B. Obermaier, et al., 1995.

TEL1, a gene involved in controlling telomere length in S. cerevisiae, is homologous to the human ataxia telangiectasia gene. Cell **82**(5): 823-9.

Hari, K. L., A. Santerre, J. J. Sekelsky, K. S. McKim, J. B. Boyd, et al., 1995. The mei-41 gene of D. melanogaster is a structural and functional homolog of the human ataxia telangiectasia gene. Cell **82**(5): 815-21.

Haupt, Y., R. Maya, A. Kazaz and M. Oren, 1997. Mdm2 promotes the rapid degradation of p53. Nature **387**(6630): 296-9.

Hirao, A., Y. Y. Kong, S. Matsuoka, A. Wakeham, J. Ruland, et al., 2000. DNA damage-induced activation of p53 by the checkpoint kinase Chk2. Science **287**(5459): 1824-7.

Houldsworth, J. and M. F. Lavin, 1980. Effect of ionizing radiation on DNA synthesis in ataxia telangiectasia cells. Nucleic Acids Res. **8**(16): 3709-20.

Huh, J. R., M. Guo and B. A. Hay, 2004. Compensatory proliferation induced by cell death in the Drosophila wing disc requires activity of the apical cell death caspase Dronc in a nonapoptotic role. Curr. Biol. **14**(14): 1262-6.

Ivanov, E. L., N. Sugawara, C. I. White, F. Fabre and J. E. Haber, 1994. Mutations in XRS2 and RAD50 delay but do not prevent mating-type switching in Saccharomyces cerevisiae. Mol. Cell. Biol. **14**(5): 3414-25.

Jaklevic, B. R. and T. T. Su, 2004. Relative contribution of DNA repair, cell cycle checkpoints, and cell death to survival after DNA damage in Drosophila larvae. Curr. Biol. **14**(1): 23-32.

Jang, J. K., D. E. Sherizen, R. Bhagat, E. A. Manheim and K. S. McKim, 2003. Relationship of DNA double-strand breaks to synapsis in Drosophila. J. Cell. Sci. **116**(Pt 15): 3069-77.

Jin, S., S. Martinek, W. S. Joo, J. R. Wortman, N. Mirkovic, et al., 2000. Identification and characterization of a p53 homologue in Drosophila melanogaster. Proc. Natl. Acad. Sci. U S A **97**(13): 7301-6.

Kastan, M. B. and D. S. Lim, 2000. The many substrates and functions of ATM. Nat. Rev. Mol. Cell Biol. **1**(3): 179-86.

Kastan, M. B., O. Onyekwere, D. Sidransky, B. Vogelstein and R. W. Craig, 1991. Participation of p53 protein in the cellular response to DNA damage. Cancer Res. **51**(23 Pt 1): 6304-11.

Kastan, M. B., Q. Zhan, W. S. el-Deiry, F. Carrier, T. Jacks, et al., 1992. A mammalian cell cycle checkpoint pathway utilizing p53 and GADD45 is defective in ataxia-telangiectasia. Cell **71**(4): 587-97.

Khanna, K. K. and M. F. Lavin, 1993. Ionizing radiation and UV induction of p53 protein by different pathways in ataxia-telangiectasia cells. Oncogene **8**(12): 3307-12.

Khosravi, R., R. Maya, T. Gottlieb, M. Oren, Y. Shiloh, et al., 1999. Rapid ATM-dependent phosphorylation of MDM2 precedes p53 accumulation in response to DNA damage. Proc. Natl. Acad. Sci U S A **96**(26): 14973-7.

Kim, S. T., D. S. Lim, C. E. Canman and M. B. Kastan, 1999. Substrate specificities and identification of putative substrates of ATM kinase family members. J. Biol. Chem. **274**(53): 37538-43.

Kitagawa, R., C. J. Bakkenist, P. J. McKinnon and M. B. Kastan, 2004. Phosphorylation of SMC1 is a critical downstream event in the ATM-NBS1-BRCA1 pathway. Genes Dev. **18**(12): 1423-38.

Lantz, V., L. Ambrosio and P. Schedl, 1992. The Drosophila orb gene is predicted to encode sex-specific germline RNA-binding proteins and has localized transcripts in ovaries and early embryos. Development **115**(1): 75-88.

Lantz, V., J. S. Chang, J. I. Horabin, D. Bopp and P. Schedl, 1994. The Drosophila orb RNA-binding protein is required for the formation of the egg chamber and establishment of polarity. Genes Dev. **8**(5): 598-613.

Lee, J. S., K. M. Collins, A. L. Brown, C. H. Lee and J. H. Chung, 2000. hCds1-mediated phosphorylation of BRCA1 regulates the DNA damage response. Nature **404**(6774): 201-4.

Li, S., N. S. Ting, L. Zheng, P. L. Chen, Y. Ziv, et al., 2000. Functional link of BRCA1 and ataxia telangiectasia gene product in DNA damage response. Nature **406**(6792): 210-5.

Lim, D. S., S. T. Kim, B. Xu, R. S. Maser, J. Lin, et al., 2000. ATM phosphorylates p95/nbs1 in an S-phase checkpoint pathway. Nature **404**(6778): 613-7.

Liu, H., J. K. Jang, N. Kato and K. S. McKim, 2002. mei-P22 encodes a chromosome-associated protein required for the initiation of meiotic recombination in Drosophila melanogaster. Genetics **162**(1): 245-58.

Liu, Q., S. Guntuku, X. S. Cui, S. Matsuoka, D. Cortez, et al., 2000. Chk1 is an essential kinase that is regulated by Atr and required for the G(2)/M DNA damage checkpoint. Genes Dev. **14**(12): 1448-59.

Llorca, O., A. Rivera-Calzada, J. Grantham and K. R. Willison, 2003. Electron microscopy and 3D reconstructions reveal that human ATM kinase uses an arm-like domain to clamp around double-stranded DNA. Oncogene **22**(25): 3867-74.

Lu, X. and D. P. Lane, 1993. Differential induction of transcriptionally active p53 following UV or ionizing radiation: defects in chromosome instability

syndromes? Cell **75**(4): 765-78.

Lustig, A. J. and T. D. Petes, 1986. Identification of yeast mutants with altered telomere structure. Proc. Natl. Acad. Sci. U S A **83**(5): 1398-402.

Madigan, J. P., H. L. Chotkowski and R. L. Glaser, 2002. DNA double-strand break-induced phosphorylation of Drosophila histone variant H2Av helps prevent radiation-induced apoptosis. Nucleic Acids Res. **30**(17): 3698-705.

Matsuoka, S., M. Huang and S. J. Elledge, 1998. Linkage of ATM to cell cycle regulation by the Chk2 protein kinase. Science **282**(5395): 1893-7.

Matsuoka, S., G. Rotman, A. Ogawa, Y. Shiloh, K. Tamai, et al., 2000. Ataxia telangiectasia-mutated phosphorylates Chk2 in vivo and in vitro. Proc. Natl. Acad. Sci. U S A **97**(19): 10389-94.

Maya, R., M. Balass, S. T. Kim, D. Shkedy, J. F. Leal, et al., 2001. ATM-dependent phosphorylation of Mdm2 on serine 395: role in p53 activation by DNA damage. Genes Dev. **15**(9): 1067-77.

McClintock, B., 1939. The behavior in successive nuclear divisions of a chromosome broken in meiosis. Proc. Natl. Acad. Sci. USA **25**: 405-16.

McKim, K. S., J. B. Dahmus and R. S. Hawley, 1996. Cloning of the Drosophila melanogaster meiotic recombination gene mei-218: a genetic and molecular analysis of interval 15E. Genetics **144**(1): 215-28.

McKim, K. S. and A. Hayashi-Hagihara, 1998. mei-W68 in Drosophila melanogaster encodes a Spo11 homolog: evidence that the mechanism for initiating meiotic recombination is conserved. Genes Dev. **12**(18): 2932-42.

McKim, K. S., J. K. Jang and E. A. Manheim, 2002. Meiotic recombination and chromosome segregation in Drosophila females. Annu. Rev. Genet. **36**: 205-32.

Meek, K., S. Gupta, D. A. Ramsden and S. P. Lees-Miller, 2004. The DNA-dependent protein kinase: the director at the end. Immunol. Rev. **200**: 132-41.

Metcalfe, J. A., J. Parkhill, L. Campbell, M. Stacey, P. Biggs, et al., 1996. Accelerated telomere shortening in ataxia telangiectasia. Nat. Genet. **13**(3): 350-3.

Moore, J. K. and J. E. Haber, 1996. Cell cycle and genetic requirements of two pathways of nonhomologous end-joining repair of double-strand breaks in Saccharomyces cerevisiae. Mol. Cell Biol. **16**(5): 2164-73.

Morgan, S. E. and M. B. Kastan, 1997. p53 and ATM: cell cycle, cell death, and cancer. Adv. Cancer Res. **71**: 1-25.

Morgan, S. E., C. Lovly, T. K. Pandita, Y. Shiloh and M. B. Kastan, 1997. Fragments of

ATM which have dominant-negative or complementing activity. Mol. Cell Biol. **17**(4): 2020-9.

Morrison, C., E. Sonoda, N. Takao, A. Shinohara, K. Yamamoto, et al., 2000. The controlling role of ATM in homologous recombinational repair of DNA damage. Embo J **19**(3): 463-71.

Moynahan, M. E., J. W. Chiu, B. H. Koller and M. Jasin, 1999. Brca1 controls homology-directed DNA repair. Mol. Cell **4**(4): 511-8.

Neuman-Silberberg, F. S. and T. Schupbach, 1993. The Drosophila dorsoventral patterning gene gurken produces a dorsally localized RNA and encodes a TGF alpha-like protein. Cell **75**(1): 165-74.

O'Neill, T., A. J. Dwyer, Y. Ziv, D. W. Chan, S. P. Lees-Miller, et al., 2000. Utilization of oriented peptide libraries to identify substrate motifs selected by ATM. J. Biol. Chem. **275**(30): 22719-27.

Oikemus, S. R., N. McGinnis, J. Queiroz-Machado, H. Tukachinsky, S. Takada, et al., 2004. Drosophila atm/telomere fusion is required for telomeric localization of HP1 and telomere position effect. Genes Dev. **18**(15): 1850-61.

Ollmann, M., L. M. Young, C. J. Di Como, F. Karim, M. Belvin, et al., 2000. Drosophila p53 is a structural and functional homolog of the tumor suppressor p53. Cell **101**(1): 91-101.

Orr-Weaver, T. L., 1991. Drosophila chorion genes: cracking the eggshell's secrets. Bioessays **13**(3): 97-105.

Page, S. L. and R. S. Hawley, 2001. c(3)G encodes a Drosophila synaptonemal complex protein. Genes Dev. **15**(23): 3130-43.

Pandita, T. K., S. Pathak and C. R. Geard, 1995. Chromosome end associations, telomeres and telomerase activity in ataxia telangiectasia cells. Cytogenet. Cell Genet. **71**(1): 86-93.

Peng, C. Y., P. R. Graves, R. S. Thoma, Z. Wu, A. S. Shaw, et al., 1997. Mitotic and G2 checkpoint control: regulation of 14-3-3 protein binding by phosphorylation of Cdc25C on serine-216. Science **277**(5331): 1501-5.

Perry, J. and N. Kleckner, 2003. The ATRs, ATMs, and TORs are giant HEAT repeat proteins. Cell **112**(2): 151-5.

Peters, M., C. DeLuca, A. Hirao, V. Stambolic, J. Potter, et al., 2002. Chk2 regulates irradiation-induced, p53-mediated apoptosis in Drosophila. Proc. Natl. Acad. Sci. U S A **99**(17): 11305-10.

Ray, R. P. and T. Schupbach, 1996. Intercellular signaling and the polarization of body

axes during Drosophila oogenesis. Genes Dev. **10**(14): 1711-23.

Riechmann, V. and A. Ephrussi, 2001. Axis formation during Drosophila oogenesis. Curr. Opin. Genet. Dev. **11**(4): 374-83.

Rivera-Calzada, A., J. P. Maman, L. Spagnolo, L. H. Pearl and O. Llorca, 2005. Three-dimensional structure and regulation of the DNA-dependent protein kinase catalytic subunit (DNA-PKcs). Structure (Camb) **13**(2): 243-55.

Robinow, S. and K. White, 1991. Characterization and spatial distribution of the ELAV protein during Drosophila melanogaster development. J. Neurobiol. **22**(5): 443-61.

Rong, Y. S., S. W. Titen, H. B. Xie, M. M. Golic, M. Bastiani, et al., 2002. Targeted mutagenesis by homologous recombination in D. melanogaster. Genes Dev. **16**(12): 1568-81.

Rozen, S. and H. Skaletsky, 2000. Primer3 on the WWW for general users and for biologist programmers. Methods Mol. Biol. **132**: 365-86.

Rudolph, N. S. and S. A. Latt, 1989. Flow cytometric analysis of X-ray sensitivity in ataxia telangiectasia. Mutat. Res. **211**(1): 31-41.

Ruohola-Baker, H., L. Y. Jan and Y. N. Jan, 1994. The role of gene cassettes in axis formation during Drosophila oogenesis. Trends Genet. **10**(3): 89-94.

Ryoo, H. D., T. Gorenc and H. Steller, 2004. Apoptotic cells can induce compensatory cell proliferation through the JNK and the Wingless signaling pathways. Dev. Cell. **7**(4): 491-501.

Sapir, A., R. Schweitzer and B. Z. Shilo, 1998. Sequential activation of the EGF receptor pathway during Drosophila oogenesis establishes the dorsoventral axis. Development **125**(2): 191-200.

Savitsky, K., A. Bar-Shira, S. Gilad, G. Rotman, Y. Ziv, et al., 1995. A single ataxia telangiectasia gene with a product similar to PI-3 kinase. Science **268**(5218): 1749-53.

Schiestl, R. H., J. Zhu and T. D. Petes, 1994. Effect of mutations in genes affecting homologous recombination on restriction enzyme-mediated and illegitimate recombination in Saccharomyces cerevisiae. Mol. Cell Biol. **14**(7): 4493-500.

Schupbach, T., 1987. Germ line and soma cooperate during oogenesis to establish the dorsoventral pattern of egg shell and embryo in Drosophila melanogaster. Cell **49**(5): 699-707.

Schupbach, T. and E. Wieschaus, 1991. Female sterile mutations on the second chromosome of Drosophila melanogaster. II. Mutations blocking oogenesis or

altering egg morphology. Genetics **129**(4): 1119-36.

Scott, D., A. R. Spreadborough and S. A. Roberts, 1994. Radiation-induced G2 delay and spontaneous chromosome aberrations in ataxia-telangiectasia homozygotes and heterozygotes. Int. J. Radiat. Biol. **66**(6 Suppl): S157-63.

Scully, R., J. Chen, A. Plug, Y. Xiao, D. Weaver, et al., 1997. Association of BRCA1 with Rad51 in mitotic and meiotic cells. Cell **88**(2): 265-75.

Sekelsky, J. J., K. S. McKim, G. M. Chin and R. S. Hawley, 1995. The Drosophila meiotic recombination gene mei-9 encodes a homologue of the yeast excision repair protein Rad1. Genetics **141**(2): 619-27.

Shieh, S. Y., J. Ahn, K. Tamai, Y. Taya and C. Prives, 2000. The human homologs of checkpoint kinases Chk1 and Cds1 (Chk2) phosphorylate p53 at multiple DNA damage-inducible sites. Genes Dev. **14**(3): 289-300.

Shieh, S. Y., M. Ikeda, Y. Taya and C. Prives, 1997. DNA damage-induced phosphorylation of p53 alleviates inhibition by MDM2. Cell **91**(3): 325-34.

Shiloh, Y., 1997. Ataxia-telangiectasia and the Nijmegen breakage syndrome: related disorders but genes apart. Annu. Rev. Genet. **31**: 635-62.

Shinohara, A. and T. Ogawa, 1995. Homologous recombination and the roles of double-strand breaks. Trends Biochem. Sci. **20**(10): 387-91.

Siliciano, J. D., C. E. Canman, Y. Taya, K. Sakaguchi, E. Appella, et al., 1997. DNA damage induces phosphorylation of the amino terminus of p53. Genes Dev. **11**(24): 3471-81.

Silva, E., 2002. Generation and Characterization of chemical-sensitive cell cycle checkpoint mutants in *Drosophila*. M.Sc. Thesis. University of Alberta: Edmonton, AB.

Silva, E., S. Tiong, M. Pedersen, E. Homola, A. Royou, et al., 2004. ATM is required for telomere maintenance and chromosome stability during Drosophila development. Curr. Biol. **14**(15): 1341-7.

Smith, G. C. and S. P. Jackson, 1999. The DNA-dependent protein kinase. Genes Dev. **13**(8): 916-34.

Smith, J. E., 3rd, C. A. Cummings and C. Cronmiller, 2002. Daughterless coordinates somatic cell proliferation, differentiation and germline cyst survival during follicle formation in Drosophila. Development **129**(13): 3255-67.

Song, Y. H., G. Mirey, M. Betson, D. A. Haber and J. Settleman, 2004. The Drosophila ATM ortholog, dATM, mediates the response to ionizing radiation and to spontaneous DNA damage during development. Curr. Biol. **14**(15): 1354-9.

Spradling, A.C., 1993. Developmental genetics of oogenesis, pp 1-70. In: The Development of *Drosophila melanogaster*. eds. Bate, M. and Martinez Arias, A. Cold Spring Harbor Press: Long Island, NY.

Staeva-Vieira, E., S. Yoo and R. Lehmann, 2003. An essential role of DmRad51/SpnA in DNA repair and meiotic checkpoint control. Embo J **22**(21): 5863-74.

Stiff, T., M. O'Driscoll, N. Rief, K. Iwabuchi, M. Lobrich, et al., 2004. ATM and DNA-PK function redundantly to phosphorylate H2AX after exposure to ionizing radiation. Cancer Res. **64**(7): 2390-6.

Styhler, S., A. Nakamura, A. Swan, B. Suter and P. Lasko, 1998. vasa is required for GURKEN accumulation in the oocyte, and is involved in oocyte differentiation and germline cyst development. Development **125**(9): 1569-78.

Su, T. T., J. Walker and J. Stumpff, 2000. Activating the DNA damage checkpoint in a developmental context. Curr. Biol. **10**(3): 119-26.

Tan, T. L., R. Kanaar and C. Wyman, 2003. Rad54, a Jack of all trades in homologous recombination. DNA Repair (Amst) **2**(7): 787-94.

Taylor, A. M., D. G. Harnden, C. F. Arlett, S. A. Harcourt, A. R. Lehmann, et al., 1975. Ataxia telangiectasia: a human mutation with abnormal radiation sensitivity. Nature **258**(5534): 427-9.

Taylor, A. M., J. A. Metcalfe, J. Thick and Y. F. Mak, 1996. Leukemia and lymphoma in ataxia telangiectasia. Blood **87**(2): 423-38.

Tibbetts, R. S., K. M. Brumbaugh, J. M. Williams, J. N. Sarkaria, W. A. Cliby, et al., 1999. A role for ATR in the DNA damage-induced phosphorylation of p53. Genes Dev. **13**(2): 152-7.

Tomancak, P., A. Guichet, P. Zavorszky and A. Ephrussi, 1998. Oocyte polarity depends on regulation of gurken by Vasa. Development **125**(9): 1723-32.

Tsukamoto, Y. and H. Ikeda, 1998. Double-strand break repair mediated by DNA end-joining. Genes Cells **3**(3): 135-44.

Uziel, T., Y. Lerenthal, L. Moyal, Y. Andegeko, L. Mittelman, et al., 2003. Requirement of the MRN complex for ATM activation by DNA damage. Embo J **22**(20): 5612-21.

Uziel, T., K. Savitsky, M. Platzer, Y. Ziv, T. Helbitz, et al., 1996. Genomic Organization of the ATM gene. Genomics **33**(2): 317-20.

Van Buskirk, C. and T. Schupbach, 1999. Versatility in signalling: multiple responses to EGF receptor activation during Drosophila oogenesis. Trends Cell Biol. **9**(1): 1-4.

van Eeden, F. and D. St Johnston, 1999. The polarisation of the anterior-posterior and dorsal-ventral axes during Drosophila oogenesis. Curr. Opin. Genet. Dev. **9**(4): 396-404.

von Wettstein, D., S. W. Rasmussen and P. B. Holm, 1984. The synaptonemal complex in genetic segregation. Annu. Rev. Genet. **18**: 331-413.

Walker, M. Y. and R. S. Hawley, 2000. Hanging on to your homolog: the roles of pairing, synapsis and recombination in the maintenance of homolog adhesion. Chromosoma **109**(1-2): 3-9.

Wang, H., M. Wang, H. Wang, W. Bocker and G. Iliakis, 2005. Complex H2AX phosphorylation patterns by multiple kinases including ATM and DNA-PK in human cells exposed to ionizing radiation and treated with kinase inhibitors. J. Cell Physiol. **202**(2): 492-502.

Wei, S., M. Rocchi, N. Archidiacono, N. Sacchi, G. Romeo, et al., 1990. Physical mapping of the human chromosome 11q23 region containing the ataxia-telangiectasia locus. Cancer Genet. Cytogenet. **46**(1): 1-8.

Wolff, T. and D. F. Ready, 1991. The beginning of pattern formation in the Drosophila compound eye: the morphogenetic furrow and the second mitotic wave. Development **113**(3): 841-50.

Wu, X., V. Ranganathan, D. S. Weisman, W. F. Heine, D. N. Ciccone, et al., 2000. ATM phosphorylation of Nijmegen breakage syndrome protein is required in a DNA damage response. Nature **405**(6785): 477-82.

Xia, S. J., M. A. Shammas and R. J. Shmookler Reis, 1996. Reduced telomere length in ataxia-telangiectasia fibroblasts. Mutat. Res. **364**(1): 1-11.

Xu, B., S. T. Kim, D. S. Lim and M. B. Kastan, 2002. Two molecularly distinct G(2)/M checkpoints are induced by ionizing irradiation. Mol. Cell Biol. **22**(4): 1049-59.

Xu, J., S. Xin and W. Du, 2001. Drosophila Chk2 is required for DNA damage-mediated cell cycle arrest and apoptosis. FEBS Lett. **508**(3): 394-8.

Xu, T. and G. M. Rubin, 1993. Analysis of genetic mosaics in developing and adult Drosophila tissues. Development **117**(4): 1223-37.

Xu, Y. and D. Baltimore, 1996. Dual roles of ATM in the cellular response to radiation and in cell growth control. Genes Dev. **10**(19): 2401-10.

Yaneva, M., T. Kowalewski and M. R. Lieber, 1997. Interaction of DNA-dependent protein kinase with DNA and with Ku: biochemical and atomic-force microscopy studies. Embo J **16**(16): 5098-112.

Yazdi, P. T., Y. Wang, S. Zhao, N. Patel, E. Y. Lee, et al., 2002. SMC1 is a downstream

effector in the ATM/NBS1 branch of the human S-phase checkpoint. Genes Dev. **16**(5): 571-82.

Yu, S. Y., S. J. Yoo, L. Yang, C. Zapata, A. Srinivasan, et al., 2002. A pathway of signals regulating effector and initiator caspases in the developing Drosophila eye. Development **129**(13): 3269-78.

Yuan, S. S., H. L. Chang and E. Y. Lee, 2003. Ionizing radiation-induced Rad51 nuclear focus formation is cell cycle-regulated and defective in both ATM(-/-) and c-Abl(-/-) cells. Mutat. Res. **525**(1-2): 85-92.

Zhao, H. and H. Piwnica-Worms, 2001. ATR-mediated checkpoint pathways regulate phosphorylation and activation of human Chk1. Mol. Cell. Biol. **21**(13): 4129-39.

Zhao, S., Y. C. Weng, S. S. Yuan, Y. T. Lin, H. C. Hsu, et al., 2000. Functional link between ataxia-telangiectasia and Nijmegen breakage syndrome gene products. Nature **405**(6785): 473-7.

Appendix A: Supplemental Primer Information

Name	Gene	Use	Strand	Start †	Length (bp)	Sequence	A.T. (°C) ‡	Product Size (bp)
1A	*atm*	PCR/Sequencing	sense	-505	22	gtgttaccaaagccatcaacaa	66	925
1B	*atm*	PCR/Sequencing	antisense	419	22	gctggaaatcacaggttagctt		
1C	*atm*	Sequencing	sense	-97	21	tctggcagaggtcactctaag		
1D	*atm*	Sequencing	antisense	-9	20	cccggcataacctgttgtaa		
2A	*atm*	PCR/Sequencing	sense	347	22	tcacacaattcaacttggaagg	63	915
2B	*atm*	PCR/Sequencing	antisense	1262	22	atcttgatgaaggggtcagaaa		
2C	*atm*	Sequencing	sense	745	18	cgtcagtttggccaagga		
2D	*atm*	Sequencing	antisense	810	20	ctgagctccggcagatattc		
3A	*atm*	PCR/Sequencing	sense	1237	22	aaattttctgacccttcatca	65	886
3B	*atm*	PCR/Sequencing	antisense	2123	22	tggaaggaacaatgtgttctga		
3C	*atm*	Sequencing	sense	1672	20	tattcgggaggattttctgg		
3D	*atm*	Sequencing	antisense	1705	20	actccaaagctcacccagaa		
4A	*atm*	PCR/Sequencing	sense	2083	22	attgcgacagatctctcaatca	65	892
4B	*atm*	PCR/Sequencing	antisense	2975	22	ggcagctgcataacatcttaaa		
4C	*atm*	Sequencing	sense	2498	21	catttcagttccagctcaagg		
4D	*atm*	Sequencing	antisense	2517	20	gccttgagctggaactgaaa		
5A	*atm*	PCR/Sequencing	sense	2888	22	gatgtgcttattgtgaccaagg	65	939
5B	*atm*	PCR/Sequencing	antisense	3827	22	gataagatcacgcactgtttgc		
5C	*atm*	Sequencing	sense	3320	21	tttgctgtgatatgcaagtcc		
5D	*atm*	Sequencing	antisense	3353	20	tgaatttcgcagtggacttg		
6A	*atm*	PCR/Sequencing	sense	3754	22	atccaattccaggggagtttat	65	903
6B	*atm*	PCR/Sequencing	antisense	4657	22	acagcatctgcaacttcacagt		
6C	*atm*	Sequencing	sense	4184	20	gcgaaagcgaaggtcagaac		
6D	*atm*	Sequencing	antisense	4233	20	ctccgacaatagctggaggt		
7A	*atm*	PCR/Sequencing	sense	4592	22	ttcggcctcttttttctagtcag	68	951
7B	*atm*	PCR/Sequencing	antisense	5543	22	ccaaactgtgacagacaacacc		
7C	*atm*	Sequencing	sense	5040	20	agacaacggactgcgagttt		
7D	*atm*	Sequencing	antisense	5101	20	attgggttgactggacttgc		
8A	*atm*	PCR/Sequencing	sense	5505	22	cgatggaagctttcttaggtgt	64	943
8B	*atm*	PCR/Sequencing	antisense	6448	21	atgggatttacaaagcctgga		
8C	*atm*	Sequencing	sense	5927	20	acctgcctgctgcctttttat		
8D	*atm*	Sequencing	antisense	5991	21	gacagactctccacgtgctct		
9A	*atm*	PCR/Sequencing	sense	6403	22	aatcaattggctgcttagatgc	67	961
9B	*atm*	PCR/Sequencing	antisense	7364	22	atcttccagcagaacgctaatc		
9C	*atm*	Sequencing	sense	6869	20	atggctgtgttcccttcaac		
9D	*atm*	Sequencing	antisense	6914	20	catcacctggcaaaaatcct		
10A	*atm*	PCR/Sequencing	sense	7339	22	tttagattagcgttctgctgga	63	939
10B	*atm*	PCR/Sequencing	antisense	8278	22	ttcttttcgcagatcatagcaa		
10C	*atm*	Sequencing	sense	7771	19	agacggcggagaaggtgac		
10D	*atm*	Sequencing	antisense	7843	20	gcgtaacgtttcatctgcac		
11A	*atm*	PCR/Sequencing	sense	8216	22	gaacagcaatacagagcgatca	64	929
11B	*atm*	PCR/Sequencing	antisense	9145	22	cttctccagcaggaaataatgg		
11C	*atm*	Sequencing	sense	8643	21	cacagtgtgggggattaaatg		
11D	*atm*	Sequencing	antisense	8698	20	accatcagagcatacgcaca		
12A	*atm*	PCR/Sequencing	sense	9114	22	aacccgttttccattatttcct	63	961
12B	*atm*	PCR/Sequencing	antisense	10075	22	ttttgaaaaacgaatgccataa		
12C	*atm*	Sequencing	sense	9563	20	ccacttttcatttggggtgt		
12D	*atm*	Sequencing	antisense	9610	20	tgctgtggtgattgcttctt		
13A	*atm*	PCR/Sequencing	sense	9999	22	tcttggcaagtgaagaatttcc	66	953
13B	*atm*	PCR/Sequencing	antisense	10952	22	gtttcgattgagatcggtgtct		
13C	*atm*	Sequencing	sense	10426	22	aagtgtttaccacccattgtcc		
13D	*atm*	Sequencing	antisense	10468	26	atgtacgttttttaaagattggggaca		
14A	*atm*	PCR/Sequencing	sense	10894	22	aacgcagctcaatctgtaatga	66	941
14B	*atm*	PCR/Sequencing	antisense	11835	20	caggagatcccagagcactt		
14C	*atm*	Sequencing	sense	11292	21	agcatttgcttactccacgag		
14D	*atm*	Sequencing	antisense	11393	20	cacccaatcccgaatctagg		
ATM5TEST1	*atm*	RT-PCR	sense	6867	20	gacatggctgtgttcccttc	62	150 / 85 *
ATM5TEST2	*atm*	RT-PCR	antisense	7017	20	cttggtcgttgaagcaggat		
p53-C1	*p53*	Test for *p53* $^{5A\text{-}1\text{-}4}$	sense	-	27	agctaatgtgacttcgcattgaacaaa	62	4000 / 7300 **
p53-C2	*p53*	Test for *p53* $^{5A\text{-}1\text{-}4}$	antisense	-	27	tcgataaacattggctacggcgattgt		

† - First position of primer on genomic sequence

‡ - Optimal annealing temperature for primer pair during PCR.

* - 150b.p. from unspliced mRNA, 85 b.p. from spliced mRNA.

** - 4 kb from $p53^{5A\text{-}1\text{-}4}$ allele, 7.3 kb from wild type *p53* allele.

Appendix B: Primary Antibody Information

Antigen	Catalog	Donor / Supplier	Host Organism	Tissue	Dilution
Hts	1B1	Hybridoma	Mouse	Ovaries	1:5
Cleaved Human Caspase-3	#9661	Cell Signaling	Rabbit	Discs	1:800
Phospho-Histone H3 (Ser10)	#06-570	Upstate	Rabbit	Discs	1:3600
LacZ (Beta-Galactosidase)	40-1a	Hydridoma	Mouse	Ovaries	1:200
Elav	9F8A9	Hybridoma	Mouse	Discs	1:100
Phospho His2Av	n/a	Kim McKim	Rabbit	Ovaries	1:500
Grk	1D12	Hybridoma	Mouse	Ovaries	1:10
Orb	4H8	Hybridoma	Mouse	Ovaries	1:100-1:150
Orb	6H4	Hybridoma	Mouse	Ovaries	1:100-1:150
BrdU	G3G4	Hybridoma	Mouse	Discs	1:20

Appendix C: Supplementary Raw Data

Section C-1: Scoring data from ionizing radiation sensitivity assay

	Eclosed Progeny (24°C)			
IR Dose	*atm*^{8} / *TM6b*	*Df / TM6b*	*atm*^{8} / *Df*	Total
0 Gy	58	47	14	119
1 Gy	96	74	1	171
2 Gy	72	65	1	138
3 Gy	66	77	0	143
4 Gy	83	62	2	147
5 Gy	79	47	0	126
6 Gy	72	68	0	140
8 Gy	86	55	0	141
10 Gy	76	66	0	142

	Eclosed Progeny (22°C)			
IR Dose	*atm*^{8} / *TM6b*	*Df / TM6b*	*atm*^{8} / *Df*	Total
0 Gy	62	63	66	191
1 Gy	76	61	62	199
2 Gy	106	90	114	310
3 Gy	77	58	65	200
4 Gy	63	85	102	250
5 Gy	116	114	99	329
6 Gy	81	63	104	248
8 Gy	96	83	95	274
10 Gy	90	71	67	228

Crosses were setup at 24°C or 22°C, which are restrictive and permissive temperatures for *atm*^{8} respectively. Both crosses were irradiated during the third larval instar, day 5 for the 24°C crosses and day 8 for the 22°C crosses. Progeny were allowed to eclose and then scored. *atm*^{8}*/TM6b* flies were identified based on the presence of *Hu*, which is present on TM6B. *Df/TM6b* flies were identified based on the presence of both *Ki*, which is present on the same chromosome as the deficiency, and *Hu. atm*^{8}*/Df* progeny were identified using the recessive marker p^{p}, which is present on the *atm*^{8} and deficiency chromosomes but not TM6b. The ratio of *atm*^{8}*/Df* progeny to total progeny was calculated for each group and used for figure 2-2e.

Section C-2: Scoring data from experiment addressing suppression of atm *lethality and developmental delay by removal of* p53.

	Cross #1		Cross #2		Cross#3	
	atm^8 p53 / TM6b X atm^1 p53 / TM6b		atm^8 p53 /TM6b X atm^1 / TM6b		atm^8 / TM6b X atm^1 / TM6b	
Days After Cross	atm^8 p53 / atm^1 p53	atm^8 p53 / TM6b or atm^1 p53 / TM6b	atm^8 p53 / atm^1	atm^8 p53 / TM6b or atm^1 / TM6b	atm^8 / atm^1	atm^8 / TM6b or atm^1 / TM6b
10	22	59	0	54	0	52
	24	76	0	52	0	57
	15	33	0	40	0	83
	2	17	0	6	0	19
(day 10 total)	**63**	**185**	**0**	**152**	**0**	**211**
11	30	38	1	41	0	35
	23	33	0	55	0	75
	29	31	0	66	0	117
(day 11 total)	**82**	**102**	**1**	**162**	**0**	**227**
12	45	70	3	99	0	91
	52	101	1	143	0	154
	23	24	0	52	0	70
	16	32	1	40	0	100
(day 12 total)	**136**	**227**	**5**	**334**	**0**	**415**
13	5	13	6	27	1	54
	21	34	3	55	0	40
	3	3	1	17	1	60
(day 13 total)	**29**	**50**	**10**	**99**	**2**	**154**
14	13	26	3	44	0	89
	0	2	1	5	4	18
	19	25	2	56	1	38
	0	0	2	2	0	4
(day 14 total)	**32**	**53**	**8**	**107**	**5**	**149**
15	0	2	3	1	3	9
	0	0	0	0	2	6
	0	1	3	38	0	51
	0	1	1	0	4	2
(day 15 total)	**0**	**4**	**7**	**39**	**9**	**68**
16	0	2	4	0	2	1
	0	0	0	0	3	2
	0	0	3	19	1	29
	0	0	0	0	3	0
(day 16 total)	**0**	**2**	**7**	**19**	**9**	**32**

The above three crosses were setup to provide atm^8 *p53* / atm^1 *p53*, atm^8 *p53* / atm^1, and atm^8 / atm^1 progeny. According to straightforward Mendelian ratios these mutant progeny would be expected to makeup one third of the total progeny. Progeny were scored to determine if removal of *p53* is capable of suppressing the lethality of *atm* progeny. In order to determine if removing *p53* also has any effect on the developmental delay associated with *atm* mutations, progeny were scored every day for seven days following the start of eclosion. For each time point, data from that time point was combined with data from all previous time points to produce a "cumulative mutant ratio". This provided an idea of how many mutant flies were able to eclose thus far for each day. These cumulative mutant ratios were used in figure 2-4d. Mutant progeny were identified based on the *atm* rough eye phenotype and the absence of the dominant marker *Hu*, which is present on TM6b.